IMPROVING PERFORMANCE AND PRODUCT SPECIFICITY OF THE CARBOXYLATE PLATFORM FOR PRODUCTION OF BIOCHEMICALS

A Dissertation

Presented to the Faculty of the Graduate School

of Cornell University

In Partial Fulfillment of the Requirements for the Degree of

Doctor of Philosophy

by

Matthew Thomas Agler

January 2012

IMPROVING PERFORMANCE AND PRODUCT SPECIFICITY OF THE CARBOXYLATE PLATFORM FOR PRODUCTION OF BIOCHEMICALS

Matthew T. Agler, Ph.D.

Cornell University, January 2012

The carboxylate platform converts organic feedstocks to short- or medium-chain carboxylates with reactions that are catalyzed by undefined mixed cultures in anaerobic systems. The undefined mixed cultures first convert substrate biomass to primary fermentation products (e.g., ethanol, acetate, propionate, lactate, n-butyrate, hydrogen, and carbon dioxide). Next, secondary fermentation reactions (e.g., carboxylate oxidation, methanogenesis, or carboxylate chain elongation) couple oxidation and reduction of primary products to achieve a final product spectrum. The most successful application of the carboxylate platform, thus far, has been anaerobic digestion, because most substrate is efficiently and almost exclusively converted to methane and carbon dioxide. Additionally, problems are relatively easy to address because of years of experience with anaerobic digesters and a good understanding of the underlying microbial processes. The carboxylate platform can also be applied to production of liquid bioproducts, such as carboxylates. Until now, this application has suffered from low product specificity and poor yields due to unclear links between operating conditions and performance and a poor understanding of the underlying microbial communities. In this dissertation, we improve carboxylate production with undefined mixed cultures by using molecular biology tools to guide engineering of carboxylate-producing systems. First, we studied the efficiencies of thermophilic bioreactors producing n-butyrate for 421 days to determine how bioreactor operating

conditions (substrate pretreatment and undissociated carboxylic acid toxicity reductions) affected the undefined mixed cultures. We used high-throughput 16S rRNA gene analysis, combined with ordination strategies, to observe the connection between development and performance of the bacterial community structure. Also, machine learning enabled us to probe the taxonomic structure to understand why performance did not increase with decreased carboxylic acid toxicity at pH 5.8. Finally, we implicated lactate in decreased n-butyrate specificity because of competing n-caproate production (i.e., lactate + n-butyrate → n-caproate), indicating that secondary fermentation reactions are important factors in determining the efficiency of carboxylate-producing systems. We concluded that *in-situ* product-specific carboxylate removal and secondary reaction control would be necessary to further decrease toxicity and increase performance of carboxylate-producing bioreactors. Because n-butyrate is relatively difficult to recover, next, we sought to study production of n-caproate, which, with a more hydrophobic nature is easier to remove from solution. Thus, we performed a functional metagenomics study of bioreactors operated at three temperatures (55^{o}C, 40^{o}C, and 30^{o}C) to produce n-caproate and n-caprylate. We combined an electron pushing strategy (i.e., ethanol supplementation to promote coupling of ethanol oxidation and short-chain carboxylate elongation) and *in-situ* product specific extraction to optimize n-caproate and n-caprylate formation. Functional metagenomics could map the dynamics between operating conditions and performance, indicating that better extraction efficiency could further improve performance. In the current setup, we achieved a maximum 52% n-caproate/n-caprylate specificity (i.e., the ratio of n-caproate and n-caprylate COD to the COD of

all other fermentation products) and maximum rates that were six times those without extraction. Further, we challenged traditional knowledge by suggesting that hydrogenotrophic methanogenesis and carboxylate production can occur simultaneously, and that the community function may have depended on management of the hydrogen partial pressure by methanogens. Overall, we showed that many principles driving product specificity in anaerobic digestion (product removal and directed secondary fermentations) also apply to efficient production of liquid carboxylates.

BIOGRAPHICAL SKETCH

Matthew T. Agler grew up in Lawrenceville, IL, located in the heart of the Midwest. After graduating from Lawrenceville High School, he pursued an undergraduate degree in Agricultural and Biological Engineering at the University of Illinois at Champaign-Urbana. In 2006, he began graduate work at Washington University in St. Louis under the direction of Dr. Largus T. Angenent. There, he met his wife, Miriam Agler-Rosenbaum. The lab (and Matthew) moved to Cornell in 2008, and there he has continued his pursuit of a Ph.D. in Biological and Environmental Engineering. Next, Matthew will pursue new adventures in Germany, happy to be back with his wife, where Miriam has been a junior professor at RWTH Aachen University since spring 2011.

This dissertation is dedicated to my wife Miriam Agler-Rosenbaum. Without you I never would have made it this far, physically, mentally, and spiritually. That is a fact. It is also dedicated to my Mother and Father, Ann and Thomas Agler, who raised me with Love, and with the opportunity and freedom to pursue a happy life. Finally, I dedicate this dissertation to my sister Leslie Caughran and her family, K.G., Kayden, Kyler, and future #3, because the support of family is everything.

ACKNOWLEDGMENTS

First, I would like to acknowledge the continuing support of my special committee: Dr. Jean Hunter, Dr. William Jewell, and Dr. Stephen Zinder. I would like to acknowledge the support of all members of the Angenent Lab, past and present. By name, I'd like to mention Ben Bocher and Dr. Marcelo Garcia, who taught me everything about running reactors. A special thanks goes out the Agricultural Waste Management Lab fraction of the Angenent Lab, especially Jack Yi, who have helped me in every way in the last three years. I would also like to thank Dr. Jeffrey Werner for making bioinformatics possible in our lab, because much of this work could not have been done without his kindness, his patience, and of course, his bioinformatics scripts. Last but not least, I owe a great deal of debt and gratitude to Dr. Largus Angenent, for taking me in, teaching me what I know, having patience when things go wrong, and providing to me the opportunity and the freedom to do some really exciting research. Thanks to everyone.

The work for the review in Chapter 2 was supported by the USDA through the National Institutes of Food and Agriculture (NIFA), grant number 2007-35504-05381

For the work described in Chapter 3, we were supported by the Illinois Department of Commerce and Economic Opportunity (grant number: 02-20701) through a grant to the National Corn to Ethanol Research Center. Finally, for the work described in Chapters 4 and 5, we were supported by the National Research Initiative of the USDA Cooperative State Research, Education and Extension Service, grant number 2007-35504-18256.

TABLE OF CONTENTS

	Biographical Sketch	iii
	Dedication	iv
	Acknowledgements	v
	Table of Contents	vi
	List of Figures	viii
	List of Tables	xi
	List of Boxes	xiii
	Preface	xiv
Chapter 1	Introduction: Central hypothesis and summary of the experiments toward that hypothesis	1
Chapter 2	Literature Review: Waste to bioproduct conversion with undefined mixed cultures: The carboxylate platform	4
	2.1 Introduction	5
	2.2 Acetate	12
	2.3 Propionate and Lactate	17
	2.4 n-Butyrate	19
	2.5 Mixed Carboxylates	21
	2.6 Outlook	21
	2.7 Acknowledgements	24
Chapter 3	Thermophilic anaerobic digestion to increase the net energy balance of corn grain ethanol	28
	3.1 Introduction	29
	3.2 Methods	33
	3.3 Results	36
	3.4 Discussion	44
	3.5 Acknowledgements	50
Chapter 4	Functional microbial community structure links operating conditions to n-butyrate production	52
	4.1 Introduction	53
	4.2 Methods	56
	4.3 Results	59
	4.4 Discussion	71
	4.5 Acknowledgements	75
Chapter 5	Directing mixed microbial cultures toward upgrading acetate, n-butyrate, and ethanol to specific medium-chain carboxylates	76
	5.1 Introduction	77

	5.2 Methods	81
	5.3 Results	86
	5.4 Discussion	97
	5.5 Acknowledgements	101
Chapter 6	Summary and recommendations for future work	103
	6.1 Summary	103
	6.2 Recommendations for future work	104
Appendix 1	Supplemental information for Thermophilic anaerobic digestion of thin stillage to increase the net energy balance of corn grain ethanol	110
Appendix 2	Hydrogenotrophic methanogen inhibition due to carboxylate toxicity	122
	A2.1 Introduction	122
	A2.2 Methods	122
	A2.3 Results	124
	A2.4 Discussion	126
	A2.5 Acknowledgements	127
Appendix 3	Supplemental information for Functional microbial community structure links operating conditions to n-butyrate production	128
Appendix 4	Supplemental information for Directing mixed microbial cultures toward upgrading acetate, n-butyrate, and ethanol to specific medium-chain carboxylates	147
Appendix 5	Protocols	151
References		167

LIST OF FIGURES

Note: AX denotes appendix X, each of which are placed in the table to follow the chapter they support

Ch 2

2.1 Hydrolysis of solid polymers to monomers and oligomers (e.g. insoluble polysaccharides, such as cellulose and hemicellulose) and subsequent conversion by primary and secondary fermentation reactions with undefined mixed cultures. 8

2.2 Chemical post-processes that convert carboxylates to bulk fuels or solvents with pure-culture biochemical, electrochemical, and thermochemical steps, or a combination thereof. 9

Ch 3

3.1 Bioreactor operating conditions and performance for anaerobic digesters treating thin stillage (R1 and R2). 41

3.2 Overall process diagram of dry-mill corn grain-to-ethanol processes. 45

A1 SUPPLEMENTAL INFORMATION FOR CHAPTER 3

A1.S1 Setup of a 5-l thermophilic anaerobic sequencing batch reactor (ASBR) for the bioconversion of thin stillage to methane (R1 and R2). 111

A1.S2 Methane yield graphs for anaerobic digesters treating thin stillage (R1 and R2). 121

A1.S3 Sludge volume index (SVI) of anaerobic digesters treating thin stillage (R1 and R2). 116

A1.S4 SEM images of biomass granules from anaerobic digesters treating thin stillage. 118

A1.S5 pH level of effluent of anaerobic digesters treating thin stillage (R1 and R2). 116

A1.S6 SEM images of individual struvite crystals from anaerobic digesters treating thin stillage. 121

A2

A2.1 Inhibition of thermophilic hydrogenotrophic methanogens in undefined mixed microbial inocula and in inocula from thermophilic bioreactors producig n-butyrate. 125

Ch 4

4.1 Fermentation product rates (as COD (g O_2) per liter bioreactor volume per day) and biogas composition in bioreactors producing n-butyrate (R_{acid}, R_{base}, and R_{heat}) 61

4.2 48-hour cycle analysis demonstrates the dynamic relationship between intermediate lactate and the acetate, n-butyrate, and n-caproate specificities (i.e., ratio of specific product in COD to all fermentation products in COD) in bioreactors producing n-butyrate (R_{acid}, R_{base}, and R_{heat}). 65

4.3 Redundancy analysis of the phylogeny described by weighted UniFrac principal coordinates of 16S rRNA genes from samples taken from bioreactors producing n-butyrate (R_{acid}, R_{base}, and R_{heat}). 67

4.4 The taxonomic structure of bioreactors bacterial communities producing n-butyrate (R_{acid}, R_{base}, and R_{heat}). 70

A3 SUPPLEMENTAL INFORMATION FOR CHAPTER 4

A3.S1 COD balance in substrate and effluent for bioreactors producing n-butyrate (R_{acid}, R_{base}, and R_{heat}). 133

A3.S2 Biological hydrolysis of solid substrate for bioreactors producing n-butyrate (R_{acid}, R_{base}, and R_{heat}). 134

A3.S3 Supplemental community structure analysis plots, including constrained vs. unconstrained redundancy analysis comparison, and principal coordinates of between-sample UniFrac distances for bioreactors producing n-butyrate (R_{acid}, R_{base}, and R_{heat}). 135

A3.S4 Rates of n-caproate production are correlated with relative abundance of the genus *Thermosinus* in bioreactors producing n-butyrate. 135

A3.S5 Bacterial community phylogenetic structure and bacterial community evenness in bioreactors producing n-butyrate (R_{acid}, R_{base}, and R_{heat}). 136

A3.S6 Community dynamics in identically operated and perturbed bioreactors portray a nonrandom community structure. 137

Ch 5

5.1 Performance comparison between an ethanol-supplemented bioreactor with *in-situ* product-specific extraction (R_p) and a bioreactor without product extraction (R_c). 87

5.2 (Constrained) redundancy analysis of SEED subsystem-based functional abundance principal coordinates for ethanol-supplemented 91

bioreactors (R_p and R_c)

5.3 100-fold bootstrapped sample-distance tree of the SEED subsystem-based functional abundance data for ethanol supplemented bioreactor communities (R_p and R_c). 93

5.4 Taxonomy distribution of the class Clostridia (other phyla are shown for comparison) in genes annotated by searching against the NCBInr database, overlaid with the n-caproate (C6)/n-caprylate (C8) specificity for ethanol-supplemented bioreactor communities (R_p and R_c). 96

A4 SUPPLEMENTAL INFORMATION FOR CHAPTER 5

A4.S1 Bioreactor setup for ethanol-supplemented bioreactors R_p (with *in*-situ product extraction) and R_c (without *in-situ* product extraction). 148

A4.S2 Volatile solids (VS) removal during bioreactor operation at three temperatures in ethanol-supplemented bioreactors (R_p and R_c). 148

A4.S3 Volcano plots based on SEED subsystem-based functional abundances comparing gene abundance changes due to temperature and extraction in ethanol-supplemented bioreactor communities (R_p and R_c). 149

A4.S4 Correlations between taxonomic groups of the chain-elongation genes and the n-caproate/n-caprylate specificity in ethanol-supplemented bioreactor communities (R_p and R_c). 149

A4.S5 Gibbs free energy of reaction (ΔG_r) for n-butyrate and ethanol oxidation at bulk bioreactor conditions during bioreactor operation for an ethanol-supplemented bioreactor with *in*-situ product extraction (R_p). 150

A4.S6 Taxonomic distribution of alcohol dehydrogenase genes in ethanol-supplemented bioreactor communities (R_p and R_c). 150

LIST OF TABLES

Note: AX denotes appendix X, each of which are placed in the table to follow the chapter they support

Ch 2

2.1 Secondary fermentation reactions and processes 11

Ch 3

3.1 Characteristics of five thin stillage samples used as substrate for the study of anaerobic digestion of thin stillage (F1-5), two thin stillage samples from different full-scale dry mill corn grain-to-ethanol facilities (Plant 1 and 2), and average values for weekly-sampled thin stillage batches during three different HRT periods for the full-scale MGP plant (no statistical data reported). 38

3.2 Elemental analysis of thin stillage (F5), R1 and R2 effluent samples, syrup, and trace element solution. 39

A1 SUPPLEMENTAL INFORMATION FOR CHAPTER 3

A1.S1 Characterization of effluent from thermophilic anaerobic digesters R1 and R2. 114

A1.S2 Calculation of the percentage of nonrenewable energy input that can be replaced by methane from thermophilic ASBRs and the change of the NEB ratio for a $3.78 \cdot 10^8$ l ethanol per year corn grain-to-ethanol plant with integrated thermophilic ASBRs. 120

A2

A2.1 n-Butyrate and n-butyric acid levels to achieve 90% inhibition of hydrogenotrophic methanogenic activity at 55^{o}C. 124

Ch 4

4.1 Composition of corn fiber (before) and hydrolysate (after) three pretreatment strategies 57

4.2 Standard state Gibbs free energy of a possible secondary fermentation coupled reaction set 144

A3 SUPPLEMENTAL INFORMATION FOR CHAPTER 4

A3.S1 Additional composition of corn fiber (before) and hydrolysate (after) three pretreatment strategies 145

A3.S2 Operating conditions for bioreactors producing n-butyrate (Period 1 through Period 4) 146

Summarized effects of changes in operating conditions for

A3.S3 bioreactors producing n-butyrate (Period 1 to Period 4) 146

A3.S4 OTUs determined by machine learning to be predictive of a bioreactor or combination of bioreactors

LIST OF BOXES

Ch 2

2.1 Predicting reaction occurrence in the carboxylate platform 25

2.2 Liquid/liquid extraction to separate acetate in the carboxylate platform 26

2.3 Biological chain elongation in the carboxylate platform 27

PREFACE

To the reader, I would like to mention that our lab specializes in long-term studies of bioreactors (in this work, ranging from 124 days to 420 days). This type of operation, combined with the high-throughput DNA sequencing techniques we performed generates massive amounts of data. I mention this because the reader will find that each of the three main research papers herein is supported by information in the appendices. The appendices are not absolutely necessary to understand the content of the chapters, but often it provides important support for arguments made in the text. This is necessary in order to keep the chapters at a readable length, and not to bog the text down with excessive amounts of data and details. We have tried to be as clear and organized as possible to make moving between chapters and appendices easy, when necessary. To that end, the LIST OF FIGURES and LIST OF TABLES places each set of appendix figures just after the chapter it supports. I hope that the reader will find that this approach is useful, and will find the supplementary information in the appendices to be valuable, when he/she is interested in further information or support.

1. INTRODUCTION

CENTRAL HYPOTHESIS AND SUMMARY OF THE EXPERIMENTS CARRIED OUT

Central Hypothesis

Efficient production of a specific carboxylate end product from lignocellulosic waste with undefined mixed microbial cultures has, thus far, been elusive because of low yields and low product specificity. Low yields have been a result of product inhibition because high levels of undissociated volatile fatty acids are toxic to fermenting microorganisms. Further, the low pH generally used to inhibit methanogens during carboxylate production increases the levels of undissociated volatile fatty acids, further inhibiting substrate conversion. To improve yields and rates of product formation, bioreactors should be designed to remove products *in-situ*. Product specificity results from the combined effect of primary fermentation pathways (i.e., carbohydrate, protein, and lipid fermentation to short-chain carboxylates and alcohols) and secondary fermentation pathways (i.e., conversion of primary fermentation products to endproducts) by constituent microbial community members to produce an array of fermentation products and to convert those to end products. To direct the microbial community structure to orient toward secondary fermentations that funnel the product spectrum to a specific endproduct, the bioreactor conditions (temperature, pH), product removal, electron acceptor availability, and electron pushing substrate (i.e., the source of energy and electrons to upgrade primary

fermentation products) must all be coordinated to drive a specific process. We investigated this hypothesis with the following experiments:

High product to substrate conversion efficiency and product specificity via anaerobic digestion for methane production and evaluating how to eliminate thermophilic hydrogenotrophic methanogenesis

- We operated two anaerobic sequencing batch reactors (ASBRs) fed thin stillage as substrate for 412 days to optimize methane production and to evaluate factors limiting its formation. CHAPTER 3.
- We analyzed suppression of hydrogenotrophic methanogenesis via carboxylic acid inhibition with n-butyrate, one valuable product of the carboxylate platform. APPENDIX 2.

Decreasing end product inhibition to improve product specificity and product formation rates in n-butyrate production with undefined mixed cultures of microbes

- We operated three ASBRs fed dilute-acid, dilute-alkali, or hot-water pretreated corn fiber for 421 days to optimize n-butyrate production CHAPTER 4.
- We performed a 16S rRNA gene survey of n-butyrate producing bioreactors at various conditions and linked bioreactor operating conditions, community structure, and performance. CHAPTER 4.

Upgrading short-chain carboxylates and dilute ethanol to medium-chain carboxylates to significantly enhance product specificity in open mixed microbial communities

- We operated two ethanol-supplemented ASBRs fed dilute-acid pretreated corn fiber for 124 days to evaluate electron pushing with ethanol at three temperatures. CHAPTER 5.
- We performed continuous *in-situ* product-specific extraction of n-caproate and n-caprylate in one bioreactor and compared ethanol utilization specifically for chain elongation of primary fermentation products to a bioreactor without product extraction. CHAPTER 5.
- We performed a functional metagenomic survey of ASBRs with varying degrees of n-caproate/n-caprylate specificity to link the environmental conditions with the community metagenome functional compositions capable of utilizing electron-pushing substrates CHAPTER 5.

CHAPTER 2.

LITERATURE REVIEW: WASTE TO BIOPRODUCT CONVERSION WITH UNDEFINED MIXED CULTURES: THE CARBOXYLATE PLATFORM

Adapted from: Agler, Wrenn, Zinder, and Angenent. Trends in Biotechnology, February 2011. 29(2):70-78

Abstract

Our societies generate increasing volumes of organic wastes. Considering that we also need alternatives to oil, an opportunity exists to extract liquid fuels or even industrial solvents from these abundant wastes. Anaerobic undefined mixed cultures can handle the complexity and variability of organic wastes, producing carboxylates that can be efficiently converted; however, to date, barriers, such as inefficient liquid product separation and persistence of methanogens, have prevented the production of bioproducts other than methane. Here, we discuss combinations of biological and chemical pathways that comprise the "carboxylate platform", used to convert waste to bioproducts. To develop the carboxylate platform into an important system within biorefineries, we must understand the kinetic and thermodynamic possibilities of anaerobic pathways, understand the ecological principles underlying pathway alternatives, and develop superior separation technologies.

2.1 Introduction

The discrepancy between the rates of discovery of new oil reserves and consumption will undoubtedly lead to a future oil crisis. Our societies are also generating an increasing quantity of organic wastes, such as industrial and agricultural wastewater. An opportunity, therefore, exists to shift the view of these waste streams from pollutant to renewable resource. In the biorefinery concept, the value of each stream must be maximized (similar to oil refineries) [Fernando et al., 2006], and such waste treatment creates an opportunity to generate additional fuels or chemicals (i.e. bioproducts), while simultaneously recycling nutrients and water. Processing steps within biorefineries, such as chemical/physical pretreatment, enzyme production, and fermentation and extraction steps, all create large volumes of wastewater that must be treated. The two best-known biorefinery platforms are the sugar platform, in which purified enzymes convert biomass into five- and six-carbon sugars as intermediate feedstock chemicals that are converted further by, for example, fermentation to fuels; and the syngas platform, in which thermochemical systems convert biomass into syngas (i.e. synthesis gas: CO, H_2, CO_2, etc.) as feedstock chemicals that are converted further by, for example, catalysis to fuels (National Renewal Energy Laboratory: www.nrel.gov/biomass/biorefinery.html). We envision a third important platform – the carboxylate platform – to convert organic feedstocks, which are often derived from industrial and agricultural wastes, to short-chain carboxylates as intermediate feedstock chemicals, using hydrolysis and fermentation with undefined mixed cultures in engineered systems under anaerobic conditions. The differences in platforms are essentially based on the method of biomass conversion and its resulting chemicals

(e.g. sugar, syngas and carboxylates), because the subsequent conversion step into bioproducts is interchangeable between platforms. The use of undefined mixed cultures in waste treatment systems is vital, because they can tolerate the complexity and variability of substrates owing to the metabolic flexibility conferred by the many members of the community [Angenent and Wrenn, 2008; Kleerebezem and van Loosdrecht, 2007]. Furthermore, they are open and anaerobic systems, which makes energetically unfavorable sterilization and aeration superfluous [Angenent and Wrenn, 2008].

The terminology "carboxylate platform" is not new, and has been used to describe an undefined-mixed-culture process to generate a mixture of carboxylates as intermediate platform chemicals toward generation of complex fuels [Holtzapple and Granda, 2009]. Carboxylates are dissociated organic acids characterized by the presence of at least one carboxyl group. The short-chain carboxylates – acetate, propionate, lactate and n-butyrate – are the main organic products of undefined mixed cultures through primary fermentation reactions (Figure 2.1b). They are themselves valuable products when separated from the culture broth, but often they are substrates for further fermentation in the same undefined mixed culture through secondary fermentation reactions (Figure 2.1c-j) or in separate bioprocesses. The carboxylates from primary fermentations can also be further processed with separate pure-culture biochemical, electrochemical and thermochemical steps (chemical post-processing step in Figure 2.2). An important carboxylate flux occurs within its undefined mixed culture; as such, anaerobic digestion is included within the carboxylate platform because short-chain carboxylates are the (pen)ultimate intermediate platform products

for gaseous methane formation (Figure 2.1). Even though pure culture and defined mixed culture studies are performed to understand the underlying ecological principles of undefined mixed communities [Read et al., 2010; Rosenbaum et al., 2011; Wittebolle et al., 2009], the commercial process to convert biomass into carboxylates must be an undefined microbial processing step to handle the complexity of the organic waste stream.

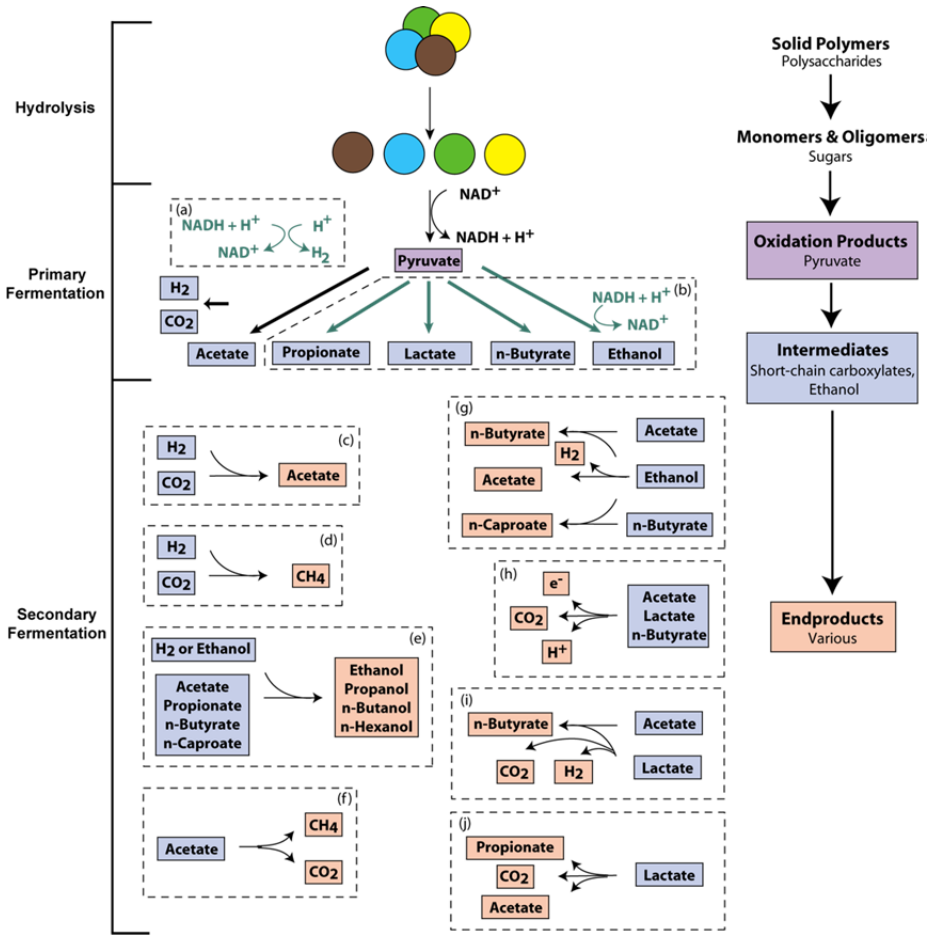

Figure 2.1. Hydrolysis of solid polymers to monomers and oligomers (e.g. insoluble polysaccharides, such as cellulose and hemicellulose) and subsequent conversion by primary and secondary fermentation reactions with undefined mixed cultures. During primary fermentation of sugars, substrates are converted to pyruvate, resulting in the production of NADH and H^+. All equivalents must be re-oxidized via H^+ reduction by: (a) NADH oxidation; or (b) NADH oxidation via reduction of pyruvate or its oxidized organic derivatives, depending upon the hydrogen partial pressure [Angenent et al., 2004]. At increasing hydrogen partial pressures, the flow of electrons from NADH shifts from H_2, acetate and CO_2 production towards formation of increasingly reduced fermentation products [McInerney et al., 1981]. CO_2 and H_2 are produced in the pyruvate oxidation reaction catalyzed by pyruvate:ferredoxin oxidoreductase. The products of primary fermentation can react further within undefined mixed cultures through several secondary fermentation reactions: (c) autotrophic homoacetogenesis; (d) hydrogenotrophic methanogenesis; (e) carboxylate reduction to alcohols with hydrogen or ethanol; (f) aceticlastic methanogenesis; (g) chain elongation of carboxylates with ethanol; (h) electricigenesis (i) lactate oxidation to n-butyrate (acetate and H^+ as electron acceptor); and (j) lactate reduction to propionate (oxidation to acetate for energy conservation).

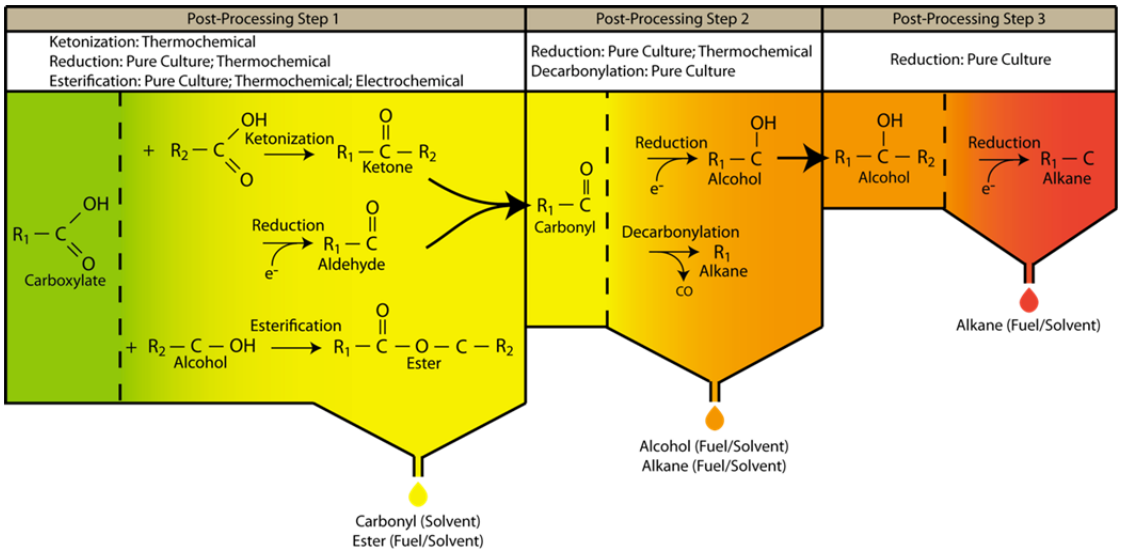

Figure 2.2. Chemical post-processes that convert carboxylates to bulk fuels or solvents with pure-culture biochemical, electrochemical, and thermochemical steps, or a combination thereof. In post-processing step 1, carboxylates are converted to esters via esterification [Holtzapple et al., 1999; Levy et al., 1981; Park et al., 2009]; are reduced to carbonyls [Glinski et al., 2007; Schirmer et al., 2010]; or ketonized to carbonyls [Gaertner et al., 2009]. In post-processing step 2, the carbonyl intermediates are converted to alkanes via decarbonylation [Schirmer et al., 2010]; or reduced to alcohols [Holtzapple et al., 1999; Tashiro et al., 2004]. Finally, in post-processing step 3, the alcohol intermediates are converted to alkanes via reduction [Belay and Daniels, 1988]. Other conversions (not shown here) are possible.

This review is a much-needed update to previous reviews [Angenent et al., 2004] because several additional bioprocessing schemes have been developed in the interim to generate energy-rich chemicals with undefined mixed cultures, rather than with pure or defined cultures. The organization of this review is based on the production and subsequent conversion of the primary fermentation end products, the carboxylate feedstock chemicals: acetate (C2), propionate and lactate (C3), n-butyrate (C4), and mixed carboxylates. In this review, we discuss how these chemicals can be further processed into high-volume fuels or industrial solvents because these bulk bioproducts would have the largest impact in an integrated biorefinery. Table 2.1 shows balanced chemical equations and their thermodynamic values under standard biological

conditions for the reactions and processes that we discuss in this review. Other chemicals that may also be generated within a carboxylate platform concept, but are not discussed here, are iso-butyrate, long-chain fatty acids, and biopolymers, such as polylactic acid.

Table 2.1. Secondary fermentation reactions and processes[a]

Reaction	Microbe	Carboxylate conversion reactions	Coupled repetitions[d]	$\Delta G_r^{o\prime}$ (kJ/mol at 37 °C)[e]	$\Delta G_r^{o\prime}$ (kJ/mol at 55 °C)[e]
(c) Carbon dioxide reduction to acetate	*Acetobacterium woodii*	$4H_2 + 2CO_2 \rightarrow acetate^- + H^+ + 2H_2O$		-86.78	-74.56
(d) Hydrogenotrophic methanogenesis	*Methanospirillum hungatei*	$4H_2 + CO_2 \rightarrow CH_4 + 2H_2O$		-125.84	-118.47
(e) Carboxylate reduction with molecular hydrogen	[b]	$acetate^- + H^+ + 2H_2 \rightarrow ethanol + H_2O$		-7.22	-4.37
		$propionate^- + H^+ + 2H_2 \rightarrow propanol + H_2O$		-7.49	-4.59
		$n\text{-}butyrate^- + H^+ + 2H_2 \rightarrow n\text{-}butanol + H_2O$		-3.58	-0.73
		$n\text{-}caproate^- + H^+ + 2H_2 \rightarrow n\text{-}hexanol + H_2O$		-7.55	-3.63
(e) Propionate reduction with ethanol	[c]	$ethanol + H_2O \rightarrow acetate^- + H^+ + 2\ H_2$	×1	7.22	4.37
		$propionate^- + H^+ + 2\ H_2 \rightarrow propanol + H_2O$	×1	-7.49	-4.59
				Total = -0.27	**Total** = -0.22
(f) Aceticlastic methanogenesis	*Methanosaeta soehngenii*	$acetate^- + H^+ \rightarrow CH_4 + CO_2$		-39.06	-43.91
(g) Chain elongation of acetate with ethanol	*Clostridium kluyveri*	$ethanol + H_2O \rightarrow acetate^- + H^+ + 2H_2$	×1	7.22	4.37
		$ethanol + acetate^- \rightarrow n\text{-}butyrate^- + H_2O$	×5	-201.68	-198.50
				Total = -194.46	**Total** = -194.13
(g) Chain elongation of n-butyrate with ethanol	*C. kluyveri*	$ethanol + H_2O \rightarrow acetate^- + H^+ + 2H_2$	×1	7.22	4.37
		$ethanol + n\text{-}butyrate^- \rightarrow n\text{-}caproate^- + H_2O$	×5	-190.00	-195.20
				Total = -182.78	**Total** = -190.83
(i) Lactate oxidation to n-butyrate	*Clostridium acetobutylicum*	$2\ acetate^- + H^+ + 2H_2 \rightarrow n\text{-}butyrate^- + 2H_2O$	×1	-47.55	-44.10
		$2\ lactate^- + H^+ \rightarrow n\text{-}butyrate^- + 2CO_2 + 2H_2$	×2.5	-209.35	-232.55
				Total = -256.90	**Total** = -276.65
(j) Lactate reduction to propionate	*Selenomonas ruminantium*	$lactate^- + H_2O \rightarrow acetate^- + CO_2 + 2H_2$	×1	28.51	25.96
		$lactate^- + H_2 \rightarrow propionate^- + H_2O$	×2	-86.63	-85.21
				Total = -58.12	**Total** = -59.25

[a]Secondary fermentation reactions correspond to those in Figure 2.1 [(h) is not shown here].

[b]Carboxylate reduction to alcohol with H_2 as the electron donor has been observed in undefined mixed cultures [Steinbusch et al., 2008].

[c]Propionate reduction with ethanol has been observed in undefined mixed cultures [Smith and McCarty, 1989].

[d]For reactions that are coupled within microbes, number of repetitions of individual reactions to achieve the total reaction.

[e]All $\Delta G_r^{o\prime}$ values are calculated considering all reactants and products to be in the aqueous phase except for H_2, CO_2 and CH_4, which are gaseous at 1 atm. $\Delta G_r^{o\prime}$ values are at biological standard state (pH = 6.82 at 37°C; 6.58 at 55°C). Reactions that are coupled by microbes are shown individually with individual and coupled (total) $\Delta G_r^{o\prime}$ values. $\Delta G_r^{o\prime}$ quantities were calculated from ΔG_f^o values from [Amend and Shock, 2001], except for n-caproate$^-$ and n-hexanol, which were calculated using the HKF equations of state [Shock and Helgeson, 1990] and thermodynamic parameters [Shock, 1995].

2.2 Acetate

When the hydrogen partial pressure is maintained at low levels in stable anaerobic digesters by scavenging hydrogenotrophic methanogens (secondary fermentation reaction in Figure 2.1d), a maximum acetate flux is maintained (mainly the primary fermentation pathway in Figure 2.1a). This maximum acetate flux explains the superiority of anaerobic digestion as an efficient biomass-to-energy conversion process because primary fermentation is directed towards acetate and hydrogen, both of which are then converted to the end product methane with secondary fermentation reactions (Figure 2.1d, f). Propionate and n-butyrate are formed during protein hydrolysis and subsequent fermentation of amino acids, regardless of the H_2 partial pressure [Nagase and Matsuo, 1982]. On the other hand, propionate and n-butyrate can only be converted to the intermediate products acetate and hydrogen by secondary syntrophic carboxylate-oxidation reactions, if these products are removed by methanogens (low H_2 partial pressure) (Box 2.1; Table I). This guarantees the maximum carbon and electron flux towards methane because almost no side-products that decrease efficiency are released from the anaerobic food web [De Schamphelaire and Verstraete, 2009]; or, in other words, the microbial process is directed to the final product (i.e. methane) with the lowest available free energy content per electron [Hanselmann, 1991]. Because anaerobic digestion is a mature technology and methane freely bubbles out without requiring additional separation processes, it is easy to understand why anaerobic digestion is the most popular waste-to-energy conversion technology worldwide. However, methane has a low monetary value, and therefore we focus here on the promises and challenges of producing liquid fuels and high-value chemicals with the carboxylate platform.

Acetate by itself is a useful chemical; or as a feedstock chemical, acetate can be processed into bulk bioproducts via secondary fermentation reactions (Figure 2.1e-i) and chemical post-processing reactions (Figure 2.2). Although a variety of chemical and biological processes can be used to transform carboxylate intermediates to valuable products, three biological processes in particular may integrate well with the production of carboxylates from complex waste streams by undefined mixed cultures. These processes are biological reduction of carboxylates to the corresponding alcohols (Figure 2.1e); biological elongation of short-chain carboxylates to longer chain products (Figure 2.1g); and bioelectrochemical systems (BES), in which biological reactions are coupled to reactions at solid electrodes to produce electric power or valuable chemicals (Figure 2.1h). Regardless of the conversion method, further processing of acetate relies on being able to separate it from the undefined mixed culture broth, because consolidated bioprocesses in which the primary and secondary fermentation reactions occur in the same bioreactor are often precluded by incompatible optimal conditions. One of the main barriers for large-scale liquid fuel and chemical production with the carboxylate platform is limitations with separation (Box 2.2). The other barrier is that hydrogenotrophic methanogenesis must be ceased.

Bioelectrochemical oxidation to electrons

Most BES research initially focused on production of electric power by bioelectrochemical oxidation of organic substrates in microbial fuel cells (MFCs) in which a solid electrode served as the electron acceptor (Figure 2.1h) [Logan et al., 2006]. Electric power is generated in MFCs by developing a natural potential difference between an anaerobic anode and an aerobic cathode. Although more complex substrates have been

used, only acetate and other short-chain carboxylates result in coulombic efficiencies appropriate for scale up [Fornero et al., 2010]. Recent studies, however, suggest that converting organic substrates, such as short-chain carboxylates, into chemical products by applying an electric potential across the electrodes has greater economic and environmental benefits than the production of electric power [Foley et al., 2010; Fornero et al., 2010]. This approach overcomes the thermodynamic limitations of the cathodic reactions by using a potentiostat to apply an electric potential between the electrodes in microbial electrolysis cells (MECs). Separation of product formation at the cathode from substrate oxidation at the anode is an inherent advantage of using a membrane-based BES to generate valuable products from complex organic wastes. Abiotic cathodes have been used to produce hydrogen [Liu et al., 2005; Logan et al., 2006], hydrogen peroxide [Rozendal et al., 2009], and sodium hydroxide [Rabaey et al., 2010], and undefined mixed cultures have been used to produce methane without the addition of mediators at potentiostatically poised cathodes (i.e. biocathodes) [Cheng et al., 2009; Villano et al., 2010]. Recent studies have demonstrated reduction of CO_2 in biocathode-based and potentiostatically poised BESs [Cao et al., 2009; Nevin et al., 2010]; and reduction of carbon dioxide into multi-carbon products (i.e. microbial electrosynthesis), such as alcohols, with all electrons originating from carboxylate oxidation at the anode, is a focus of ongoing research.

Biological reduction to alcohols

Biological reduction of carboxylates, such as acetate, n-butyrate and n-caproate, to the corresponding alcohols has been observed in separate secondary fermentation bioprocesses (Figure 2.1e) [Steinbusch et al., 2008; Steinbusch et al., 2010]. The

thermodynamic free energy under biological standard conditions (Table 2.1) is smaller than the biologically limit for cellular functions (Box 2.1) [Kleerebezem and Stams, 2000; Thauer et al., 1977]; therefore, the hydrogen partial pressure must be maintained at elevated levels (~1.5 atm). Because hydrogen would be available in a biorefinery that includes the carboxylate platform, it is an attractive reducing agent. Unfortunately, very low rates of alcohol production from acetate (0.07 g ethanol l^{-1} day^{-1}) have been observed under these conditions [Steinbusch et al., 2009]. Alternatively, acetate can also be reduced to ethanol with an artificial mediator and a mixed culture at the cathode of a BES [Steinbusch et al., 2010], where electrons donated from the cathode provide the required reducing power.

High-rate consolidated bioprocesses for producing ethanol from acetate cannot be envisioned because high hydrogen partial pressures are required to drive acetate reduction and very low partial pressures are required to sustain high rates of acetate production. Thus, a secondary-fermentation bioprocess with two separate streams of acetate and hydrogen would be required. The ethanol concentrations obtained in batch experiments with an undefined mixed culture (0.17 g/l at an acetate conversion efficiency of ~55%) [Steinbusch et al., 2008] are too low for economical recovery of the product by *ex situ* distillation, and the maximum concentration that can be achieved (<1.1 g/l at pH 4.5) is limited by the required threshold free energy for this reaction [Steinbusch et al., 2009]. Therefore, it might be necessary to remove ethanol continuously during the acetate reduction process to maintain sufficiently low product concentrations and high fluxes. Because ethanol is polar, continuous extraction of ethanol would be difficult, and

further conversion to longer-chain chemicals that are easier to separate from the aqueous medium (e.g. medium-chain carboxylates, described below) might be a solution.

Chain elongation to medium-chain carboxylates

An undefined mixed culture capable of reducing acetate to ethanol (Figure 2.1e) can also produce n-butyrate (0.61 g/l) by further reaction of ethanol with acetate (Figure 2.1g; Box 2.3) [Steinbusch et al., 2009]. Thus, these two secondary fermentation processes allow one undefined mixed culture to convert acetate and hydrogen to n-butyrate by elongation of the acetate carbon chain. Further optimization is needed to accelerate the production rates, but conversion of the intermediate ethanol to n-butyrate is logical because, as discussed above, ethanol accumulation renders the biological reduction reaction thermodynamically unfeasible. It is important to understand that hydrogenotrophic and aceticlastic methanogens must be completely inhibited by heat-shocking the inoculum, lowering the pH, or by adding a methanogenic inhibitor (e.g. 2-bromoethanosulfonic acid), because methanogenesis competes with the desired reaction. (Comment from the author: This is an example of the old paradigm thinking which was prevalent at the time of publication of this chapter. Later in this thesis we find that hydrogenotrophic methanogenesis *can* occur simultaneously with chain elongation under the right bioreactor conditions, and we hypothesize that it may even be desirable. [CHAPTER 5])

Further chain elongation reactions can also occur, ultimately converting acetate to n-caproate (C6) (Figure 2.1g) and even n-caprylate (C8). n-Caproate concentrations of 8.27 g/l and n-caprylate concentrations of 0.32 g/l have been observed when acetate and hydrogen (or ethanol) are provided to undefined mixed cultures [Steinbusch, 2010].

These concentrations approach the solubility limits for these carboxylates (n-caproate: 10.19 g/L; n-caprylate: 0.79 g/L). The rate of n-caproate formation is promising (0.49 g/L/day) at neutral pH [Steinbusch, 2010]. Both of these compounds have excellent energy densities, may be relatively easy to separate from the fermentation broth, and both can be precursors for production of biodiesel and fuel alkanes by chemical post-processing reactions (Figure 2.2) [Gaertner et al., 2009]. These chain-elongation reactions proceed most effectively when ethanol is available as the reducing agent and when reduction of acetate to ethanol occurs at a relatively slow rate; however, it may be necessary to add a separate stream of ethanol to economically produce n-caproate and n-caprylate. This ethanol may have to come from the sugar platform in the biorefinery concept because of the cumbersome production and extraction of ethanol from undefined mixed cultures. An in-depth economic analysis is needed to investigate if the higher energy density of a fuel derived from medium-chain carboxylates and the superior separation characteristics warrant the use of ethanol in an integrated biorefinery.

2.3 Propionate and lactate

Propionate

Propionate is one of the reduced products of primary fermentation at elevated levels of hydrogen (Figure 2.1). Under anaerobic conditions, propionate can only be oxidized when the hydrogen partial pressure is extremely low (Box 2.1; Table I). Microbial production of propionate from industrial waste has been studied primarily with pure cultures and has been plagued by microbial toxicity of the accumulating undissociated propionic acid at low pH values [Colomban et al., 1993]. To circumvent propionate

accumulation, *in-situ* extraction provides some improvement over traditional fermentation, but the short chain length of propionate makes it relatively difficult to extract [Ozadali et al., 1996].

Undefined mixed cultures can reduce propionate to propanol (Figure 2.1e). Relatively high rates of propionate reduction to propanol (0.49 g l^{-1} day^{-1}) have been observed in a continuous-flow bioreactor when propionate and ethanol are provided (Figure 2.1e) [Smith and McCarty, 1989], even though the calculated free energy of the coupled reaction is below the expected threshold value (Table 2.1; Box 2.1). Others have shown propionate-to-propanol reduction in the absence of ethanol oxidation at elevated hydrogen partial pressure, but the rates are lower (0.03 g l^{-1} day^{-1}), even though the calculated free energy change is sufficient (Box 2.1) [Steinbusch et al., 2008]. The preference for ethanol as a reducing agent might be attributed to the availability of a simple mechanism for energy conservation during ethanol oxidation.

Biological chain elongation can be used to convert propionate into n-valerate (i.e. addition of two carbon atoms) [Ding et al., 2010; Smith and McCarty, 1989]. The process is similar to that described for elongation of the acetate carbon chain (C2), except that uneven chain-length carboxylates, such as n-valerate (C5) and n-heptanoate (C7), are produced. n-Butyrate (C4) and n-caproate (C6) are also produced in this process because ethanol is oxidized to acetate – which can start the even-chain carboxylate elongation process – to provide energy for microbial growth (Table 2.1).

Lactate

Lactate fermentation (Figure 2.1) dominates primary fermentation in undefined mixed cultures when high concentrations of easily degradable substrate are available, because

the lactate pathway enables rapid disposal of reducing equivalents [Russell and Hino, 1985]. This phenomenon of lactate accumulation occurs in the rumen with diets high in grain [Owens et al., 1998] and in fermentation processes used to preserve plant material, such as in silage and sauerkraut fermentation [Stiles, 1996]. In fact, bio-energy crops, such as maize, are sometimes ensiled as a pretreatment and storage step before anaerobic digestion at full-scale installations (primary and secondary fermentations in different processes). To our knowledge, mixed cultures have not been used specifically to produce useful quantities of pure lactate, but pure cultures have been used to produce lactate in an optically pure (only D- or L-isomer) form [John et al., 2007] aided by *in situ* lactate extraction [Tong et al., 1998].

Lactate can be oxidized and reduced by secondary fermentation reactions to other carboxylates with undefined mixed cultures, such as in the gut [Belenguer et al., 2007]. For example, lactate oxidation to n-butyrate (Figure 2.1i) is catalyzed by *Clostridium acetobutylicum* [Diez-Gonzalez et al., 1995]. However, this reaction must be coupled to acetate reduction to become energetically feasible (Table 2.1), effectively converting both acetate and lactate to n-butyrate. Another secondary fermentation pathway is lactate reduction to propionate (Figure 2.1j), which is catalyzed by *Selenomonas ruminantium* [Chen and Wolin, 1977]. In this pathway, energy is conserved as ATP during acetate production while it is coupled to lactate reduction (Table 2.1), resulting in the conversion of three molecules of lactate into one molecule of acetate and two molecules of propionate. The former pathway to convert lactate into n-butyrate may actually add more value than the latter pathway, because chemicals with a higher carbon chain are generally energetically superior and easier to separate.

2.4 n-Butyrate

n-Butyrate is usually a product in undefined-mixed-culture acidogenic systems, from both primary and secondary fermentation pathways. It has often been found to be the most important side product during biological hydrogen production with dark fermentation [Zhang et al., 2003]. Similar to propionate and lactate, n-butyrate production with undefined mixed cultures has been largely ignored. Problems with bacterial production with pure cultures include low yields owing to product toxicity at lower pH levels and product streams contaminated with co-products, such as acetate and propionate [Zigová and Šturdík, 2000]. Because of a longer carbon chain for n-butyrate compared with acetate and propionate, the extraction of n-butyrate might become feasible in the future, especially by using ionic liquids [Li et al., 2002; Marták and Schlosser, 2008]. Pure culture fermentation studies have already reported improved n-butyrate yields and product purity with *in-situ* liquid/liquid extraction, and this technology should considerably improve the prospects of producing n-butyrate with undefined mixed cultures [Wu and Yang, 2003].

n-Butyrate is an excellent feedstock for the production of n-butanol with pure cultures of *Clostridium* sp., using organic electron donors (Figure 2.2) [Tashiro et al., 2004]. Therefore, we have proposed coupling n-butyrate production by an undefined mixed culture with a pure culture bioprocess that would reduce n-butyrate to n-butanol (sugars are necessary for reducing equivalents) [Angenent and Wrenn, 2008]. Recently, the feasibility of reducing n-butyrate to n-butanol with an undefined mixed culture has been demonstrated by using high partial pressures of H_2 (Figure 2.1e), although this biological

reduction is slow. Others have also found chain elongation of n-butyrate with undefined mixed cultures [Ding et al., 2010; Segers et al., 1981; Smith and McCarty, 1989; Smith and McCarty, 1989]; but, to our knowledge, never by feeding a separate stream of n-butyrate.

2.5 Mixed carboxylates

Rather than optimizing the production and separation of a single carboxylate as a bulk feedstock, researchers have developed systems for which the product spectrum is mixed and variable. In some cases, the carboxylate products are converted into a blend of liquid fuels and organic chemicals by chemical post-processing (Figure 2.2). For example, one system has converted wastes into carboxylates using an undefined mixed culture, followed by electrochemical conversion into either esters (Figure 2.2) or a mixture of alkanes and alcohols [Levy et al., 1981]. The authors proposed using liquid/liquid extraction to remove and concentrate the carboxylates before post-processing. Another system, the MixAlco process, has been tested for many different feedstocks [Holtzapple et al., 1999]. For example, fermentation studies with pretreated municipal solid waste and sugarcane bagasse as substrate have achieved up to 69% and 60% degradation of volatile solids with maximum total carboxylate concentrations of 20.5 g/L and 18.7 g/L, respectively [Chan and Holtzapple, 2003; Thanakoses et al., 2003]. The MixAlco system concentrates the carboxylates by drying and calcium precipitation. The carboxylate mixture is thermally decomposed to ketones, and the ketones are catalytically hydrogenated to a mixture of alcohols (Figure 2.2).

2.6 Outlook

The volume of organic waste will drastically rise when crude lignocellulosic or algal biomass is converted to liquid biofuels in biorefineries using the sugar and syngas platforms. Integration of the carboxylate platform into the biorefinery concept would increase bioproduct formation and recover nutrients and water that can be recycled within the biorefinery, thereby serving as a crucial component of biorefineries. Anaerobic digestion is the only bioprocess within the carboxylate platform that is currently utilized for complex waste treatment on a large scale because production of liquid chemicals presents important scientific and technical challenges that production of gaseous methane does not. Three major barriers must be overcome: (i) the separation barrier (efficient separation of carboxylates from fermentation broth); (ii) the methanogen barrier (economic inhibition of hydrogenotropic methanogens); and (iii) the ecology barrier, (directing the microbial process to generate the target carboxylates at sufficient rates).

Two promising research directions are being pursued to overcome the separation barrier. First, lab-scale bioelectrochemical systems have used ion-exchange membranes to separate production of organic chemicals at cathodes from anaerobic microbial processes that occur at anodes [Nevin et al., 2010; Steinbusch et al., 2010]. Second, medium-chain carboxylates, such as n-caproate and n-caprylate, have been produced by undefined mixed cultures at promising rates [Steinbusch et al., 2011]. For the first time, this would allow undefined mixed cultures to produce liquid chemicals with an energetic value that is equivalent to n-butanol and with chemical characteristics that ensure superior extraction.

These developments provide incentives to seriously address the methanogen barrier.

The n-caproate and n-caprylate experiments described in this review were all performed by adding bromoethane sulfonic acid [Steinbusch et al., 2009; Steinbusch et al., 2011], which is too expensive for use at a large scale. If a cheaper chemical that selectively inhibits methanogens cannot be developed, two alternative methods must be pursued: periodic heat shock, or low pH (~5.5). The former might be possible when enough waste heat is available in the biorefinery to perform this periodic activity to enrich for spore-forming bacteria while inhibiting methanogens. The latter might be especially effective at a combination of low pH and high concentrations of carboxylic acids, owing to a relatively high abundance of the inhibiting undissociated form. These methods could be aided by managing trace elements carefully; for example, cobalt is not available in corn-derived waste, and its continued absence severely limits methanogenic activity [Agler, et al., 2008].

We must realize, however, that these methods, such as the slightly acidic conditions (pH ~5.5), might be incompatible with the conditions needed to overcome the ecology barrier. Microbial ecology cannot be uncoupled from thermodynamic considerations, and this interplay is important to predict and manage the behavior of complex communities. The environmental conditions, in turn, determine which reactions are thermodynamically feasible and which microbes are selected [Hanselmann, 1991]. Indeed, the relative product composition of sugar-fed acidogenic bioreactors with high hydrogen partial pressures has been affected by environmental conditions [Ren et al., 1997; Segers et al., 1981; Zoetemeyer et al., 1982]. In a full-scale system, several environmental conditions will be varying constantly owing to the complexity and variability of organic wastes. It is, therefore, important to perform experiments to predict which environmental conditions

have the largest effects on community composition. A combined approach of high-throughput metagenomics and massive environmental data monitoring is necessary to find correlations between environment and community [Werner et al., 2011b]. In addition, ecological principles such as parallel metabolic pathway richness [Hashsham et al., 2000], community evenness [Wittebolle et al., 2009], and resistance, resilience, or redundancy [Allison and Martiny, 2008] can aid in selecting for superior communities that can sustain a stable bioprocess. Based on all this knowledge, the engineer must make decisions on how to design, inoculate and operate the full-scale system to obtain the sufficient kinetic rates and yields for a viable bioproduct. We realize, however, that some breakthroughs, such as better separation technologies, still need to be made before success can be achieved.

2.7 Acknowledgements

The work for this review was supported by the USDA through the National Institutes of Food and Agriculture (NIFA), grant number 2007-35504-05381.

Box 2.1. Predicting reaction occurrence

The food web of the undefined mixed culture is made up of a network of reactions in which microorganisms convert one or more substrates (S_1) into products (P_1) (Figure I). Modeling of the sequence of reactions that will occur for a specific set of operating conditions might help engineers optimize the product spectrum. In any biological system, there are two prerequisites for a reaction to proceed in space and time: (i) a catalyst is present to drive the reaction; (ii) the reaction is thermodynamically favorable. The microorganisms in the undefined mixed culture are the catalysts (i.e. their enzymes) that decrease the activation energy (E_a) of the transition state, resulting in increased kinetic rate constants (Eqn 1) and reaction rates (Eqn 2) (Figure I). The second requirement dictates that the available free energy of reaction, which is a function of the temperature, pressure, and substrate and product activities (Eqn 3), is below an energetic threshold (ΔG_{thr}). Thus, if the required microorganism is available in a culture, the environmental conditions (e.g. pH, temperature, pressure) must be maintained to favor the reaction of interest ($\Delta G_r < \Delta G_{thr}$).

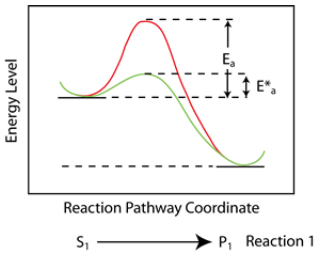

$k = k_o \cdot e^{-E_a/RT}$ Eqn 1

$r = k \cdot [S_1]$ Eqn 2

$\Delta G_r = \Delta G^o_r + RT \ln \frac{[P_1]}{[S_1]}$ Eqn 3

ΔG^o_r is a function of environmental conditions such as pH, temperature (T), pressure

[ ] denotes solute concentration, which is often used in practice in place of activity

Figure I. Reaction coordinate diagram and equations to calculate reaction kinetics and thermodynamics. The presence of microbial catalysts decreases the activation energy E_a to E^*_a so that the rate of reaction is increased with increasing rate constants (Eqns 1 and 2). Environmental conditions, microbial biochemistry, and substrate (S_1) and product (P_1) activities affect the thermodynamic feasibility of a reaction (Eqn 3).

Table I. Thermodynamic considerations for secondary oxidation reactions

Microbes	Carboxylate oxidation reactions	$\Delta G_r^{o'}$ (kJ/mol at 37°C)[a]	$\Delta G_r^{o'}$ (kJ/mol at 55°C)[a]
Syntrophospora bryantii	$acetate^- + H^+ + 2H_2O \rightarrow 4H_2 + 2\ CO_2$	86.96	74.56
or	$propionate^- + 2H_2O \rightarrow acetate^- + CO_2 + 3H_2$	68.53	60.74
Syntrophomonas wolfei	$n\text{-butyrate}^- + 2H_2O \rightarrow 2\ acetate^- + H^+ + 2H_2$	47.55	44.07

[a]All $\Delta G_r^{o'}$ values are calculated considering all reactants and products to be in the aqueous phase except for H_2, CO_2, and CH_4, which are gaseous at 1 atm. $\Delta G_r^{o'}$ values are at biological standard state (pH = 6.82 at 37°C and 6.58 at 55°C). $\Delta G_r^{o'}$ quantities were calculated from ΔG_f^o values from Ref. [Amend and Shock, 2001].

The energetic threshold is the amount of energy that must be conserved in a reaction pathway. Here, we show an example of how this threshold was calculated for the specific oxidation reaction of n-butyrate to acetate. In this reaction, 1 ATP is produced by substrate-level phosphorylation; however, up to 2/3 ATP is reinvested in a proton gradient with a combined $\Delta G_{thr} \approx$ -23.3 kJ/mol [Schink, 1997]. For many reactions throughout our review where the biochemistry has been poorly defined, we have used this ΔG_{thr} value as a conservative approximation. Note that in the text we have used the free energy nomenclature for standard biological conditions ($\Delta G_r^{0'}$) to compare ΔG_{thr} to free energy numbers of specific reactions in Table 1. Research has shown, however, that certain reactions (including n-butyrate oxidation) have occurred when ΔG_r was above -10 kJ/mol (Table I). Indeed, modelers have been able to explain biological metabolic activity under these conditions ($\Delta G_r > \Delta G_{thr}$) by allowing the energy required to produce ATP and pump protons to be variable, depending on environmental conditions [Jin, 2007; Kleerebezem and Stams, 2000]; but for such modeling efforts, a detailed knowledge of the biochemical pathways is required.

Box 2.2. Liquid/liquid extraction to separate acetate

Currently, acetate is primarily produced petrochemically or via microbial fermentations that convert yeast-derived ethanol to acetate, but it may also be possible to develop an undefined-mixed-culture process with high acetate yields. To do so, it is useful to consider two systems with a high acetate flux: a termite gut and an anaerobic digester. In both systems, a maximum acetate flux from polysaccharide breakdown (Figure 2.1a) occurs because a low hydrogen partial pressure is maintained by scavenging homoacetogens (Figure 2.1c) [Leadbetter et al., 1999; Odelson and Breznak, 1983] and hydrogenotrophic methanogens (Figure 2.1d) [Chen and Wolin, 1977]. However, accumulating the product acetate would quickly inhibit these hydrogenotrophs, resulting in rising hydrogen partial pressures and a shift towards increasingly reduced fermentation products. Anaerobic digesters can maintain a sustainably high acetate flux because acetate is converted and removed by aceticlastic methanogens (Figure 2.1f). Termites have another strategy: they take up acetate. Thus, to produce acetate at high yields, both hydrogen and acetate should be maintained at low concentrations in the mixed culture.

One possibility to remove acetate from our engineered systems is with continuous liquid/liquid extraction by using membranes (i.e. perstraction) [Ozadali et al., 1996]. This separation technology has been shown to improve carboxylate yields and selectivity for pure cultures and may hold promise for undefined mixed cultures [Tong, Y et al., 1998; Wu and Yang, 2003]. Liquid/liquid extraction of organic acids is traditionally achieved by contacting the fermentation broth with an organic solvent phase (often a substituted amine or phosphine, such as trioctylphosphine oxide, dissolved in an alkane), followed by contact of the organic phase with an aqueous alkaline phase. In this way, undissociated acids move along a pH gradient and the dissociated form of the carboxylate concentrates in the alkaline phase. Dissolution in the organic phase is particularly effective for relatively hydrophobic acids, such as n-butyrate and n-caproate (although it is much easier to separate the C6 n-caproate than the C4 n-butyrate), while shorter chain molecules, such as the C2 carboxylate acetate and the C3 carboxylate propionate, have always presented greater challenges [Li et al., 2002]. Extraction of acetate has become more feasible recently by using ionic liquids as the organic phase [McFarlane et al., 2005].

Box 2.3. Biological chain elongation

Biological chain elongation includes reversed β-oxidation of carboxylates – the addition of a two-carbon acetyl-CoA derived from ethanol, which has been described for a pure culture of *C. kluyveri* [Barker et al., 1945]. Although reversed β-oxidation of acetate with ethanol is thermodynamically feasible ($\Delta G_r^{0'}$ < -23.3 kJ/mol), it cannot gain ATP, and the oxidation of ethanol to acetate is required to conserve the necessary energy. The latter reaction has a positive free energy in acidogenic systems with high hydrogen partial pressures, and thus the ethanol oxidation and reversed β-oxidation reactions must be coupled (Table 2.1). The combined process has a sufficiently negative free energy under biological standard conditions ($\Delta G_r^{0'}$ = -194.5 kJ/mol at 1 atm and 37°C) (Table 2.1). Through this process, 5 mol ethanol and 5 mol acetate are converted to 5 mol n-butyrate for every 1 mol ethanol oxidized to acetate [Seedorf et al., 2008]. It has been known for decades that *C. kluyveri* can also generate n-caproate [Barker et al., 1945], which is a C6 carboxylate. The process is analogous to n-butyrate formation through chain elongation, and results in the same two-carbon-atom elongation, but now through reversed β-oxidation of n-butyrate with ethanol ($\Delta G_r^{0'}$ = -182.8 kJ/mol for n-butyrate at 1 atm and 37°C) (Table 2.1).

CHAPTER 3.

THERMOPHILIC ANAEROBIC DIGESTION TO INCREASE THE NET ENERGY BALANCE OF CORN GRAIN ETHANOL

Adapted from: Agler, Garcia, Lee, Schlicher, and Angenent. Environmental Science and Technology, September 2008. 42(17):6273-6279

Note: Supplementary information can be found in Appendix 1 and is denoted in this text as A1.SX, where X denotes the appendix section.

Abstract

U.S. production of fuel ethanol from corn grain has increased considerably over the last 10 years. Intense debate regarding the true environmental impact of the overall production process has been ongoing. The present study evaluated the utilization of thin stillage (a major by-product of the dry-mill corn grain-to-ethanol process) in lab-scale thermophilic anaerobic sequencing batch reactors for conversion to methane. We found that augmentation of cobalt as a growth factor to the thermophilic anaerobic digestion process is required. After reaching sustainable operating performances, the methane potential in the bioreactors was 0.254 l CH_4/g total chemical oxygen demand (TCOD) fed. Together with a reduction in the mass of solids that needs drying, methane generation translates to a 51% reduction of natural gas consumption at a conventional dry mill, which improves the net energy balance ratio from 1.26 to 1.70. At the design hydraulic retention time of 10 days, the digesters achieved TCOD, biodegradable COD, volatile solids, and total solids removal efficiencies of 90%, 75%, 89%, and 81%,

respectively. We also found that struvite precipitation occurred in the thermophilic digesters during the course of the study, resulting in possibilities for nutrient recovery.

3.1 Introduction

Current attitudes towards the environment and a political movement that desires to reduce dependence on foreign oil have bolstered liquid biofuel production in the U.S.A. In addition, restrictions on the fuel additive methyl tertiary butyl ether (MTBE) have promoted ethanol production, resulting in the virtual replacement of MTBE in the U.S.A. by a 5-10% addition of ethanol to petroleum-based fuel [Solomon et al., 2007]. Total annual U.S.A. ethanol production has increased considerably between 1997 and 2005 from ~ $5 \cdot 10^6$ to ~ $15 \cdot 10^6$ m^3, mostly from corn (*Zea mays* ssp. *mays*) grain (called kernel in the corn-to-ethanol industry) [Solomon et al., 2007]. Corn grain-to-ethanol plants based on dry grinding (i.e., dry mill) constituted to 67% of U.S.A. corn-ethanol production in 2005 with wet grinding (i.e., wet mill) making up the difference. Further growth in ethanol production is anticipated to be primarily by constructing dry mills because of the relatively lower capital costs [Belyea et al., 2006; Bothast and Schlicher, 2005].

Creating a sustainable biofuel industry requires a holistic assessment that takes into consideration numerous factors, such as deforestation, crop production methods, nonrenewable energy and water consumption, and world food supplies. Some of the environmental-based criticism of corn grain-to-ethanol has mainly focused on the small positive net energy balance that is achieved [Farrell et al., 2006; Hill et al., 2006; Solomon et al., 2007; WSTB, 2007]. For example, Hill et al. [2006] calculated through

life-cycle assessment that 26% more energy is gained from ethanol than is contained in nonrenewable fuels required for its production (i.e., a 1.26 net energy balance ratio), but that this gain is mostly due to energy credit of coproduced animal feed. They found a relatively large input of 0.60 units energy per one unit ethanol-energy output for processing the corn grain into ethanol and animal feed (or a 62.5% energy requirement for operating the processing facility out of all the energy inputs). The remaining energy requirements stem from the processing facility construction and laborer household energy use (1%), all energy requirements for farming (31.3%), and crop and biofuel transportation (5.2%) [Hill et al., 2006].

Because of the small positive net energy balance, corn grain-to-ethanol has been suggested only to be an intermediate step until more favorable technology has been scaled up [Schnoor, 2006]. Because ethanol from corn grain is a reality, the net energy balance can be improved in the immediate future by, for example, finding alternative uses for process streams (e.g., thin stillage) [Farrell et al., 2006; Rausch and Belyea, 2006]. In dry mills, thin stillage is the centrate of distillation bottoms (i.e., the residue after ethanol is distilled from "beer") and is partially recycled as fermentation broth for ethanol production or dehydrated in evaporators to produce syrup. Usually, less than a 50% recycle ratio for thin stillage as fermentation broth (called backset in the corn-to-ethanol industry) can be utilized due to solids build up and toxicity to yeast by lactic acid, acetic acid, and/or sodium [Egg et al., 1985; Ingledew, 2003; Shojaosadati et al., 1996]. Evaporation requires a large energy dedication (often from waste heat), but it enables some of the condensed water to be recycled as make-up water in the fermentation process. Syrup is added to wet distillers' grains (WDG) and flash dried (often with steam

from natural gas) to produce distillers' dried grains with solubles (DDGS), which is sold as animal feed (wet distillers' grains dried without syrup is also known as distillers' dried grains [DDG]).

Anaerobic digestion of thin stillage (called biomethanation in the corn-to-ethanol industry) may be an advantageous process step compared to evaporation and syrup drying because energy is recovered in the form of biogas, which could substantially increase the net energy balance. Anaerobic digestion of stillage from various fermentation feedstocks, such as cane molasses, beet molasses, whey, wheat, and grapes, has been previously studied with a diverse group of bioreactor types, including continuously stirred tank reactors (CSTR) and upflow anaerobic sludge blanket (UASB) reactors [Bories et al., 1988; Hutnan et al., 2003; Machado and Sant'Anna, 1987; Wilkie et al., 2000]. For thin stillage treatment from corn grain feedstock, Ganapathi [1984] used continuous-flow mesophilic (35ºC) digestion with a CSTR, but this was after complete physical removal of the solids and subsequent dilution with water. Another published study was by Schaefer et al. [2008], who studied thermophilic (55ºC) anaerobic treatment of thin stillage in semi batch-fed continuously-stirred digesters.

Due to high total chemical oxygen demand (TCOD) concentrations of ~ 100 g/l in thin stillage, cost-efficient digestion requires very high organic loading rates, and thus increased degradation kinetics, to enable reduced bioreactor volumes. Thermophilic anaerobic digestion is, therefore, advantageous compared to mesophilic anaerobic treatment of thin stillage because of higher metabolic rates [Hutnan et al., 2003; Mackie and Bryant, 1995; Wilkie et al., 2000]. In addition, fats, oils, and grease (FOG), which are common at high concentrations in thin stillage from dry mills without fractionation of

the corn grain, can accumulate in mesophilic digesters by forming a foam layer, and cause operating problems by washing out active biomass [Jeganathan et al., 2006]. This is not a problem in thermophilic digesters due to sufficient solubilization and degradation of FOG at higher temperatures [Reimann et al., 2002]. In many cases, however, due to high effluent volatile fatty acid (VFA) concentrations and increased heating costs, thermophilic digestion has been largely ignored [Lettinga, 1995; Speece et al., 2006]. Recent work by Speece et al. [2006] has removed the first limitation of high VFA concentrations by supplementing prominent trace elements to prevent inhibition of methanogenesis. It was already known that trace elements are important in the function of many methanogenic enzymes [Thauer, 1998], that they are scarce in most digester substrates [Speece, 1996], and that addition of trace elements has been credited with causing dramatic improvements in bioreactor performance [Fathepure, 1987; Murray and van den Berg, 1981], but it seems even more imperative for thermophilic digestion [Speece et al., 2006]. The second limitation of increased heating costs is not valid for thermophilic digestion of thin stillage because the whole stillage is already hot after leaving the distillation column.

This study sought to ascertain the applicability of an integrated method of thermophilic anaerobic digestion of thin stillage from dry mill corn grain-to-ethanol plants by utilizing anaerobic sequencing batch reactors (ASBRs). By allowing biomass to settle in the ASBR before decanting effluent vs. no settling in completely-stirred digesters, the concentration of active biomass is increased and the sludge retention time (SRT) is elongated compared to the hydraulic retention time (HRT), to pursue higher volumetric degradation rates (high-rate vs. low-rate digestion). We will also discuss

whether thermophilic digestion with high-rate systems is a better use of thin stillage than evaporation and syrup drying to produce animal feed. From preliminary calculations, we have estimated a substantial increase in the net energy balance ratio when thin stillage is treated with thermophilic anaerobic digestion.

3.2 Methods

Experimental Setup and Operation

The experimental setup of replicates bioreactor 1 (R1) and bioreactor 2 (R2) is given in the supporting information (A1.S1 and Figure A1.S1). Each of the bioreactors was inoculated by adding 1.7 l of thermophilic anaerobic sludge from an anaerobic digester treating a mixture of primary and waste activated sludge at a municipal wastewater treatment plant (Western Lake Superior Sanitary District, Duluth, MN) to 3.3 l of de-ionized water. After inoculation, 10 l of natural gas was bubbled through each bioreactor to ensure anaerobic conditions after which the digesters were allowed 24 h to acclimate before feeding commenced. Thin stillage samples were received periodically from the National Corn-to-Ethanol Research Center in Edwardsville, IL, which is a demonstration-scale dry mill (~ 1/200 the size of a full-scale plant), and were stored at -20^{o}C in 1-l bottles until a day before feeding. Five different thin stillage samples were received from the dry mill and fed consecutively (F1-5); each had somewhat different characteristics and each was fed for different periods of time (Table 3.1). From day 78 to day 106 of the operating period, 5 mL of a modified trace element solution according to Zehnder et al. [1980] (Table 3.2) and Angenent et al. [2002] was added weekly to R1. To R2, we added a 5-mL solution of only $FeCl_3 \cdot 4H_2O$ (10 g/l) on day 85 of the operating period;

$FeCl_3 \cdot 4H_2O$ (10 g/l) and $CoCl_2 \cdot 6H_2O$ (2 g/l) on days 92 and 99; and $CoCl_2 \cdot 6H_2O$ (2 g/l) on day 106. From day 113 until the end of the operating period, a solution of $CoCl_2 \cdot 6H_2O$ (2 g/l) was added to both bioreactors at a rate of 1 ml/10 g influent TCOD once a week. All trace element solutions in this study contained EDTA (1 g/l) and HCl (1 ml concentrated HCl/l). A more detailed rationale for this augmentation is given in A1.S3.

The semi-batch ASBRs (R1 and R2) were sequenced through a 24-h cycle with an instant feeding period, a 23-h react period with intermittent mixing, a 58-min settling period (no mixing), and a 2-min decanting period (the volume of feeding and decant solution was the same). Initially, intermittent mixing of the ASBRs was every h for one min, but this was changed to every 15 min for one min on day 69 of the operating period in an attempt to circumvent accumulation of rapidly settling solids. The HRT was decreased in a stepwise manner from 40 days (with an organic loading rate of 2.42 g TCOD/l/d) to 7 days (10.71 g TCOD/l/d) on day 392 after which the HRT was maintained at an 8-day HRT (9.37 g TCOD/l/d) from days 394-417. The HRT was shortened upon achieving pseudo steady-state conditions when stable biogas production rates (within 10% of average values), total VFA concentrations, volatile solids (VS) concentrations, and pH levels were achieved and after a minimum time period of one HRT, except at the 40 and 25-day HRTs during which the bioreactors were operated for 22 and 21 days, respectively.

We estimated the methane potential and methane yield by plotting the specific volumetric methane production rates against TCOD loading rates or removal rates, respectively, and forcing a linear regression of the points through zero on the y-axis. The

specific biogas production rate was found by calculating the average biogas production rate (corrected to standard temperature and pressure) during each organic loading rate, except for two periods; the unstable period of R1 (days 284-362) and the time for both bioreactors beyond the 10-day HRT. The latter data were not included because both bioreactors were not able to handle the increase in the hydraulic pressure to an HRT of 7-8 days and/or an organic loading rate of 9.37-10.71 g TCOD/l/d. The specific volumetric methane production rate is the product of the specific biogas production rate and the average methane content of the biogas during a TCOD loading rate. Correlation of daily biogas production values were corrected for and linear regression were performed using the "AUTOREG" and "GLM" procedures, respectively, in SAS software, version 9.1 (SAS Institute Inc., Cary, NC, USA).

Physical and Chemical Analysis

All periodic analyses for evaluating digester performance were performed according to *Standard Methods* [Clesceri et al., 1998], unless otherwise indicated. Daily measurements included pH, biogas production, and room temperature and ambient pressure (to correct biogas production to standard conditions). Total VFA (distillation method), total solids (TS), VS, TCOD, soluble chemical oxygen demand (SCOD) (closed-reflux titrimetric method), and total ammonium (i.e., free ammonia and ammonium) concentration (electrode model Orion 9512, Thermo Electron Corporation, Beverly, MA) analysis were performed at least weekly. FOG and sludge volume index (SVI) measurements were also performed periodically. Methane concentration in the biogas was measured bi-weekly with a gas chromatograph (Series 350, Gow-Mac Instrument Co., Bethlehem, PA) with a thermal conductivity detector. The GC column

was a 4’ x 1/8” o.d. 20% DC-200 on Chromosorb P AW-DMCS, 80/100 mesh (Varian, Inc., Palo Alto, CA). The temperatures for injection port, detection, and column were 50^{o}C, 115^{o}C, and 25^{o}C, respectively. Elemental analysis of influent and effluent was performed with an inductively coupled plasma mass spectrometer (ICP-MS) (Model 7500 ICP-MS ChemStation, Agilent, Santa Clara, CA) equipped with an SP-5 autosampler. Precipitate analysis was performed with a scanning electron microscope (SEM) with a 15-kV accelerating voltage (Model S-4500, Hitachi High-Technologies America, Schaumburg, IL) equipped with an energy dispersive x-ray spectroscopy (EDX) microanalysis system (Noran, Madison, WI). Further analysis on the precipitate was done by x-ray powder diffraction using Cu Kα radiation (Geigerflex D-MAX/A, Rigaku, The Woodlands, TX). Software by Materials Data, Inc. (Livermore, CA) was used to control the diffractometer. Soluble protein concentration was measured in the influent and effluent using the colorimetric BCA Protein Assay kit (Pierce Biotechnology, Rockford, IL). Total protein was measured by the same method, but prior to analysis the sample was heated in 0.1M NaOH for 10 min at 90^{o}C, centrifuged at 9,300 x g for 20 min after which the supernatant was analysed. Colorimetric analysis was done using an end point reading in a 96-well plate at 562 nm and ambient temperatures (SPM Synergy HT, Bio-Tek, Winooski, VT). The method for calculating the nitrogen mass balance and measuring the N composition of the precipitate is included in A1.S2.

3.3 Results

Thin Stillage Characteristics

We measured the COD and solids concentrations for seven different thin stillage samples, five from a demonstration-scale dry mill (F1-5 used as substrate in this study), and two from different full-scale corn grain-to-ethanol dry mills. In addition, we showed published data from one full-scale dry mill (Table 3.1). The average TCOD concentrations for the F1-5 samples were from 74-97 g/l, while they were 96-182 g/l for thin stillage from the three different full-scale plants (Table 3.1). The SCOD accounted for 36-53% of the TCOD in the feed substrate from the National Corn to Ethanol Research Center, which was in the same range compared to thin stillage from the full-scale plants (39, 54, and 53-63%). The VS concentration in the substrate batches was lower than those from the full-scale plants (32 to 45 g VS/l compared to 59-84, 84 and 94 g VS/l) (Table 3.1), and VS contributed 87-92% and 90-92% to the TS in the substrate and the thin stillage from full-scale plants, respectively.

Table 3.1. Characteristics of five thin stillage samples used as substrate for this study (F1-5), two thin stillage samples from different full-scale dry mill corn grain-to-ethanol facilities (Plant 1 and 2), and average values for weekly-sampled thin stillage batches during three different HRT periods for the full-scale MGP plant (no statistical data reported). Standard deviations are given for the variations in averages with n being the number of measurements for the F1-5 samples.

Thin Stillage Sample [days fed]	SCOD (g/l)	TCOD (g/l)	VS (g/l)	TS (g/l)
F1 [0-106, 219-238]	39±10, n=14	97±19, n=12	37.29±3.08, n=6	42.09±3.14, n=6
F2 [107-163]	35±6, n=6	97±29, n=6	45.17±4.30, n=3	49.93±3.91, n=3
F3 [164-218]	36.5±11, n=7	77.5±5.5, n=5	37.11±0.44, n=5	41.87±0.46, n=5
F4 [239-295]	39±4, n=7	73.5±13, n=8	31.55±0.57, n=3	36.01±0.56, n=3
F5 [295-416]	33.5±2, n=14	75±12, n=13	31.85±1.51, n=4	36.63±1.60, n=4
Plant 1	71±12.5, n=5	182±4, n=4	93.76±1.05, n=3	104.30±0.93, n=3
Plant 2	66±3, n=5	123±7, n=5	84.44±1.04, n=3	92.82±1.04, n=3
MGP plant, ave for 30-day HRT*	59	97.1	61.9	68.9
MGP plant, ave for 20-day HRT*	76	121	83.5	90.3
MGP plant, ave for 15-day HRT*	51	96.1	59.1	65.9

* From the Midwest Grain Processors (MGP) ethanol plant, Lakota, IA [Schaefer and Sung, 2008].

Differences in COD and solids concentrations can be accounted for by varying operating conditions in the dry mill. For example, the solids concentrations from the demonstration-scale facility were lower compared to the full-scale facilities due to a relatively larger capacity of the centrifuge at the demonstration facility compared to a full-scale facility. Elemental analysis of one of the feed substrates (F5) showed that cobalt was not present in detectable concentrations (Table 3.2). In addition, magnesium, phosphorus, and potassium were all present in relatively high concentrations of $3.70 \cdot 10^2$, $4.14 \cdot 10^3$, and $5.56 \cdot 10^3$ mg/l, respectively, while manganese, iron, nickel, copper, and zinc were detected at lower concentrations (Table 3.2). FOG levels were 3.81 and 2.05 g/l in F4 and F5, respectively. The influent total ammonium concentration remained below 30 mg NH_4^+-N/l over the course of the study, and the total protein concentration in F5 was $7.2 \cdot 10^3$ mg/l (SE = 41.7 mg/l, n = 3). pH values of the thin stillage varied from 3.46 to 4.35.

Table 3.2. Elemental analysis of thin stillage (F5), R1 and R2 effluent samples, syrup, and trace element solution.

Element	F5 (mg/l)	R1 effluent (mg/l)	R2 effluent (mg/l)	Belyea et. al * (mg/kg dry basis)	Zehnder et. al ** (mg/l)
Mg	$3.70 \cdot 10^{2}$	$1.66 \cdot 10^{1}$	$1.40 \cdot 10^{1}$	6870±437	-
P	$4.14 \cdot 10^{3}$	$3.37 \cdot 10^{2}$	$3.53 \cdot 10^{2}$	15200±1280	-
K	$5.56 \cdot 10^{3}$	ND	$5.43 \cdot 10^{3}$	23200±1340	-
Mn	1.17	<DL	<DL	29.2±6.30	$1.39 \cdot 10^{2}$
Fe	$6.61 \cdot 10^{-1}$	$5.78 \cdot 10^{-1}$	$6.58 \cdot 10^{-1}$	138±33.3	$2.38 \cdot 10^{3}$
Co	<DL	2.71	2.77	<DL	$4.95 \cdot 10^{2}$
Ni	$1.25 \cdot 10^{-1}$	$9.60 \cdot 10^{-2}$	$1.00 \cdot 10^{-1}$	4.9±0.90	$3.51 \cdot 10^{1}$
Cu	$1.95 \cdot 10^{-1}$	$2.16 \cdot 10^{-1}$	$2.42 \cdot 10^{-1}$	6.3±3.30	$1.42 \cdot 10^{1}$
Zn	6.24	$6.35 \cdot 10^{-1}$	$8.8 \cdot 10^{-1}$	126±21.5	$2.40 \cdot 10^{1}$
Na	ND	ND	ND	2360±305	$1.63 \cdot 10^{1}$
Al	ND	ND	ND	10.8±1.10	$1.01 \cdot 10^{1}$
Mo	ND	ND	ND	0.8±0.02	$2.64 \cdot 10^{1}$
Sr	ND	ND	ND	2.6±3.40	-

* Values given are for syrup (product of evaporation of thin stillage) [Belyea et al., 2006]
** Trace Element Solution [Zehnder et al., 1980]
<DL = less than detection level, ND = not determined.

Bioreactor Operation and Performance

R1 and R2 were operated similarly over the operating period with step-wise increases in the organic loading rates except during unstable periods due to trace element limitations in both bioreactors (days 70-106 of the operating period: A1.S3) and an accidental oxygen influx in R1 (days 284-362: A1.S.4). In addition, the five changes in the feed batch were implemented simultaneously for both bioreactors on days 107, 164, 219, 239, and 295 (Table 3.1), which resulted in changing organic loading rates within periods of similar HRTs. Therefore, the performances for R1 and R2 were similar with analogous trends of volumetric biogas production rates following step-wise increases in organic loading rates over the operating time or changing organic loading rates within HRT periods during times of stable performances with low total VFA concentrations

(Figures 3.1A and 3.1B). This is reflected in statistically (95% confidence interval) similar methane potentials and methane yields for both bioreactors (0.253 and 0.254 l CH_4/g TCOD fed; and 0.278 and 0.284 l CH_4/g TCOD removed, for R1 and R2, respectively, with R^2 values of 0.99). A methane potential of 0.254 l CH_4/g TCOD fed, which was estimated from the combined data of both bioreactors, is used subsequently in this paper (Figure A1.S2). The methane concentrations in the biogas of both bioreactors were also similar and were on average 59.6% (SE = 5.1%, n=30) and 59.7% (SE = 5.3%, n=36) for R1 and R2, respectively.

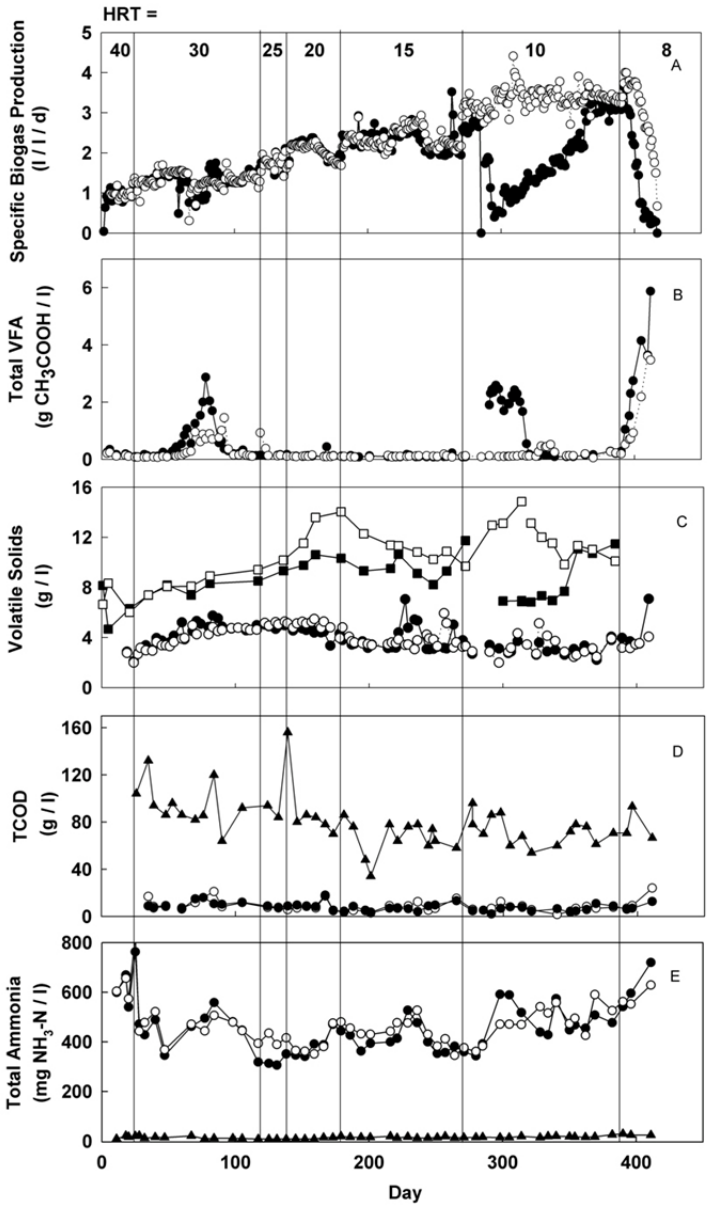

Figure 3.1. Bioreactor operating conditions and performance for R1 and R2: A. Volumetric biogas production rate over the operating period; B. Effluent volatile fatty acid concentration over the operating period; C. Volatile solids concentration over the operating period; D. Influent and effluent chemical oxygen demand over the operating period; and E. Total ammonium concentrations over the operating period (▲ – F1-5 (substrate); ● – R1; ○ – R2; ■ – R1 Biomass; □ – R2 Biomass). Vertical lines indicate periods with different HRTs.

The solids and COD removal efficiencies were determined for each HRT period (Figures 3.1C and 3.1D). The 10-day HRT is the design HRT for this study because a stable performance was found for an extended period of operating time at this hydraulic loading. At the HRT of 10 days and an organic loading rate of 7.5 g TCOD/l/d, the removal efficiencies for R1 and R2 were similar, but because more data for R2 is available compared to R1 (10 HRT periods of stable performance vs. 3 HRT periods) we report the information from R2 here (data for R1 in A1.S4). The mean TCOD removal efficiency for R2 measured (effluent vs. influent) at the 10-day HRT was 92.2%, which included removal due to methane generation and biomass accumulation in the high-rate bioreactor (biomass was wasted naturally with the effluent, but this occurred periodically and not during the COD measurements at a 10-day HRT). The relative TCOD removal efficiency due to methane formation not including biomass accumulation was 81.1%. This efficiency was calculated from the ratio of the methane yield (0.284 l CH_4/g TCOD removed) to the maximum methane yield (0.350 l CH_4/g TCOD removed). By multiplying the measured and methane formation TCOD removal efficiencies, we estimated the efficiency due to biodegradation to be 74.7% at a 10-day HRT. The biodegradation of VS resulted in a measured 80.3% removal efficiency of TS since VS accounted for 88% of TS in thin stillage. The SCOD removal efficiency based on the TCOD concentration of the influent and the SCOD concentration of the effluent was 95.8% (Table A1.S1). Despite the shorter HRT of 10 days at the end of the operating time compared to the longer HRT of 40 and 30 days at the beginning of the operating period, the TCOD, VS, and TS removal efficiencies were higher (Table A1.S1) because of significantly lower effluent TCOD ($\alpha = 0.01$), VS ($\alpha = 0.01$), and TS ($\alpha = 0.05$)

concentrations. This was due to the better settleability of the biomass, which may have resulted in longer SRTs at the end of the operating period compared to the beginning of the operating period. Biomass characteristics of the bioreactor contents and effluent throughout the operating period are shown in Figure 3.1C (volatile solids) and described in A1.S5 and Figures A1.S3 and A1.S4.

Nutrient and Element Removal

The total ammonium concentration in the effluent was stable through the end of the 10-day HRT with average concentrations of 450 mg NH_4^+-N/l (SE=96.2, n=49) and 467 mg NH_4^+-N/l (SE=88.0, n = 49) for R1 and R2, respectively (Figure 3.1E). The resulting high alkalinity levels in the effluent varied with feed and loading rate, but remained between 2,000 and 3,000 mg/l as $CaCO_3$ through the 10-day HRT (data not shown). As a result, the pH values of the bioreactor contents were stable without any addition of alkalinity or acid (except after accidental oxygen influx) even during the initial start-up period (Figure A1.S5). The nitrogen balance during the 10-day HRT operating condition (see details in A1.S2) shows that the increase in total ammonium concentration in the effluent compared to the influent was due to protein degradation. It also shows an approximately equal concentration of total nitrogen in the influent and the effluent with concentrations of 1180, 1180, and 1190 mg/l N for the influent, R1 effluent, and R2 effluent, respectively. ICP-MS analysis on R1 and R2 effluent during the 10-day HRT period showed a 96% magnesium removal in both bioreactors when compared to influent levels (Table 3.2), and 92% and 91% phosphorus removals in R1 and R2, respectively.

Over the operating period, a ~ 10-cm layer of white precipitate accumulated in the bottom cone of both bioreactors. SEM/EDX analysis showed that this precipitate

contained Mg, P, and O with 16.12% ± 0.74 and 28.93% ± 1.58 (atomic basis) for Mg and P, respectively, which explained the reduction in Mg and P levels in the effluent compared to thin stillage. SEM photographs of the crystals resembled struvite (i.e., $MgNH_4PO_4 \cdot 6H_2O$) (Figure A1.S6A), and the x-ray powder diffraction spectrum of the precipitate was similar to struvite's standard spectra although an amorphous phase peak was present (Figure A1.S6B). We found that the precipitate only contained 0.286 moles of N per mole of precipitate (an equal molar amount is anticipated for crystalline struvite). Because of the relatively low levels of N in the precipitate and a slow accumulation of struvite due to Mg limitations, we were able to close the nitrogen balance without accounting for struvite precipitation in the bioreactors.

3.4 Discussion

We operated two similar thermophilic, high-rate anaerobic bioreactors to investigate if anaerobic digestion of thin stillage is a more energetically favorable approach compared to evaporation and syrup drying, which is the conventional process in corn grain-to-ethanol dry mills. A basic schematic of the conventional process of corn grain-to-ethanol fermentation and a conceptual process with an integrated anaerobic digester is shown in Figure 3.2. We propose a system based on this study that includes thermophilic anaerobic digestion, biomass recovery, and recycling of digester effluent as make-up water. To successfully advance the process technology through this change, the net energy balance ratio must be improved considerably, while recovering nutrients, improving the quality of animal feed, and reducing water consumption.

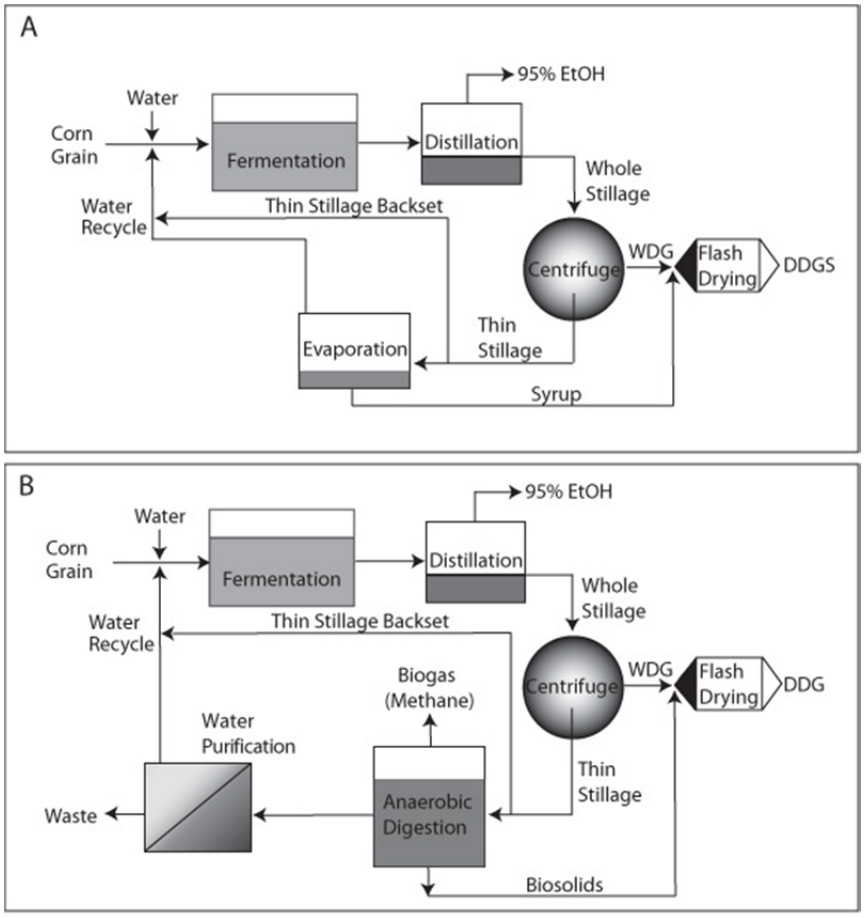

Figure 3.2. Overall process diagram of dry-mill corn grain-to-ethanol processes: A. Conventional facility; and B. Conceptual process diagram with an integrated anaerobic digester (water purification technology and purification requirements are not yet determined).

Digester Methane as an Energy Supplement

The generated methane from thin stillage digestion will partially replace nonrenewable fuels (often natural gas) as energy inputs in the ethanol production process. Using the combined methane potential from R1 and R2 of 0.254 l CH_4/g TCOD fed combined with full-scale data, we anticipate a 51% reduction in required energy input from nonrenewable fuels for a $3.8 \cdot 10^8$ l ethanol per year corn grain-to-ethanol dry mill (see details in A1.S6). This estimation included a projected reduction of 45% in the mass of produced animal feed (DDG vs. DDGS) and the resulting circumvention of flash

drying syrup (with steam from natural gas) (Table A1.S2 and Figure 3.2). Currently, approximately a third of the total energy input is recovered as waste heat and provides the energy for thin stillage evaporation. Since an integrated anaerobic digestion process would make evaporation of thin stillage redundant, the leftover heat is still available, and therefore a new application for it can be found. However, we have not included this available energy in the calculations for the anticipated 51% energy input reduction because some of this waste heat may be necessary to recover make-up water from digester effluent. Stover et al. [1984] found a higher anticipated reduction in energy input of 60% based on methane potential data from Ganapathi [1984] due to accounting for the available energy from waste heat by not having to evaporate thin stillage. If these authors had not included waste heat recovery, their anticipated energy input reduction for corn processing would have been 40%. The absence of suspended solids in the thin stillage substrate of the Ganapathi [1984] study is one contributing reason for a lower energy input reduction compared to ours. Schaefer et al. [2008] published an energy input reduction at the processing plant of 43% based on their methane potential with low-rate thermophilic anaerobic digestion of thin stillage without any correction for the considerable lower mass of produced animal feed. We also estimated a 43% energy input reduction from our data when we did not account for a lower mass of DDG vs. DDGS, however, this is an over simplification, and animal feed quantity reductions should be included in the calculations.

To our knowledge, this is the first report on thin stillage digestion with a high-rate anaerobic digester system. We obtained a shorter design HRT of 10 days and a higher organic loading rate of 7.50 g TCOD/l/d with prolonged stable performance compared to

Schaefer et al. [2008], who were able to achieve stable operating conditions at a 20-day HRT and an organic loading rate of 6.1 g TCOD/l/d with thermophilic low-rate digesters. The shorter HRT will directly result in smaller bioreactor volumes, and thus reduced construction costs. Therefore, we anticipate that high-rate anaerobic digestion will be preferential to low-rate digestion and that other high-rate bioreactor configurations should be evaluated.

Nutrient Recovery

For a practical corn-to-ethanol industry, nutrient recovery for plant growth, yeast fermentation, and animal growth is critical. Direct recycle of up to 50% of thin stillage to the ethanol fermenters [Egg et al., 1985; Shojaosadati et al., 1996] will provide nutrients, such as phosphorus (4,140 mg/l, Table 3.2), for yeast metabolism. Subsequently, an integrated anaerobic digestion technology can aid in nutrient recovery because nutrient species are not oxidized and lost to the atmosphere from the process and remain in a closed nutrient cycle, while they are liberated from the VS matrix. Indeed, we were able to obtain a closed nitrogen balance for both bioreactors during formation of total ammonium from protein degradation. Magnesium, phosphorus, and relatively minor amounts of nitrogen were removed from the digester solution by the generation of struvite, which was a mixture of crystalline and amorphous phases, and precipitated out to accumulate on the bottom of the bioreactor over the operating period. Our results with x-ray powder diffraction were similar to the identification of struvite by Wang et al. [2005], including an amorphous region. A close to complete removal of the incoming magnesium was obtained, indicating magnesium to be the limiting species for struvite formation. The precipitated struvite must be removed from a full-scale digester to

prevent any operating problems, but it can be used as a slow-release fertilizer for plant growth [Bridger et al., 1962].

Animal Feed Improvement

In the conventional processing scheme of dry mills (Figure 3.2A), thin stillage is evaporated to syrup, added to wet distiller's grains (WDG), and flash dried to produce distiller's dried grains with solubles (DDGS), which is used as animal feed. After integrating anaerobic digesters in the dry-mill plant, syrup will no longer be added to WDG (Figure 3.2B), leaving only distiller's dried grains (DDG) as a higher value animal feed because of increased protein concentrations due to a relatively lower concentration of salts. Long-term effects on animals fed with DDGS may be of concern due to high concentrations of certain elements that stem from syrup (e.g., potassium has a laxative effect and is present at levels of 1.5% in syrup [Table 3.2]) [Rausch and Belyea, 2006; Wilkie et al., 2000]. Our ICP-MS analysis confirmed high levels of both potassium and phosphorus in thin stillage samples (Table 3.2). By degrading VS from thin stillage in anaerobic digesters, a considerably lower quantity of animal feed (DDG) will be produced albeit at a higher relative protein content. As mentioned above, we anticipate this reduction to be 45% of the total mass of animal feed based on the dry weight of WDG and syrup per quantity of corn grain (Table A1.S2). Currently, animal feed is an important product to ensure economic viability of corn grain ethanol, especially since demand has recently outpaced the increase in supply mostly due to recent growth in exports [*USDA*, 2008]. Thus, for anaerobic digestion of thin stillage to be economical, the increased value of a higher quality feed plus the savings due to reduced natural gas consumption must be higher than reduced revenue due to the loss in feed quantity.

Cobalt Augmentation

We discovered that augmentation of the trace element cobalt is necessary for successful long-term anaerobic digestion of thin stillage under thermophilic conditions (A1.S3). Cobalt is an important factor in enzymatic catalysis of methyl group transfer in methanogenesis [Fathepure, 1987; Murray and van den Berg, 1981; Thauer, 1998]. We found cobalt levels to be below detection in thin stillage because cobalt is not added as a trace element during yeast fermentation in corn-to-ethanol plants. This is in agreement with Belyea et al. [2006], who found that syrup (evaporated thin stillage) contained below-detection levels of cobalt (Table 3.2). Augmenting cobalt will add cost (~ $0.4 – $1.20/1,000 kg TCOD), which must be taken into consideration during a full life cycle and economic assessment of the integrated digester system. Codigestion of thin stillage with animal manure would also supplement enough cobalt to sustain long-term anaerobic digestion. For example, cow manure contains levels of cobalt of ~ 2 mg/kg (dry basis) [Capar et al., 1978]. However, codigestion of thin stillage with animal manure as an integrated technology would result in a digester effluent that is much harder to purify and recycle as make-up water for yeast fermentation. It seems, therefore, an unlikely alternative due to considerably higher water consumption rates at the dry mill.

Outlook

Based on the estimated reduction of 51% for the nonrenewable energy input to process corn grain, the energy input at the facility is anticipated to be 0.30 instead of 0.60 units per unit energy output for ethanol based on published life cycle assessment data (a 45.2% instead of a 62.5% nonrenewable energy requirement for operating the processing facility out of all the energy inputs) [Hill et al., 2006]. Such a decrease in nonrenewable

energy input per output would increase the net energy balance ratio from 1.26 to 1.70, which would make corn grain-to-ethanol a more acceptable technology as an existing intermediate step towards lignocellulosic-to-energy technology with a much higher net energy balance. Our calculation included a 45% reduction in animal feed quantity and a resulting loss in energy credit (from 0.203 to 0.112 by using the Hill et al. [2006] data) and a 45% lower mass that needs flash drying with nonrenewable energy (17% of nonrenewable fuel in a conventional dry mill goes to flash drying of animal feed [Hill et al., 2006]). However, the calculation did not include the energetic costs to physically replace the evaporator with the integrated digester system (this will be a relatively small fraction of the energy input because the percentage of energy input per unit of ethanol energy output for construction of the entire conventional dry mill is 0.2% [Hill et al., 2006]); the improved quality in animal feed (DDG vs. DDGS); nor the available waste heat from circumventing thin stillage evaporation. Since the anaerobic digester will be integrated within the dry mill, all changes will cascade through the plant, affecting water, mass, and energy balances, and to firmly establish the net energy balance ratio, an extensive life cycle and economic assessment should be performed after the changes have become apparent. Further work is necessary to establish the level of purification of recycled anaerobic digester effluent in the dry mill to prevent inhibition of yeast fermentation. Finally, we must assess a new water balance, especially since we project a considerable increase in water reuse (and thus decrease in water consumption) in part due to not releasing water to the atmosphere by circumventing syrup drying.

3.5 Acknowledgements.

This work was supported by the Illinois Department of Commerce and Economic

Opportunity (grant number: 02-20701) through a grant to the National Corn to Ethanol Research Center. We acknowledge the support of this center in providing thin stillage and thank Dr. Brian Wrenn (National Corn to Ethanol Center, Edwardsville, IL), Jelte Lanting (Biothane, Camden, NJ), and anonymous reviewers for critically evaluating the manuscript, and Elijah Thimsen (Washington University) for analysis of struvite.

CHAPTER 4.

FUNCTIONALLY PREDICTIVE MICROBIAL COMMUNITY STRUCTURE LINKS OPERATING CONDITIONS TO n-BUTYRATE PRODUCTION

Adapted from: Agler, Werner, Iten, Cotta, Dien, and Angenent. Submitted to Microbial Biotechnology, August 2011.

Note: Supplementary information can be found in Appendix 3 and is denoted in this text as A3.SX, where X denotes the appendix section.

Abstract

Corn fiber was evaluated as a lignocellulosic feedstock for n-butyrate production using the carboxylate platform. Corn fiber was pretreated by dilute-acid, dilute-alkaline, or hot-water regimes and fermented to n-butyrate using an undefined mixed cultures of microbes. During an operating period of 419 days, the maximum n-butyrate yield from corn fiber was 23% (i.e., the ratio of n-butyrate produced in chemical oxygen demand [COD] to corn fiber substrate in COD) with a maximum n-butyrate specificity of 59% (i.e., the ratio of n-butyrate produced in COD to all fermentation products in COD). Further, we observed that the bacterial community was stable and predictive - variation of 41% in phylogenetic structure among communities was predicted by the combination of n-butyrate specificity and the undissociated short-chain carboxylic acid concentration. In addition, the relative abundances of specific taxonomic groups were predictive of performance, and we used these community-based predictions to link operating

parameters to performance with statistical certainty. We found that a community structure with improved n-butyrate yield and specificity can be shaped by a decrease in short-chain carboxylic acid toxicity through product dilution and by the occurrence of beneficial secondary fermentations, such as conversion of lactate and acetate into n-butyrate. These two strategies -- product removal and secondary fermentation reactions directed toward product of interest -- may have broad applications for the carboxylate platform because they are beneficial for anaerobic production of methane and, as demonstrated here, for n-butyrate production.

4.1 Introduction

The carboxylate platform includes at least one bioprocessing step that converts biomass through hydrolysis and fermentation pathways to short-chain carboxylates (possibly as intermediate products) with undefined mixed cultures of microbes under anaerobic conditions [Agler et al., 2011]. Anaerobic digestion has been the most successful application to date of the carboxylate platform because it converts lignocellulosic feedstocks to a single end product - methane - with high yield and specificity [Kleerebezem and van Loosdrecht, 2007]. Researchers are now exploring production of carboxylates as end products (e.g., n-butyrate and n-caproate), rather than methane, to be utilized as biofuels or as replacements for petroleum in bulk industrial chemical production [Agler et al., 2011; Holtzapple et al., 1999; Steinbusch et al., 2009; Steinbusch et al., 2011]. n-Butyrate is a versatile carboxylate product that can be reduced to the biofuel n-butanol [Grethlein et al., 1991; Richter et al., 2011], incorporated into food and fragrance esters [Shu et al., 2011], and used directly as an inhibitor of microbial

growth [Butkus et al., 2011]. Abundant and low-value agricultural feedstocks, such as corn fiber (i.e., mostly pericarp [outer skin] of corn kernel), wheat straw, manure, and corn stover (i.e., mostly stalks and leaves of the corn plant), are currently used in anaerobic digestion for methane production, and therefore are good candidates for conversion to relatively higher-value carboxylates. These feedstocks are already collected with existing technology and they do not compete with human food production [Ragauskas et al., 2006]. Production of carboxylates, such as n-butyrate from agricultural waste lignocellulose, however, has not been commercialized because of important factors that contribute to low product yields (i.e., the ratio of product to substrate) and low product specificity (i.e., the ratio of product to all fermentation products).

The first important factor that specifically limits the product yield is biomass recalcitrance to microbial digestion of carbohydrate present within the plan cell wall matrix. Biomass recalcitrance can be overcome using chemical/physical pretreatments, such as dilute-acid, dilute-alkali, or hot-water strategies that improve microbial and/or enzymatic degradation rates by opening up the cell wall matrix [Hendriks and Zeeman, 2009; Mosier et al., 2005a]. Each of dilute-acid [Dien et al., 1999], dilute-alkaline [Saha and Bothast, 1999], and hot-water [Mosier et al., 2005b] strategies have been reported, specifically, to be effective for corn fiber pretreatment. Dilute-acid pretreatment hydrolyzes the hemicellulose, often to monosaccharides, thereby exposing the cellulose fibers [Noureddini and Byun, 2010]. Dilute-alkali pretreatment removes hemicellulose by extraction [Kim and Holtzapple, 2005]. Finally, hot-water pretreatment can be used instead of dilute-acid pretreatment to circumvent the need for corrosive chemicals while

the mode of action is similar although hydrolysis of solubilized hemicellulose to monosaccharides is limited [Mosier et al., 2005a].

Once biomass recalcitrance is overcome and substrate can be converted to fermentation products, accumulation of carboxylates is the second important factor that limits both product yield and product specificity. For example, carboxylic acid toxicity can directly inhibit efficient primary fermentation reactions (i.e., conversion of substrate to acetate, lactate, propionate, n-butyrate, and ethanol [Agler et al., 2011]) by inhibiting hydrolysis of particulates, such as cellulose [Russell and Wilson, 1996b]. Researchers usually maintain a low pH to promote carboxylate specificity by inhibiting the secondary fermentation pathway (i.e., conversion of primary fermentation products into end products [Agler et al., 2011]) that leads to methane [Van Kessel and Russell, 1996], but such a change in operating conditions considerably increases the toxicity of carboxylates to all community members by increasing the fraction of undissociated carboxylic acids. This toxicity, therefore, also inhibits community members that perform secondary fermentation reactions that have the potential to increase product specificity.

The third important factor that limits efficient product yields and specificity is a lack of understanding of the relationships between bioreactor operating conditions, microbial community structure, and bioreactor performance. The complex and undefined microbial communities of the carboxylate platform are difficult to control, but at the same time they provide a major advantage; the phylogenetic and functional diversity in carboxylate bioreactors allows them to be robust in response to perturbations, such as variations in operating conditions or substrates [Hashsham et al., 2000; Werner et al., 2011b]. In addition, lignocellulose feedstocks, such as corn fiber, are often rich in hemicelluloses,

and thus pentose polysaccharides. These pentoses are easily metabolized by mixed cultures, but are often problematic for pure cultures [Enari and Suihko, 1983]. To maintain these advantages and simultaneously improve product yields and specificity, we must improve our understanding of the factors controlling structure and function of the microbial community [Kleerebezem et al., 2008; Lee et al., 2009; Temudo et al., 2007]. The exact nature of the responses of community structure to environment, however, is difficult to predict. Recently, Werner et al. [2011b] linked the conditions and performance of anaerobic digesters to the structures of their bacterial communities (measured via high-throughput 16S rRNA gene surveys) using computational ecological tools, including constrained ordination and machine learning. Here, we hypothesized that a similar approach could provide insight into the structure and dynamics of thermophilic n-butyrate production from pretreated lignocellulosic feedstock, by allowing us to precisely link environmental and performance gradients, including the optimization of n-butyrate yields.

4.2 Methods

Corn fiber pretreatment, bioreactor setup, and bioreactor operation

Corn fiber (Aventine ethanol wet-milling plant [Pekin, IL]) was treated in fluidized sand bath reactors at 160^{o}C for 20 min in dilute acid (0.5% w/w H_2SO_4), dilute alkali (1:10 $Ca(OH)_2$ to dry biomass), or distilled water (Table 4.1, Table A3.S1, and Table A3.S2). Four identical thermophilic (55^{o}C) anaerobic sequencing batch bioreactors (ASBRs) that were maintained at a pH of 5.5 were inoculated with a mix of inoculum from three sources. Details are given in the supporting information.

Table 4.1. Composition of corn fiber before and after pretreatment

Treatment	TS [g l^{-1}]	VS [g l^{-1}]	TCOD [g l^{-1}]	SCOD [g l^{-1}]	Glucose [mM]	Xylose [mM]	Arabinose [mM]
Dilute Acid	51.77 ± 3.71 (n = 15)	50.63 ± 3.15 (n = 15)	84.86 ± 6.52 (n= 9)	44.50±2.51 (n = 6)	53.79 ± 3.06 (n = 2)	52.45 ± 1.74 (n = 2)	29.17 ± 3.39 (n= 2)
Dilute Alkali	63.69 ± 6.66 (n = 15)	56.06 ± 6.60 (n = 15)	93.87 ± 26.89 (n= 15)	37.50±5.53 (n=6)	0.67 ± 0 (n = 2)	0.27 ± 0.09 (n = 2)	1.03± 0.14 (n= 2)
Hot Water	56.39 ± 8.68 (n = 15)	55.68 ± 9.24 (n = 15)	80.60 ± 15.09 (n= 13)	26.00±1.92 (n=6)	1.44 ± 0 (n = 2)	6.06 ± 0.47 (n = 2)	15.15 ± 1.84 (n= 2)
None	[1]67.50	[1]66.99	[2]96.22 ± 12.41 (n= 8)	5.40±2.42 (n=4)	NA	NA	NA

[1]No Standard deviation is provided for the nonpretreated TS and VS because it was calculated based on how much corn fiber was added to water.
[2]Nonpretreated TCOD is calculated based on the COD of dry corn fiber and addition of 67.5 dry g TS to 1 l of water.
The value following ± represents the standard deviations, and n= represents the number of replicates. TS , VS, TCOD, and SCOD measurements were performed once or twice for each batch of substrate, depending on variability in replicates. Glucose, xylose, arabinose, and lactate were only performed for the first two batches of substrate.

Chemical analysis

All measurements were performed according to *Standard Methods* [APHA, 1998], unless otherwise indicated. We measured biogas production, ambient temperature, and ambient pressure daily. Every week we evaluated the hydrogen content of the biogas by gas chromatography. Other weekly measurements of the effluent were TS and VS, short-chain carboxylates, alcohols, and soluble and total COD. Monthly, we measured the concentration of effluent soluble carbohydrates. We also characterized weekly the mixed liquor VS, TS, and sludge volume index (SVI), after day 163. We sampled the inoculum and biomass for subsequent microbial community analysis four times during startup and several times during steady state in each of Period 1-4. Details about the operating procedures of the chemical analysis are provided in the supporting information.

DNA extraction, amplification, and data preparation

We extracted DNA from bioreactor mixed liquor samples during each Period 1–4, using the MoBio PowerSoil 96-well gDNA isolation kit (MoBio Labs, Inc, Carlsbad,

CA) and subsequently amplified the V1-V2 region of 16S rRNA genes using universal bacterial primers 8F (including 454 primer 'A') and 338R (including 454 primer 'B' and a unique barcode for each sample). We quantified the dsDNA in the amplified product, pooled the samples in equimolar concentrations, and sequenced on the Roche 454 pyrosequencing platform using Titanium chemistry (Engencore, Columbia, SC). Details can be found in the supporting information. Nucleotides have been submitted to the MG-RAST database under reviewer login BEE6940. We used the QIIME 1.2.1 pipeline [Caporaso et al., 2010] to denoise, quality filter, split sequences into the proper samples, and pick OTUs at 97% sequence identity. We assigned taxonomy to the OTUs according to the GreenGenes database [Werner et al., 2011a]. We also used QIIME to determine the Gini coefficient and weighted and unweighted UniFrac distances between samples. We only report weighted UniFrac distances here because sample clustering was more informative than in unweighted UniFrac. We used principal coordinate decomposition to graphically display the phylogenetic distances between samples.

(Constrained) redundancy analysis

We used redundancy analysis in the Vegan community ecology package for R [Oksanen et al., 2011] to evaluate which metadata gradients were most predictive of community structure. Unconstrained redundancy analysis is essentially a principal component decomposition of principal coordinates. Redundant coordination is useful because the new axes can be constrained by metadata gradients. Essentially, the original principal coordinates are given a score based on how they fit to the chosen environmental or performance gradients, and then the samples are scored based on the weighted principal coordinate scores. Thus, when used with UniFrac principal coordinates, a good

correlation of the constrained and unconstrained axes indicates that the gradient could predict variation in phylogeny. We initially constrained the model with the gradients that fit best to the unconstrained model, and then we removed insignificant gradients (ANOVA $p > 0.05$) and non-unique gradients (variance inflation factor > 10).

Machine learning to identify predictive OTUs to explain patterns

To narrow down the OTU table to OTUs that could help explain patterns between bioreactors, we used nearest shrunken centroids (NSC) analysis in the Pamr 1.4 package for R [Tibshirani et al., 2002] to identify OTUs that were predictive of the pairs R_{acid} vs. R_{base}/R_{heat}, R_{base} vs. R_{acid}/R_{heat}, and R_{heat} vs. R_{acid}/R_{base} during Period 1-3. These resulting OTUs are ones that together could identify a single bioreactor against the other two with at least 92% confidence. We first trimmed the entire OTU table to include only OTUs present in 3 or more samples, and OTUs that had at least 4 sequences in any given sample. The resulting table contained 189 OTUs. Before performing NSC, we normalized OTU counts in each sample by the total number of sequences in the sample. In the predictive OTU table, we reported OTUs that were made up >3% of the relative abundance of a given sample.

4.3 Results

Pretreatment of lignocellulosic biomass

We pretreated corn fiber with dilute-acid, dilute-alkali, and hot-water strategies, each of which resulted in different biomass hydrolysates (Table 4.1, Table A3.S1). Dilute-acid pretreatment achieved the largest reduction in total solids (TS) and volatile solids (VS) from corn fiber compared to dilute-alkali and hot-water pretreatments, resulting in the

highest soluble chemical oxygen demand (SCOD) concentration of 45 g l^{-1}. This solution included the monosaccharides glucose (primarily from starch), and xylose and arabinose (from hemicellulose) at considerable concentrations (Table 4.1). Dilute-alkali pretreatment resulted in a SCOD concentration of 38 g l^{-1}, which was lower than dilute-acid pretreatment but higher than hot-water treatment. We only detected low levels of monosaccharides in the dilute-alkali hydrolysate (Table 4.1), and we determined that most of the soluble carbohydrates were polysaccharides (most likely xylan; details on xylan analysis in supporting information). The hot-water pretreatment strategy resulted in a SCOD concentration of 26 g l^{-1} with considerable concentrations of xylose and arabinose monosaccharides from hemicellulose (Table 4.1).

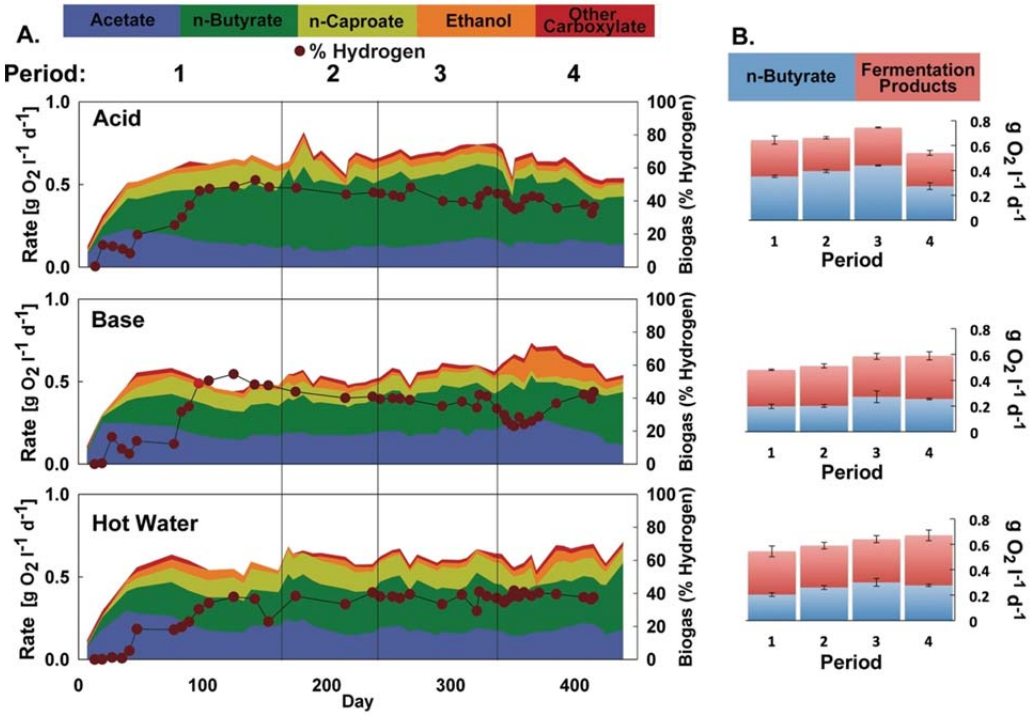

Figure 4.1. Fermentation product rates (as COD (g O_2) per liter bioreactor volume per day) and biogas composition in R_{acid}, R_{base}, and R_{heat}: A. Individual short-chain carboxylate and ethanol production rates in R_{acid}, R_{base}, and R_{heat} during the 419-day operating period; and B. Average with standard deviation of n-butyrate and total fermentation product rates in each period, averaged for three stable points at the end of each period. Time periods signify the following major changes in operating conditions: startup and stable operation (Period 1), decrease in HRT from 25 d to 20 d (Period 2), decrease in HRT from 20 d to 15 d (Period 3), increase in pH from 5.5 to 5.8 (Period 4).

Bioreactor operating conditions and performances

We operated three thermophilic (55°C) bioreactors (designated: R_{acid}, R_{base}, and R_{heat}) by feeding dilute-acid, dilute-alkali, or hot-water pretreated corn fiber hydrolysate, respectively. These three bioreactors were operated continuously for 419 days at a constant VS and COD loading rate (Table A3.S2; Figure 4.1). A fourth thermophilic bioreactor fed nonpretreated corn fiber was discontinued after day 100 due to poor performance (supporting information). We divided the entire study into four periods by adjusting the operating conditions (shortening HRT to dilute substrate and products and

lowering pH to reduce the concentrations of undissociated carboxylic acids) in each sequential period to decrease carboxylic acid toxicity (Table A3.S2). During the first operating period (Period 1) from day 1 to 163, a 25-d HRT and pH of 5.5 was maintained. After an initial start-up period (supporting information), stable concentrations of short-chain carboxylates and ethanol were achieved for all bioreactors (Figure 4.1). During the second operating period (Period 2) from day 164 to 243, a shorter HRT of 20 days was applied while a pH of 5.5 was maintained. Similarly, during the third operating period (Period 3) from day 244 to 337, an even shorter HRT of 15 days was applied at a pH of 5.5. Since our loading rates were constant throughout the entire operating period, we accomplished shorter HRTs by adding more water to the pretreated corn fiber substrate solution during Period 2 and 3. This dilution decreased the concentration of carboxylates but increased the fermentation product rates (i.e., the combined production rates of acetate, propionate, iso-butyrate, n-butyrate, iso-valerate, n-valerate, n-caproate, and ethanol in COD); these rates increased 15-22% between Period 1 and 3 for all bioreactors (Table A3.S3). Further, the dilution also increased the n-butyrate specificity (i.e., the ratio of n-butyrate produced in COD to all fermentation products in COD); these specificities increased 8-24% between Period 1 and 3 for all bioreactors (Table A3.S3). During the final period (Period 4) from day 338 to 419, we increased the pH to 5.8 and maintained the 15-d HRT. The pH increase resulted in a reduction in the concentration of undissociated carboxylic acids by ~50% at the end of Period 4 (Table A3.S3). However, this pH change did not have the preferred outcome because fermentation product rates, n-butyrate specificity, and n-butyrate yields (i.e., the ratio of n-butyrate produced in COD to corn fiber substrate in COD) stayed similar or

declined between Period 3 and 4 for all bioreactors (Table A3.S3). For future n-butyrate studies with pretreated corn fiber, we, therefore, do not recommend increasing the pH above 5.5.

Effect of pretreatment strategy on rates and n-butyrate specificity

The fermentation product rates were the highest in R_{acid} compared to the other bioreactors during Period 1-3 (Table A3.S3) because dilute-acid hydrolysate consisted of the highest concentration of monosaccharides (Table 4.1), which was completely fermentable by the mixed community (Figure A3.S1). The dilute-alkaline hydrolysate was characterized by very low concentrations of monosaccharides (Table 4.1) and in R_{base} the available soluble polysaccharides were not completely fermented (Figure A3.S1). This resulted in the poorest fermentation product rates for R_{base} compared to the other bioreactors. The fermentation product rates for R_{heat} were intermediate (between R_{acid} and R_{base}) because of two reasons: 1. intermediate concentrations of easily-fermentable monosaccharides in hot-water hydrolysate; and 2. the biomass in R_{heat} was consistently the best settling of the three bioreactors (Figure A3.S2), resulting in the longest solids retention times and the most efficient biological VS removal efficiencies (Figure A3.S2).

The n-butyrate specificity was also the highest for R_{acid} compared to the other bioreactors (Table A3.S3). We are not completely sure why, but hypothesized that the higher concentration of monosaccharides in dilute-acid hydrolysate compared to the other hydrolysate substrates promoted n-butyrate production through primary fermentation reactions. In addition, the interplay of primary and secondary fermentation pathways to produce n-butyrate, and secondary fermentation pathways to remove n-butyrate in the complex food web played a role. For both hypotheses the microbial community

dynamics are important. To study the second hypothesis, we performed batch tests with mixed liquor from R_{acid} at thermophilic conditions and 48-h bioreactor cycle analyses (i.e., 48-h is the period from one feeding to the next). One secondary pathway that produces n-butyrate is present in cow rumen through the coupling of lactate oxidation and acetate reduction (i.e., lactate + acetate → n-butyrate) [Agler et al., 2011; Counotte and Prins, 1981]. Indeed, our batch experiment (see supporting information) and *in-situ* cycle analysis showed that lactate was an important intermediate product from primary fermentation in R_{acid} (1.67 mM at 19 h in Figure 4.2A). The subsequent disappearance of lactate accumulation during the cycle and simultaneous decrease in acetate specificity (i.e., the ratio of acetate produced in COD to all fermentation products in COD) showed that secondary fermentation was indeed occurring (Figure 4.2A). In addition to a modest increase in n-butyrate specificity, we observed a distinct and temporary increase in n-caproate specificity (i.e., the ratio of n-caproate produced in COD to all fermentation products in COD) with a peak around 28 h during the cycle analysis for R_{acid} (Figure 4.2A). This phenomenon indicates the existence of a hereto-unknown secondary fermentation pathway (i.e., lactate + n-butyrate → n-caproate) under thermophilic conditions. Although the pathway has not been described in literature, one possible mechanism would couple oxidation of lactate to butyrate with reduction of butyrate and acetate to caproate (Table 4.2). The other known possible secondary fermentation pathway to produce n-caproate, which occurs through the coupling of ethanol oxidation and n-butyrate reduction (i.e., ethanol + n-butyrate → n-caproate) [Agler et al., 2011; Seedorf et al., 2008], did not occur in our thermophilic bioreactor studies even after repeated trials (data not shown).

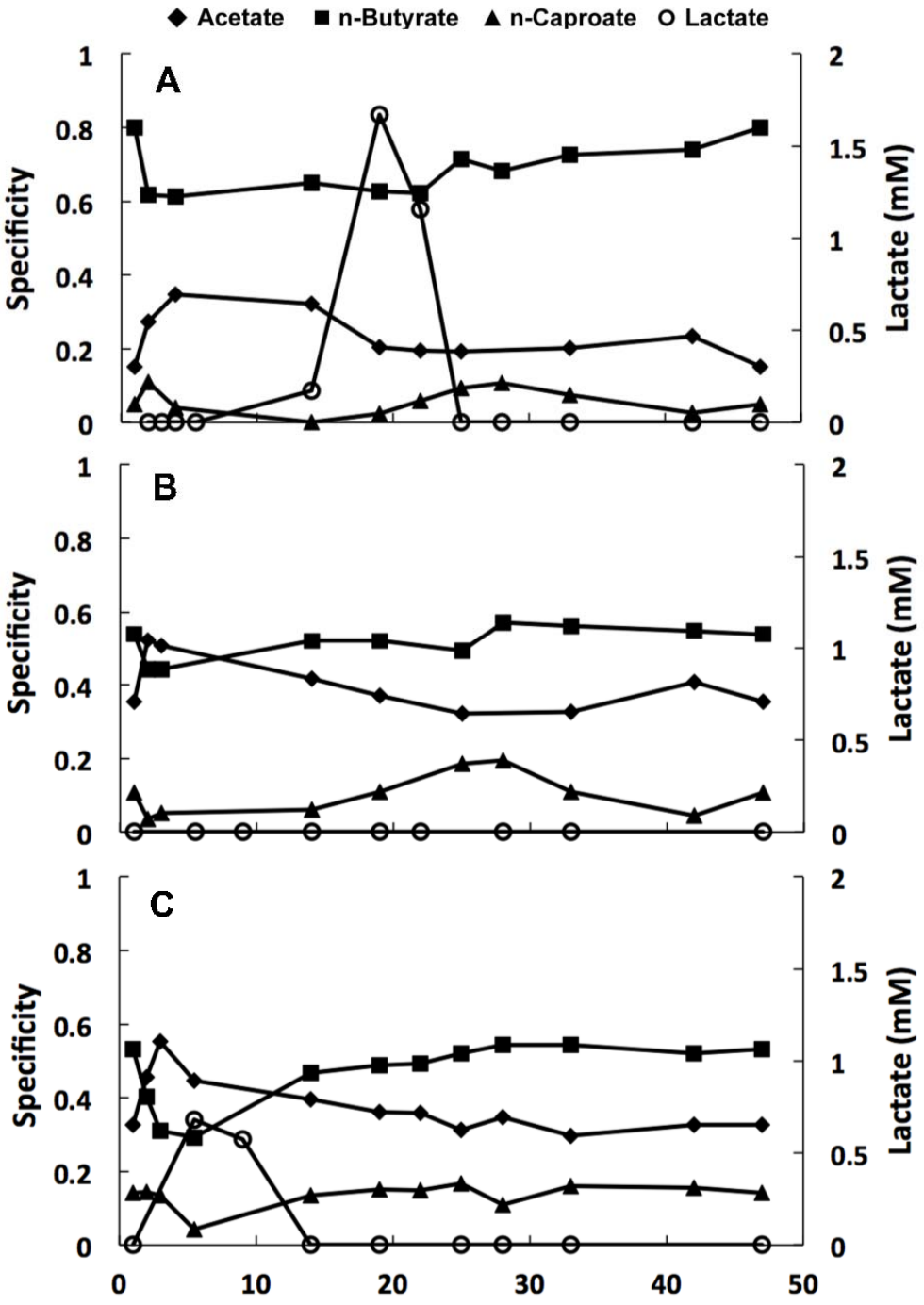

Figure 4.2. 48-hour cycle analysis demonstrates the dynamic relationship between intermediate lactate and the acetate, n-butyrate, or n-caproate specificities (i.e., ratio of specific product in COD to all fermentation products in COD) in R_{acid} (A), R_{base} (B), and R_{heat} (C).

Even though no lactate accumulated in R_{base}, a peak in the n-caproate specificity within the 48-h cycle suggests that secondary fermentation occurred (Figure 4.2B). We did measure primary fermentation of substrate to lactate (0.68 mM at 5.5 h in Figure 4.2C) during the cycle analysis for R_{heat}, and removal of lactate concurrent with increases in both n-butyrate specificity and n-caproate specificity (Figure 4.2C). This result showed that both secondary fermentation pathways -- lactate + acetate → n-butyrate and lactate + n-butyrate → n-caproate -- played important roles along with primary fermentation in producing n-butyrate. Thus, from this data it is apparent that both primary and secondary fermentation pathways to form n-butyrate were important in all bioreactors. However, we did not perform flux analyses to determine the relative importance for each of these pathways. The final concentrations of n-caproate were indicative, however, that conversion of n-butyrate into n-caproate had the highest relative importance in R_{heat} compared to the other two bioreactors. For optimization of the n-butyrate specificity, however, this secondary fermentation pathway is disadvantageous and should be repressed.

Table 4.2. Standard state Gibbs free energy of a possible[a] secondary fermentation coupled reaction set

Reaction	Carboxylate conversion reactions	$\Delta G_r^{o'}$ (kJ/mol at 37 °C)[b]	$\Delta G_r^{o'}$ (kJ/mol at 55 °C)[b]
Lactate oxidation to n-caproate[a]	acetate$^-$ + n-butyrate$^-$ + H^+ + $2H_2$ → n-caproate$^-$ + $2H_2O$	-45.22 -83.75	-45.50 --93.02
	2 lactate$^-$ + H^+ → n-butyrate$^-$ + $2CO_2$ + $2H_2$	**Total** = -128.97	**Total** = -138.52

[a]To our knowledge, the actual mechanism of n-caproate formation from lactate and n-butyrate has not been described. The individual reactions shown here are presumed, and are shown as being coupled within a single microbe.

[b]All $\Delta G_r^{o'}$ values are calculated considering all reactants and products to be in the aqueous phase except for H_2 and CO_2, which are gaseous at 1 atm. $\Delta G_r^{o'}$ values are at biological standard state (pH = 6.82 at 37°C; 6.58 at 55°C). The reactions that are coupled are shown individually with individual and coupled (total) $\Delta G_r^{o'}$ values. $\Delta G_r^{o'}$ quantities were calculated from ΔG_f^{o} values from [Amend and Shock, 2001], except for n-caproate$^-$, which was calculated using the HKF equations of state [Shock and Helgeson, 1990] and thermodynamic parameters [Shock, 1995].

Bacterial community structure

We compared the structure of bacterial communities via high-throughput sequencing of bacterial 16S rRNA gene amplicons of 70 samples representing at least three time points for each of the Periods 1-4 from R_{acid}, R_{base}, and R_{heat} (Figure 4.3A).

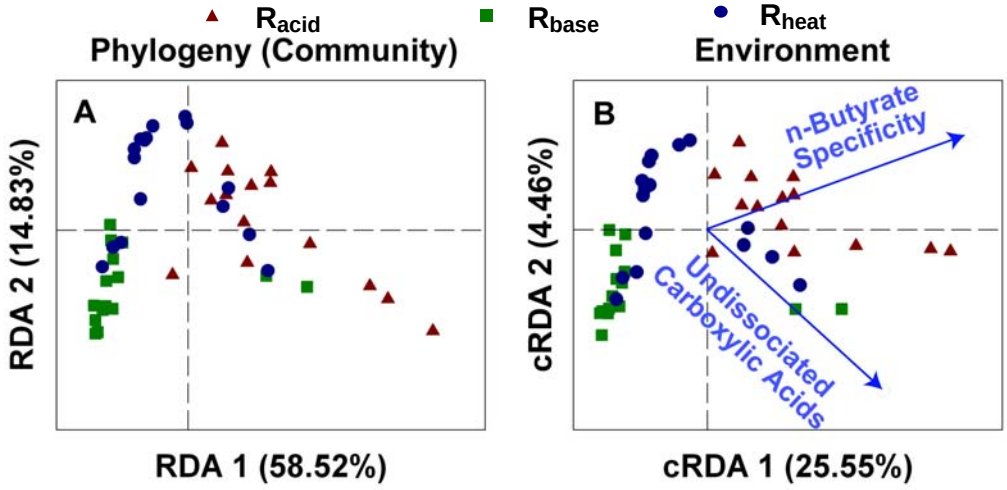

Figure 4.3. Redundancy analysis of the phylogeny described by weighted UniFrac principal coordinates: A. Unconstrained redundancy analysis showing as much of the UniFrac distance between samples as possible in two dimensions demonstrates that bioreactors were clearly differentiated after Period 1 (see Figure A3.S3D for points colored by period); and B. The undissociated short-chain carboxylic acids concentration and the n-butyrate specificity gradients predict ~41% of the community phylogenetic variation between samples in constrained redundancy analysis.

Our primary measure of bacterial community structure was weighted UniFrac distances with principal coordinates analysis [Lozupone and Knight, 2005] in which phylogenetic relationships between operational taxonomic units (OTUs) and abundances of OTUs are taken into account. However, due to long-term operating periods, we were restricted to one bioreactor for each pretreatment. To test whether the bacterial communities for each of these nonreplicated bioreactors were primarily dependent on operating conditions rather than influenced by random fluctuations, we operated two additional identical bioreactors for over 200 days using dilute-acid hydrolysate (supporting information). We found that the communities in the replicated bioreactors

were very similar to each other and stable and resilient over the operating period, which validates our results with nonreplicated bioreactors. To find statistically relevant relationships between bacterial community structure and bioreactor operating conditions and performances, we used constrained ordination of the UniFrac principal coordinates. We determined that the constrained ordination technique was able to explain 41% of the variation in the bacterial community structure for R_{acid}, R_{base}, and R_{heat} (i.e., 41% of the first two unconstrained ordination axes [Figure 4.3A]) by the two combined gradients for undissociated short-chain carboxylic acid concentration (function of both environmental conditions and performance) and n-butyrate specificity (function of performance) (Figure 4.3B). Moreover, a direct comparison of constrained and unconstrained axes revealed that the community structure could be associated with not only within-bioreactor performance differences, but also between-bioreactor performance differences (R^2=0.99 for RDA 1 vs. cRDA 1; Figure A3.S3A and Figure A3.S3B). Indeed, the community structures were grouped by pretreatment (between bioreactors) or by period (within bioreactors) (Figure A3.S3D), indicating that operating conditions determined the community structure, which caused changes in the bioreactor performance.

Bacterial taxonomic structure

Assignment of taxonomy to bacterial OTUs clearly demonstrated differences between reactors (Figure 4.4A), so we used a machine-learning method (i.e., nearest shrunken centroids) to find important taxa by automatically selecting OTUs that were predictive of pretreatment regimes (i.e., specific bioreactors). Indeed, some of the predictive OTU set had taxonomy assignments that could allow us to speculate about physiology of specific OTUs to improve our understanding of differences in performance between bioreactors

during Period 1-3 (Table A3.S4). For example, one of the two OTUs that were predictive of R_{acid} belonged to the family *Lachnospiraceae* (the other was a *Clostridium*, for which the diverse physiology is not specific enough to be useful), and was present after an initial start-up period (Figure 4.4A). *Lachnospiraceae* likely contributed to relatively higher n-butyrate specificities in R_{acid} than the other bioreactors, because several genera (i.e., *Butyrivibrio, Roseburia,* and *Anaerostipes*) in that family are known to produce mostly n-butyrate from carbohydrates utilizing primary fermentation pathways [Cotta and Forster, 2006]. Next, we found a group of predictive OTUs within the genus *Thermoanaerobacterium* of which some were specific to R_{base} and some predictive of both R_{acid} and R_{heat} (Figure 4.4B). Members of *Thermoanaerobacterium* are well-known xylan and xylose fermenters and some species have pH optima near or below our bioreactor conditions [Lee et al., 1993; Liu et al., 1996; Ren et al., 2008]; the specific OTU that was solely identified in R_{base} may, thus, have been xylan degraders because dilute-alkaline pretreated corn fiber hydrolysate contained almost no xylose in contrast to the other two hydrolysates. We also found that the presence of all *Thermoanaerobacterium* OTUs was positively correlated to fermentation product rates during Period 1–4 (Figure 4.4C). During Period 4 in which the pH had been increased to 5.8, the *Thermoanaerobacterium* abundance decreased (Figure 4.4D), which may explain the deterioration of all performance parameters in, for example, R_{acid} (discussed earlier for Period 4). Finally, the presence of OTUs within *Thermosinus* spp. was positively correlated with rates of n-caproate formation in all three bioreactors (Figure A3.S4). This genus is placed in the *Veillonaceae* family, and includes the mesophilic bacterium *Megasphaera elsdenii* that was able to grow on lactate by generating acetate, n-butyrate,

and n-caproate [Marounek et al., 1989], suggesting that our OTUs within the genera *Thermosinus* are likely candidates to perform the newly described thermophilic secondary fermentation pathway to convert lactate and n-butyrate into n-caproate.

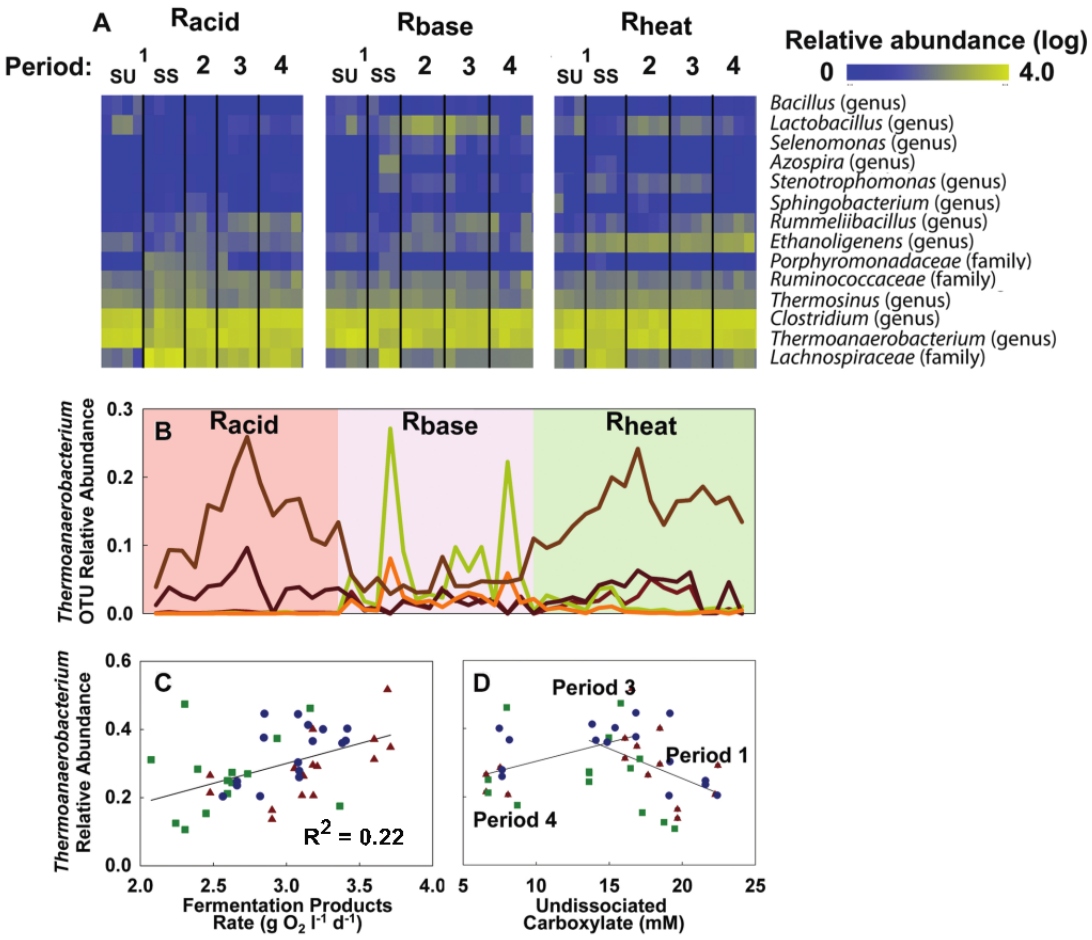

Figure 4.4. The taxonomic structure of the bioreactors reflects differences in overall community structure and performance: A. Heatmap of the relative abundance (logarithmic scale) of major taxonomic groups in R_{acid}, R_{base}, and R_{heat}. SU in Period 1 indicates the period of time after inoculation until stable bioreactor performance, and SS indicates steady-state conditions; B. *Thermoanaerobacterium* spp. OTU speciation in R_{acid}, R_{base}, and R_{heat} in Period 1-3 reflects speciation of pentose units as xylan (alkali pretreatment) vs. xylose (dilute-acid and hot water pretreatment); C. *Thermoanaerobacterium* spp. relative abundance corresponded to total fermentation production rates; and D. *Thermoanaerobacterium* spp. relative abundance increased with end product dilution at pH 5.5, but the pH shift to 5.8 was detrimental to the community (no R^2 values given, lines are intended to show trend).

4.4 Discussion

n-Butyrate specificity was predictable based on community and taxonomic structure

We showed that the performance of bioreactors in regards to n-butyrate specificity was predictable based on the structure of the bacterial community. Further, even though community structures between bioreactors were similar due to generally analogous operating conditions, the communities were sensitive to difference in substrate (i.e., hydrolysate) composition. Our work agrees with other sequencing efforts that have found stable carboxylate-producing populations that were linked, theoretically, to performance [Kim et al., 2006; Ren et al., 2007]. It is important that this has now been shown for acidogenic mixed culture communities with enough sequencing depth for statistical certainty so that further work in isolating factors contributing to improved bioreactor performance can continue.

n-Butyrate-producing communities were uneven

Previous work has suggested that bioreactor stability is positively correlated to evenness in ecosystem populations; a higher evenness (i.e., lower Gini coefficient) resulted in more robust systems [Werner et al., 2011b; Wittebolle et al., 2009]. Our systems were associated with high Gini coefficients (ranging from ~0.6 to 0.8), similar to those found with other high-depth sequencing efforts in thermophilic acidogenic systems [Hollister et al., 2010]. A small increase in evenness during Period 3 was outside of statistical certainty (Figure A3.S5), so it is unclear if minor gains in n-butyrate specificity would be correlated with evenness as a result of, for example, the onset of secondary fermentation pathways (i.e., the coupling of lactate oxidation and acetate reduction to n-butyrate). The uneven bacterial populations in our bioreactors could have been a

response to high temperatures, product toxicity, or both, or the higher unevenness may be determined after future research to be a characteristic of thermophilic communities compared to their mesophilic counterparts. Regardless, we predict that manipulation of environmental conditions to promote secondary fermentation processes that improve system functionality (e.g., lactate + acetate → n-butyrate) will also improve community evenness and increase culture productivity and n-butyrate specificity. This is already true for anaerobic digesters with optimized methane production pathways [Werner et al., 2011b].

Carboxylic acid inhibition limits pentose-rich substrate conversion to n-butyrate

Product buildup and toxicity, especially with undissociated carboxylic acids, are commonly implicated in incomplete conversion of substrate to fermentation products [Russell and Wilson, 1996b; Wu and Yang, 2003]. We found that diluting the undissociated carboxylic acid concentrations, via applying shorter HRTs, while maintaining a constant pH during Periods 2-3, led to a bacterial community structure with enhanced fermentation product rates. Specifically, our results showed that the abundance of *Thermoanaerobacterium* spp., which are well-known pentose saccharide (xylan and xylose) fermenting bacteria [Lee et al., 1993], was positively correlated to fermentation product rates (Figure 4.4B-4.4D). We anticipated that an increase in pH from 5.5 to 5.8 during Period 4 would further promote pentose degradation due to lower undissociated carboxylic acid concentrations, but this did not occur. Rather, an increase in pH negatively affected the relative abundance of *Thermoanaerobacterium* spp. even though this pH increase, indeed, considerably reduced the concentration of undissociated carboxylic acids, and thus also reduced toxicity. The nonoptimum growth of

Thermoanaerobacterium spp. at the slightly higher pH decreased the conversion efficiency of our pentose-rich substrate, and places *Thermoanaerobacterium* spp. with other bacteria that are superior at conditions of low pH/high carboxylate concentrations because of mechanisms preventing the toxic effects of carboxylic acids (e.g., [Russell and Wilson, 1996b]). The complex interactions between substrate type, population dynamics, environmental conditions, and product inhibition also explain ambiguities between studies [Vavilin et al., 2008], and the effects of changes in pH are clearly not universal for mixed communities due to the growth optima of different populations for each substrate type.

Better control over secondary fermentation processes can improve functionality

Mathematical models describing mixed culture carboxylate production have typically focused only on primary fermentation and have simply predicted a metabolic shift toward n-butyrate specificity at low pH levels because of energetic costs in transport of carboxylic acids out of the cell at low pH [Lee et al., 2009; Rodriguez et al., 2006]. We discovered that secondary fermentation pathways considerably affected product specificities through the flux of the primary fermentation product lactate. Lactate had been identified as an intermediate in both mesophilic and thermophilic systems, and has been widely studied as a precursor in a pathway to generate n-butyrate (lactate + acetate → n-butyrate) in colon and rumen microbial communities [Belenguer et al., 2007; Duncan et al., 2004; Kim et al., 2003]. To our knowledge, this secondary fermentation pathway had not been implicated in bioreactors designed for carboxylate-specific production. We also observed the occurrence of another secondary fermentation pathway (lactate + n-butyrate → n-caproate), which was maybe carried out by bacteria in the

genera *Thermosinus*. Our results show that future bioreactor studies and mathematical efforts should focus on these secondary fermentation pathways to affect product specificity.

Continuous, long-term, and specific production of n-butyrate

We showed continuous production of carboxylates from pretreated lignocellulose for operating periods exceeding 400 days. By combining pretreatment, biological hydrolysis, and fermentation, we achieved a maximum fermentation product yield from corn fiber of ~40% (on a COD basis, which is equivalent to 0.56 g COD/g VS added) and n-butyrate yields exceeding 23% (on a COD basis, which is equivalent to 0.33 g COD/g VS added). Compared to anaerobic digestion of lignocellulose for methane production, we achieved a yield that was only half that of typical yields (e.g., producing methane from grasses [Tong et al., 1990]). Therefore, there is considerable room for improvement of carboxylate production. More research is needed to better understand the effects of decreasing short-chain carboxylic acid toxicity and the occurrence of beneficial secondary fermentations on performance that we observed in this study. To shape carboxylate-producing communities that are as effective as anaerobic digestion communities, we must follow broad rules that apply to both anaerobic digestion and carboxylate production: 1. remove the products (primary fermentation products are converted to methane, which freely bubbles out in anaerobic digesters); and 2. direct all secondary fermentation pathways towards the product of interest (methane has the lowest free energy content per electron, which even allows the anaerobic oxidation of organic intermediates in anaerobic digesters [Angenent and Kleerebezem, 2011]). To address these needs, we are currently integrating membrane-based extraction [Wu and Yang,

2003] with mixed culture bioreactors to specifically remove the product of interest. This will not only reduce product toxicity by lowering the undissociated carboxylic acid concentrations, but also will promote secondary fermentation pathways that increase specificity. Under these operating conditions, however, secondary reactions that decrease specificity must be prevented as much as possible by manipulation of environmental conditions and the application of ecological theory.

4.5 Acknowledgements

We acknowledge Joseph G. Usack and Dr. Miriam Agler-Rosenbaum for reviewing the manuscript. We also thank Dr. Wei Zhang for her help with DNA extraction and amplification. The project was supported by the National Research Initiative of the USDA Cooperative State Research, Education and Extension Service, grant number 2007-35504-18256.

CHAPTER 5.

DIRECTING MIXED MICROBIAL CULTURES TOWARD UPGRADING ACETATE, N-BUTYRATE, AND ETHANOL TO SPECIFIC MEDIUM-CHAIN CARBOXYLATES

This chapter is not yet published

Note: Supplementary information can be found in Appendix 4 and is denoted in this text as A4.SX, where X denotes the appendix section.

Abstract

We studied chain-elongation reactions that couple ethanol oxidation to n-butyrate reduction (i.e., n-butyrate + ethanol → n-caproate) in mixed communities of microbes to upgrade miscible ethanol and short-chain carboxylate products derived from biomass into better extractable medium-chain carboxylates (n-caproate and n-caprylate). To do so, two bioreactors were operated with mixed communities under anaerobic conditions to convert ethanol and dilute-acid pretreated corn fiber to primarily n-caproate and n-caprylate. Promising chain elongation rates were achieved when both electron pushing (addition of ethanol as an external chemical source of energy and electrons) and *in-situ* product extraction (continuous removal of hydrophobic and acidic end products) were applied. However, environmental conditions such as the operating temperature needed to be optimized. Indeed, the n-caproate/n-caprylate carboxylate specificity (i.e., the ratio of n-caproate and n-caprylate in COD to all other fermentation products in COD) improved

from 12% at 55°C to 52% at 30°C in the bioreactor with *in-situ* extraction and from 6% to 18% in the bioreactor without *in-situ* extraction. Surprisingly, methane production proceeded via carbon dioxide reduction with hydrogen and low hydrogen pressures did not apparently negatively affect the process. This is a paradigm shift because completely inhibiting methane production had been described as an absolute requirement. We used the metagenome of the communities to link with statistical certainty the operating conditions - temperature and extraction - to the ability of the bioreactors to utilize ethanol as the electron pushing substrate. Further, gene taxonomy results indicated that chain elongation might be catalyzed by more complex consortium of microbes than previously described.

5.1 Introduction

The carboxylate platform produces commercially valuable bioproducts from biomass with undefined mixed communities of microbes [Agler et al., 2011; Holtzapple et al., 1999]. For example, the potential products n-caproate and n-caprylate are valuable commodities in the lubricant industry, the food and fragrance industry, and others that usually rely on petrochemical production of carboxylates [Gaertner et al., 2009]. Until now, researchers have not been able to produce carboxylates with high enough product specificity with mixed communities in engineered bioreactors. In these systems, microbes utilize the best available electron acceptors to extract energy from the system by oxidizing primary fermentation products (i.e., acetate, ethanol, propionate, lactate, and n-butyrate) to the most energetically favorable end products, usually only methane and carbon dioxide if methanogen populations are active. In methanogen-

inhibited systems, the best biologically available electron donors are relatively reduced primary fermentation products (e.g., ethanol and lactate) and the only available electron acceptors are relatively more oxidized fermentation products (e.g., acetate and n-butyrate) [Angenent and Kleerebezem, 2011]. Therefore, secondary-fermenting microorganisms thrive in this environment by coupling, for example, ethanol oxidation to reduction of n-butyrate (e.g., ethanol + n-butyrate → n-caproate) [Duncan et al., 2004; Ding et al. 2010; Steinbusch et al., 2011]. The end product spectrum is achieved when electron donors are depleted – typically resulting in a diverse array of carboxylates [Borja et al., 2005]. Thus, a driving force, such as an electron pushing substrate (i.e., an exogenous supply of electron donor), is required to drive fermentation products toward a product of interest.

The carboxylate platform system with the highest product specificity, thus far, is anaerobic digestion. These systems convert nearly all substrate to methane through carboxylate intermediates, because in well-functioning digesters protons are available electron acceptors for secondary fermentation reactions that oxidize carboxylates to acetate and hydrogen [Schink, 1997]. Secondary-fermenting methanogens then split acetate to methane and carbon dioxide and/or oxidize hydrogen and reduce carbon dioxide to methane [Thauer, 1998]. Thus, in anaerobic digesters the sources of energy and electrons for secondary fermentations leading to methane are carboxylates and hydrogen, which are continuously supplied by primary and secondary fermentation reactions. Researchers first demonstrated the same principle for carboxylate-producing bioreactors by continuously adding ethanol as an electron donor and acetate as electron acceptor. In their systems with mixed cultures of microbes at pH 7 with chemical

methanogen inhibition, the result was formation of mostly n-caproate and n-caprylate [Steinbusch et al., 2011]. More recently, we found that in bioreactors producing n-butyrate from corn fiber, lactate oxidation was coupled to reduction of acetate to produce n-butyrate [Agler et al., 2011]. We hypothesized, therefore, that external addition of an electron donor to undefined mixed cultures (i.e., electron pushing) could boost beneficial secondary fermentations.

Besides beneficial secondary reactions, other undesirable reactions may compete for energy and electrons. For example, in the same study to optimize n-butyrate production, we showed that n-caproate production from lactate and n-butyrate was lowering the n-butyrate specificity (i.e., the ratio of n-butyrate in COD to all fermentation products in COD), while n-butyrate production from lactate and acetate was increasing this specificity [Agler et al., 2011]. When ethanol is the electron pushing substrate to reduce short-chain carboxylates to n-caproate and n-caprylate, competing reactions could include, for example, ethanol oxidation coupled to reduction of propionate to propanol [Smith and McCarty, 1989]. Regardless, additional efforts, such as *in-situ* product removal, are needed to specifically and rapidly remove the product of interest to provide a competitive advantage to desirable secondary fermenters. This technique would also reduce carboxylate toxicity, which is crucial for microbial activity [Russell and Wilson, 1996a]. Membrane-based extraction is one option for direct carboxylate removal that has already been shown to be effective for pure culture fermentations [Wu and Yang, 2003]. For efficient extraction, n-caproate and n-caprylate are ideal products because they are relatively easy to remove with typical extraction systems [Zigová and Šturdík, 2000] and

the maximum solubility of the undissociated acid is relatively low (~11 g l^{-1} and 0.68 g l^{-1} for n-caproate and n-caprylate, respectively).

The complex microbial ecosystems that catalyze the carboxylate platform are promising for production of biochemical, such as n-caproate, because they are robust, resilient, and are functionally diverse [Hashsham et al., 2000; Werner et al., 2011b]. These systems feature a complex and difficult-to-predict food web, however, and attempts to directly link operating conditions and performance have yielded conflicting results because researchers have not considered unintended effects to microbial interactions. Molecular biology tools, such as metagenomic analysis of undefined mixed microbial communities, have recently been applied to better understand complex microbial communities [Martin et al., 2006; Schluter et al., 2008]. Only recently has work revealed that ecological tools applying correlation and regression (i.e., constrained ordination) to functional metagenomic analysis (studying community metagenome relationships *via* the functional structure of the metagenome) can statistically correlate environmental parameters with community function [Dinsdale et al., 2008; Gianoulis et al., 2009]. Thus, we suggest that applying functional metagenomics and ecological theory to the carboxylate platform will contribute to our understanding of processes, such as electron pushing, which may have complex and difficult to predict interactions with operating parameters. Here, we operated two bioreactors degrading pretreated corn fiber and supplemented them with ethanol to promote chain-elongation reactions that upgrade the product spectrum to higher-value n-caproate and n-caprylate. We combined a functional metagenomic survey with constrained ordination of 12 bioreactor samples to determine the dynamic effects of operating conditions (three temperatures and product-

specific extraction) on the function of bioreactors. Further, we evaluated the taxonomic structure of chain-elongation genes to gain insights into how the community performs the chain-elongation function at these conditions.

5.2 Methods

Bioreactor operation

We operated two ethanol-supplemented anaerobic sequencing batch bioreactors (ASBRs) treating dilute-acid pretreated corn fiber for 124 days to direct metabolism toward medium-chain carboxylates (n-caproate and n-caprylate). The dilute-acid pretreated corn fiber was the same as described in our previous work converting dilute-acid pretreated corn fiber to n-butyrate [Agler et al., 2011]. Two strategies were employed to direct the community to produce primarily n-caproate and c-caprylate in the liquid fraction. First, we added ethanol to both bioreactors at a rate of 0.75 g l^{-1} d^{-1} to encourage chain-elongation of acetate and n-butyrate that was produced during primary fermentation to n-caproate and n-caprylate and to encourage reduction of carbon dioxide to methane. Second, we performed *in-situ* product specific extraction of n-caproate and n-caprylate in one bioreactor (R_p), while products only left the other bioreactor in the effluent (R_c). Both bioreactors were previously operated for ~119 days at a thermophilic temperature (55^{o}C) and a pH of 5.5 with supplemented ethanol. After operating at 55^{o}C, we reduced the temperature to 40^{o}C, and after 33 days we reduced the temperature to 30^{o}C to promote a microbial community structure more efficient at the desired chain-elongation reactions.

In-situ product-specific extraction

We incorporated an in-line continuously recirculating membrane-based liquid/liquid extraction system (a system diagram is given in Figure A4.S1). To ensure extraction specificity, the system was designed to extract the more hydrophobic carboxylates (medium-chain) by employing a light mineral oil based solvent with 3% tri-n-octylphosphine oxide as a "carrier" molecule (Sigma-Aldrich, Inc). Further, we ensured that only acidic molecules could be extracted by regenerating the solvent with a borate buffer solution maintained at pH=9 with automated addition of 5M NaOH. Thus, the driving force of extraction was the concentration gradient of undissociated acids while non acidic molecules (e.g., ethanol) were not removed. To control for potentially negative affects of the solvent on the microbial community, both R_p and R_c were in contact with the solvent continuously. However, regeneration of the solvent only occurred for R_p, so carboxylates were not extracted from R_c (Figure A4.S1). To provide a large aqueous/solvent contact area while maintaining separation of the phases, we used commercially available hollow-fiber membrane units, each providing ~0.5 m^2 of membrane surface area (Membrana, Inc). Two membrane units in series were located at the bioreactor broth/solvent interface and the solvent/aqueous alkaline interface. The bioreactor broth and aqueous alkaline solution were each continuously recirculated from the reservoir through the membrane and back at ~10mL min^{-1}. The solvent was continuously recirculated between the bioreactor broth and aqueous alkaline regenerant. We never experienced noticeable reductions in extraction rates due to reduced solvent capacity, and we only replaced it when a leak occurred.

Chemical analysis

We monitored the chemical oxygen demand (COD) and volatile and total solids (VS and TS) levels in the substrate and effluent weekly or bi-weekly during the operating period, according to *Standard Methods* [APHA, 1998]. Every day we measured the biogas production and recorded the temperature and pressure to standardize the measurements. Biogas composition was measured weekly. For hydrogen composition we used a Gow-Mac Series 580 GC (Gow-Mac, Inc) with a 5' x ¼" stainless column packed with 60/80 Carboxen 1000 packing material (Supelco, Inc). The temperature of the column, injector, and detector were 100, 110, and 105^{o}C, respectively, and the current to the TCD detector was 70 mA. Carbon dioxide and methane were measured with an SRI 8610C GC with a 1m x ¼" Rt-XLSulfur column (Restek, Inc). The temperature of the column, injector, and detector were 40^{o}C, 25^{o}C, and 101^{o}C, respectively, and the current was 167 mA. We determined the composition of the effluent and the stripping solution by measuring the individual carboxylate and ethanol concentration after every 48-h cycle of feeding. Individual carboxylates were measured with an HP 5890 Series II GC equipped with an autosampler with a 15m x 0.53mm Nukol column. Ethanol was measured with the same GC setup and a Supelco 6' ¼" x 2mm glass column packed with 10% CW-20M (treated with 0.01% H_3PO_4) on 80/100 Chromasorb WAW support.

DNA isolation and metagenomic analysis

We collected biomass directly from bioreactors by mixing them for 5 min, rapidly sampling, centrifuging 2-mL vials of sample at 10,000 rpm for 10 min, disposing of supernatant, then freezing at -80^{o}C until further analysis. We isolated whole community genomic DNA (gDNA) from 12 bioreactor biomass samples (4 from R1 and 8 from R2) with the MoBio PowerSoil DNA Isolation Kit (MoBio, Inc). DNA extracted from

samples from 55°C and 40°C operating periods resulted in low concentrations of DNA, so we concentrated DNA by ethanol precipitation so that all samples had at least 10 ng/ul, measured with the PicoGreen dsDNA measurement kit (Invitrogen, Inc). Samples were sequenced with an Illumina HiSeq 2000 sequencing system in two lanes (6 samples in each lane), resulting in 10-15 million high quality and nonredundant reads per sample. We filtered the sequences for quality, using a trimming threshold of two consecutive low-quality bases, no unknown bases, and a final minimum length of 75 bp, and removal of identical sequences, using the QIIME 1.3.0 pipeline [Caporaso et al., 2010], and uploaded them to MG-RAST [Meyer et al., 2008] for further analysis.

We annotated sequencing reads in MG-RAST based on SEED subsystem-based functional abundances, with a minimum 50% identity and an e-value cutoff of 1×10^{-3}. Next, we created a QIIME-style table using subsystem-based functions instead of OTUs so that we could calculate between-sample Pearson distances to compare gene functional profiles. Pearson distances were calculated based on a table generated from the mean of 100 rarefactions at a depth of 350,000 sequences per sample. We then generated principal coordinates of the subsystem-based Pearson distances to visualize the relatedness of sample metagenome structures. We also used ANOVA in the QIIME package to determine genes that shifted in abundance with statistical significance ($p < 0.05$ with a 3-fold abundance shift) between the operating categories temperature (55°C vs. 30°C) and extraction (extraction/no extraction).

To evaluate how operating or performance gradients described the subsystem-based function of the metagenome, we used redundancy analysis of the Pearson distance principal coordinates in the Vegan community ecology package for R [Oksanen et al.,

2011]. Redundancy analysis is essentially a principal component decomposition of principal coordinates. The resulting principal components are known as "unconstrained principal components", and they show as much separation as possible between samples on two axes. Constrained principal components are made by using gradients, such as operating conditions or performance variables, to recreate the unconstrained principal components. Thus, in our application using subsystem-based between-sample distances, a good correlation between constrained and unconstrained axes indicates that the constraining variables are predictive of the subsystem-based function of the metagenome. Next, we constrained the entire set of principal coordinates by one operating or performance variable at a time and plotted them against one another (operating conditions vs. performance). The type of correlation between the constraints is useful in identifying the dynamic between operating condition-explained metagenome functional composition and performance-explained functional composition, thus, linking the operating conditions and performance through the community metagenome.

We used USEARCH version 4.2.133 [Edgar, 2010] to search against the NCBInr database, which we divided into 29 equal parts to increase the speed of searches. We queried 4 million sequence reads against each part of the database with a 10^{-6} e-value cutoff and 70% sequence identity (USEARCH does not count gaps, so this corresponds to ~60% identity in a BLAST search). We used a last common ancestor (LCA) algorithm to annotate the taxonomy and function of genes. After annotation, we summarized the taxonomy results for the whole metagenome and two processes within the metagenome: 1. The chain-elongation pathway catalyzed by *Clostridium kluyveri* [Seedorf et al., 2008],

and 2. Both the NAD- and NADP-dependent alcohol dehydrogenases (EC 1.1.1.1 and EC 1.1.1.2).

5.3 Results

Bioreactor operation and performance

We operated two ethanol-supplemented anaerobic bioreactors converting dilute-acid pretreated corn fiber to carboxylates. We supplemented ethanol (i.e., electron pushing) as a source of energy and electrons for microorganisms that couple ethanol oxidation to reduction of short-chain carboxylates (acetate and n-butyrate), resulting in medium chain carboxylates (n-caproate and n-caprylate) [Agler et al., 2011; Steinbusch et al., 2011]. We compared performance between a bioreactor with *in-situ* product specific extraction (R_p) and one without extraction (R_c) at three different operating temperatures to optimize the chain elongation reactions leading to n-caproate and n-caprylate (Figure 5.1). Here, we report n-caproate/n-caprylate specificity (i.e., the ratio of n-caproate and n-caprylate in COD to all other carboxylates in COD) and carboxylate production rates (i.e., the rate of formation of a carboxylate or a group of carboxylates in COD) as the total of products collected in the effluent and in the extraction system.

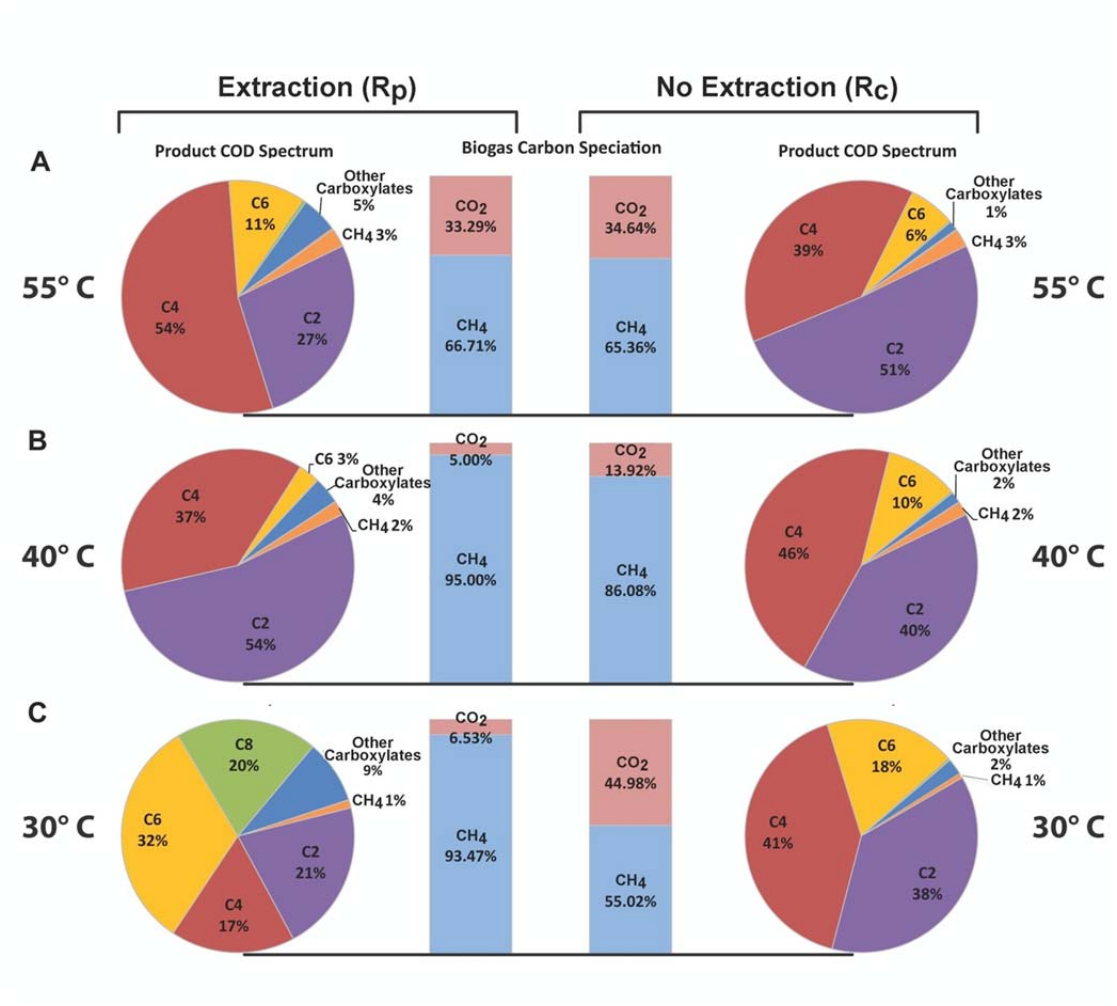

Figure 5.1. Performance comparison between a bioreactor with *in-situ* product specific extraction (R_p) and a bioreactor without product extraction (R_c). A. Fermentation product specificities in chemical oxygen demand (COD) and biogas carbon speciation at 55°C; B. Fermentation product specificities COD biogas carbon speciation at 40°C; and C. Fermentation product specificities COD speciation and biogas carbon speciation at 30°C

The first operating condition we tested was 55°C, corresponding to typical thermophilic bioreactor conditions. At this temperature, the n-caproate/n-caprylate specificity was 11% and 6% for R_p and R_c, respectively, (Figure 5.1A) and about two-thirds of the biogas carbon was in methane. To promote chain elongation in the bioreactors, we decreased the temperature to 40°C, but the n-caproate/n-caprylate specificity only changed marginally, indicating that this temperature was still not

optimum for chain elongation (Figure 5.1B). Carbon dioxide reduction to methane was more complete, with 95% and 85% of biogas carbon in the form of methane for R_p and R_c, respectively (Figure 5.1B). Even though some carbon dioxide may have been reduced to acetate at 40°C, it could not have been responsible for the increase in acetate specificity in R_p at 40°C because the acetate production rate increase from 0.011 mol acetate C l^{-1} d^{-1} at 55°C to 0.023 mol acetate C l^{-1} d^{-1} at 40°C was very large compared to the total available biogas carbon at 55°C (0.0018 mol C l^{-1} d^{-1}). Finally, we decreased the bioreactor temperature to 30°C, resulting in the maximum n-caproate/n-caprylate specificity for R_p of 52% and for R_c of 18% (Figure 5.1C). The n-caproate/n-caprylate production rate was six times higher in R_p compared to R_c (1.16 vs. 0.19 g COD l of bioreactor^{-1} d^{-1}) and the total carboxylate production rate (i.e., the combined rate of formation of acetate, propionate, is butyrate, n-butyrate, iso valerate, n-valerate, n-caproate and n-caprylate in COD) in R_p was more than double that of R_c (2.10 vs. 0.97 g COD l^{-1} d^{-1}). Hydrolysis of the corn fiber substrate was relatively consistent throughout the entire operating period (Figure A4.S2), indicating that the increase in specificity and product rates was due to higher rates of ethanol utilization in R_p (~89% of the supplied ethanol was utilized in R_p vs. ~30% in R_c). The portion of biogas carbon as methane at 30°C was higher in R_p with 95% methane compared to 55% in R_c (Figure 5.1C). The methane production rates were also higher in R_p, with 0.116 g COD l^{-1} d^{-1} vs. 0.026 g COD l^{-1} d^{-1} in R_c. We attribute the lower methane production rates in R_c to accumulation of toxic n-caproate concentrations without product extraction [Butkus et al., 2011].

The community metagenome structure

We used the community metagenome structure of R_p and R_c to understand the dynamics between operating conditions and bioreactor utilization of the electron-pushing substrate ethanol to upgrade acetate and n-butyrate to n-caproate and n-caprylate and to reduce carbon dioxide to methane. We sequenced the metagenome of a total of 12 samples (8 from R_p and 4 from R_c); one sample from each bioreactor was collected at 55^{o}C, one from each at 40^{o}C, and 6 from R_p and two from R_c at 30^{o}C. The 30^{o}C samples were collected at various levels of n-caproate/n-caprylate specificity so that we could evaluate changes in the structure along performance gradients. Using barcoded sequencing on the Illumina HiSeq platform, we obtained an average of 12.5 million high-quality reads sample^{-1} (average 98.2 bp per sequence) after filtering. Our primary measure of community metagenome structure was principal coordinate analysis of SEED subsystem-based functional abundances, using Pearson distances to compare gene functional profiles between samples. In redundancy analysis of the functional subsystem-based principal coordinates, we could visualize 85% of community metagenome inertia (i.e., variation) on two axes (Figure 5.2A).

To find statistical correlation between operating conditions, metagenome functional composition, and performance, we performed constrained ordination of the functional subsystem-based principal coordinates. We constrained the distances between samples with the operating variables temperature (55^{o}C, 40^{o}C, and 30^{o}C) and extraction (extraction or no extraction), and found that the variables described 98% of the inertia described by the metagenomic functional data (98% is calculated by the total inertia described by cRDA 1 and cRDA 2 divided by the total inertia described by RDA1 and RDA 2, multiplied by 100)(Figure 5.2B). Next, to link bioreactor performance and

metagenomic functional shifts due to operating conditions, we again constrained the functional subsystem-based principal coordinates with three variables one at a time: 1. rate of ethanol consumption (performance), 2. temperature (operating condition), and 3. extraction (operating condition). Because higher productivity corresponded with increased ethanol utilization, we reasoned that the rate of ethanol consumption should describe the sum of electron pushing pathways (n-caproate, n-caprylate, and methane production) that were active, and thus the overall performance of the bioreactors. We plotted each of the operating condition-constrained axes against the performance-constrained axis (Figure 5.2C and 5.2D), and found that the aspects of metagenome functional composition that were determined by the bioreactor operating conditions also explained bioreactor performance ($R^2 = 0.56$ for temperature and $R^2 = 0.93$ for extraction Figure 5.2C and 5.2D), although the relationships were different (nonlinear for temperature and linear for extraction). The nonlinear relationship for temperature explains that the community metagenome was capable of efficient ethanol utilization at 30^oC. The linear correlation for extraction and performance indicates that extraction continuously altered the same metagenome functional composition that corresponded to performance. Thus, extraction efficiency is directly correlated to performance improvements.

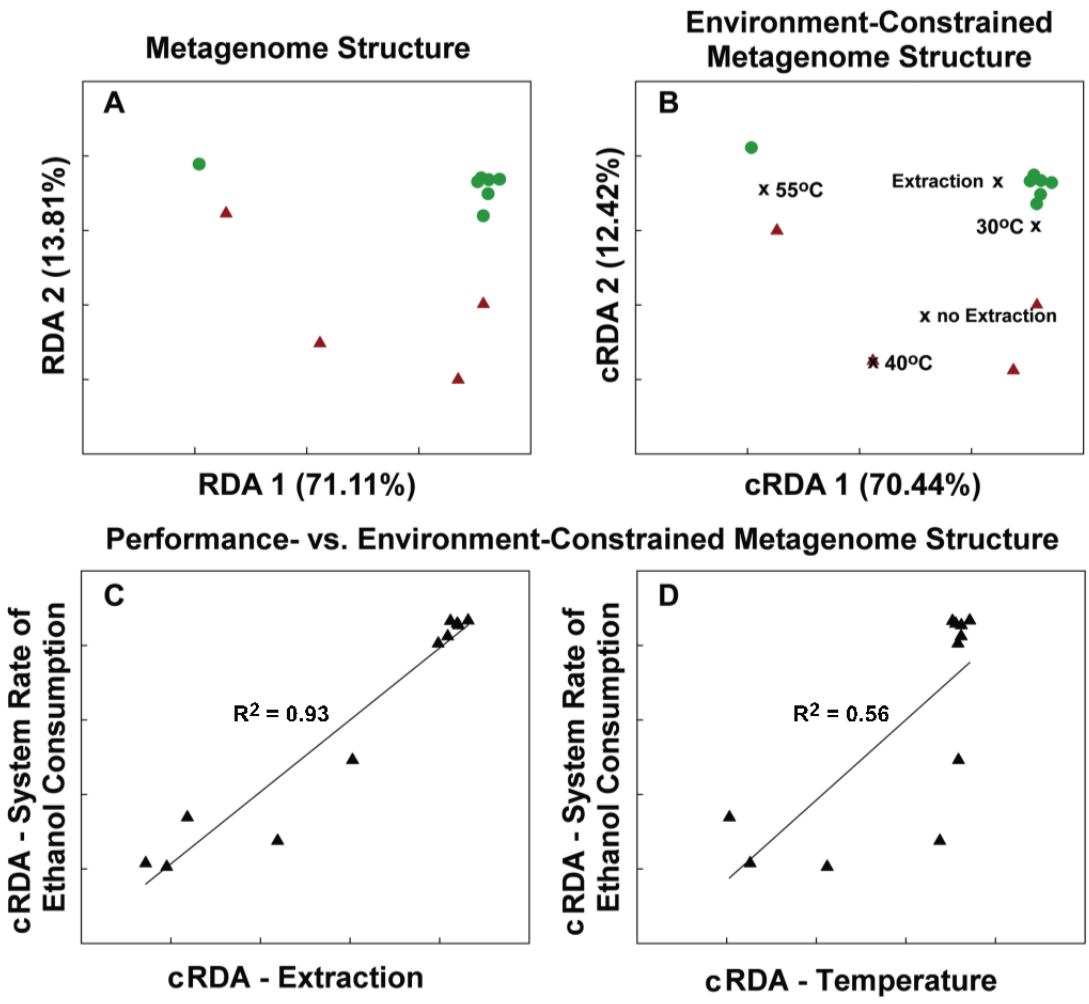

Figure 5.2. (Constrained) redundancy analysis of SEED subsystem-based functional abundance principal coordinates. Green circles correspond R_p samples and red triangles correspond to R_c samples. A. Unconstrained redundancy analysis showing as much of the functional abundance-based distance between samples as possible on two axes; B. The operating categories temperature and extraction predict ~98% of the unconstrained functional abundance-based distance between samples; C. One-dimensional constrained redundancy analysis comparison of the constraints rate of ethanol consumption (performance) and extraction (operating conditions) display a linear dynamic relationship between the variables; and D. One-dimensional constrained redundancy analysis comparison of the constraints rate of ethanol consumption (performance) and temperature (operating conditions) display a nonlinear dynamic relationship between the variables.

To further validate the inference that operating conditions dictated the metagenomic functional composition and that the functional composition was indicative of performance, we created a 100-fold bootstrapped sample-distance tree of the same

subsystem abundance data (again using Pearson distances). In the bootstrapped tree, bioreactor samples clustered by temperature, regardless of whether or not extraction was performed on the sample. Within the group of 30^{o}C samples, clustering was by whether the sample derived from R_p (extraction) or R_c (no extraction) (Figure 5.3). Furthermore, within the group of extraction samples at 30^{o}C, samples corresponding to the highest n-caproate/n-caprylate specificity clustered closely together (blue shading in Figure 5.3). Gene plots (Figure A4.S3) describing the significance of changes in gene abundance due to temperature or extraction further showed that both operating conditions had substantial effects on the community metagenome structure (529 and 101 significant genes for temperature and extraction, respectively at $p < 0.05$ and a 3-fold relative abundance shift). Therefore, the bioreactor operating conditions determined the metagenome functional structure of the mixed microbial communities, and the functional structure, in turn, was correlated with ethanol utilization for electron pushing.

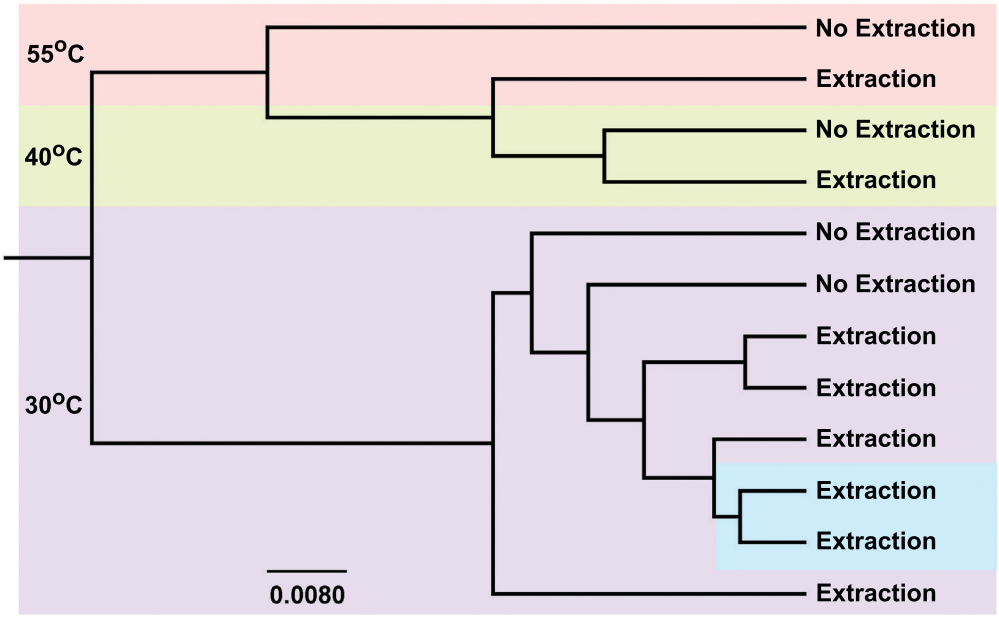

Figure 5.3. 100-fold bootstrapped sample-distance tree of the SEED subsystem-based functional abundance data, demonstrating sample clustering first based on temperature, then based on extraction or no extraction. The pair of samples shaded in blue represent samples with the highest n-caproate/n-caprylate specificity.

Gene taxonomy and performance

We already determined that the community metagenome functional composition could predict the ability of the bioreactors to accept ethanol as an electron-pushing substrate. Next, we wanted to determine if we could correlate the taxonomic distribution of genes in the bioreactor with n-caproate/n-caprylate specificity. Annotation of short shotgun-genome sequences with taxonomy should be performed carefully because the results are biased by both the database and how well conserved specific genes are between species. Thus, we searched against NCBInr, a relatively large database of gene taxonomy, and used an LCA algorithm to assign genes with hits to multiple organisms to the last common ancestor of the multiple hits. Even with these strategies, we expect bias in gene taxonomy results, therefore, we use the analysis as a tool to probe taxonomy and form hypotheses. First, we examined the distribution of taxonomy for genes assigned to

the class Clostridia in the entire metagenome of the samples (Figure 5.4A), because we expected *Clostridium kluyveri* or a similar organism to perform the chain elongation reactions [Seedorf et al., 2008]. From this analysis, it was apparent that the overall taxonomic distribution was primarily affected by temperature, with a large shift within Clostridia from primarily genes assigned to Thermoanaerobacterales to primarily genes assigned to Clostridiales. We were not able to directly correlate abundance of any Clostridia taxonomic groups with n-caproate/n-caprylate specificity.

Next, we examined the taxonomic distribution for only the metabolic pathway that *Clostridium kluyveri* uses to elongate acetate to produce n-butyrate (the same or analogous genes are used to produce n-caproate [Seedorf et al., 2008]). We found that in samples with the highest n-caproate/n-caprylate specificity, 65-75% of genes were assigned to the class Clostridia. We were surprised to find that genes assigned to the family *Clostridiaceae* (which includes *Clostridium kluyveri*) were decreasing during the operating period at 30^{o}C; note that *Clostridium kluyveri* has already been implicated in chain elongation with ethanol in undefined mixed culture fermentations at pH 7 [Steinbusch et al., 2011]. We did find two correlations to n-caproate/n-caprylate specificity at 30^{o}C: the entire order Clostridiales (R^2 = 0.87) and the family *Syntrophomonadaceae* (R^2=0.93) (Figure A4.S4). Bacteria in *Syntrophomonadaceae* (e.g., *Syntrophomonas wolfei*) are typically found in syntrophic relationships with hydrogenotrophs in anaerobic digesters, where they oxidize carboxylates [McInerney et al., 1981]. We do not expect that this was its role in these chain-elongating bioreactors for two reasons. First, *Syntrophomonas sp.* oxidation reactions are inhibited by minor buildup of carboxylates (~20 mM acetate) [Beaty and McInerney, 1989] and carboxylate

levels in our bioreactors were much higher. Second, we calculated that oxidation of n-butyrate at bulk bioreactor conditions was only marginally thermodynamically favorable at 30°C (ΔG_r = -3 kJ/mol to 0 kJ/mol, Figure A4.S5), probably not enough to support growth [Kleerebezem and Stams, 2000]. It is more likely that these *Syntrophomonadaceae* operated in a reductive fashion, similar to *Syntrophomonas wolfei* grown in pure culture on crotonate, wherein it uses an electron bifurcating pathway (oxidation of some of the crotonate for energy and reduction of some of the crotonate) similar to *Clostridium kluyveri* to produce n-butyrate and n-caproate [Beaty and McInerney, 1989]. If a *Syntrophomonadaceae* sp. was partly responsible for chain elongation, it is surprising that relatively few genes were assigned to the family in the whole metagenome taxonomic distribution (Figure 5.4A). However, other factors, such as poor specificity in taxonomic identification for *Syntrophomonadaceae* genome sequences, could obscure the population in the overall community.

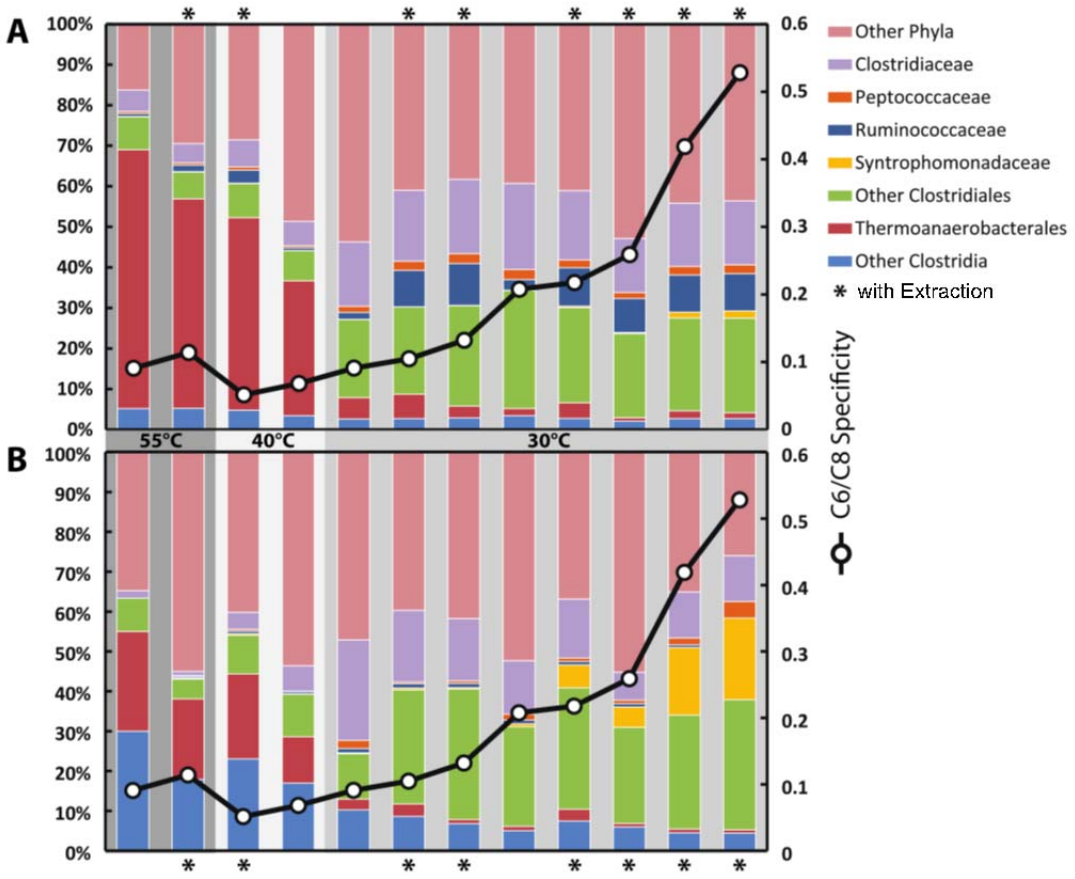

Figure 5.4. Taxonomy distribution of the class Clostridia (other phyla are shown for comparison) in genes annotated by searching against the NCBInr database, overlaid with the n-caproate (C6)/n-caprylate (C8) specificity. Bars with a * symbol are samples taken from the bioreactor with *in-situ* product extraction (R_p). The bars are organized first by temperature (from left to right), then in order of increasing n-caproate/n-caprylate specificity within temperatures; A. Taxonomic distribution within the class Clostridia for the entire metagenome; and B. Taxonomic distribution within the class Clostridia for the chain elongation pathway from acetate to n-butyrate [Seedorf et al., 2008].

Alcohol dehydrogenase gene taxonomy

Syntrophomonadaceae were correlated with n-caproate/n-caprylate specificity and these organisms have been shown to metabolize crotonate to n-butyrate and n-caproate reductively, but we found no evidence in the literature to indicate that it could elongate short-chain carboxylates with ethanol. Potentially, other microbes oxidized ethanol and *Syntrophomonadaceae* used an intermediate metabolite to produce n-caproate and n-

caprylate. We looked at the taxonomic distribution of alcohol dehydrogenase genes in our bioreactors to determine how genes were distributed among groups of organisms (Figure A4.S6). The gene distribution for ethanol oxidation, compared to chain elongation, was much more broadly distributed among bacterial taxa. Specifically, in the four samples with the highest n-caproate/n-caprylate specificity, about 20-25% of ethanol oxidation genes were assigned to various Clostridia, 5-15% were assigned to Bacilli (mostly the family Lactobacillaceae), and 15-25% were assigned to Actinobacteria (mostly the family Bifidobacteriaceae) (Figure A4.S6). We did not find significant correlations of taxonomy to performance. The wide distribution amongst taxa may indicate that several organisms were involved in ethanol oxidation. We calculated at bulk conditions during operation at 30^{o}C in R_p, that ethanol oxidation directly to acetate and hydrogen was thermodynamically favorable (Figure A4.S5), which makes oxidation by multiple species of microbes very likely.

Only a few alcohol dehydrogenase genes were assigned to Archaea (not shown), indicating that a direct coupling of ethanol oxidation and carbon dioxide reduction by a single methanogen (e.g., *Methanogenium organophilum* [Frimmer and Widdel, 1989]) was unlikely. Therefore, we expect that hydrogen utilized for carbon dioxide reduction to methane was produced when ethanol was oxidized, either directly to acetate and hydrogen, or with a coupling reaction such as chain elongation that also produced some hydrogen (Figure A4.S5).

5.4 Discussion

Bioreactor functionality is accurately linked to operating conditions through metagenomics

We determined via metagenomic analysis of carboxylate bioreactors that the variables temperature and extraction had significant effects on metagenomic functional composition of the bioreactors. Dinsdale et al. [2008] first showed that this was possible by using functional metagenomic data to show that environment (i.e., operating conditions) corresponds to metagenomic structure. In our bioreactors, temperature affected the functional metagenome content the most, which is expected because microbial colonization of diverse temperatures has required distinct evolutionary changes [Berezovsky and Shakhnovich, 2005]. The nonlinear (i.e., threshold) correlation of performance to the metagenome functional composition caused by temperature in our bioreactors is the expected, since 30^{o}C was the only temperature at which the bioreactor community could catalyze chain elongation with ethanol. Extraction was also important, and the linear correlation to performance through functional composition indicates that bioreactor metagenomes exhibited a smooth transition from no extraction and poor ability to utilize ethanol to extraction and rapid ethanol utilization. Because the main function of extraction is to remove end products, we can predict that the transition to communities allowing more electron pushing would continue along this gradient if product removal were more efficient.

Metagenome taxonomy implicates chain elongation by a consortium of microbes

We found that supplementing ethanol to bioreactors converting dilute-acid pretreated corn fiber to carboxylates at 30^{o}C while simultaneously performing *in-situ* product-specific extraction adjusts the product spectrum from primarily acetate and n-butyrate to

higher-value n-caproate and n-caprylate. Steinbusch et al. [2011] already determined in methanogen-inhibited mixed culture ethanol supplemented fermentations at pH 7, that acetate and n-butyrate are converted to n-caproate and n-caprylate. They suggested that *Clostridium kluyveri* dominated the process, but they only used selective sequencing methods (i.e., DGGE band isolation followed by cloning and sequencing). Here, we found that within genes in the chain elongation pathway, the taxonomic group correlated with n-caproate/n-caprylate specificity was the family *Syntrophomonadaceae*. Because *Syntrophomonas* sp. are known to reduce crotonate to n-butyrate and n-caproate [Beaty and McInerney, 1989], and because bioreactor conditions made oxidation of short-chain carboxylates by these species unlikely, our results suggest that species within *Syntrophomonadaceae* may have participated in chain elongation. Further, alcohol dehydrogenase genes were dispersed throughout a wide variety of taxa, and we did not find evidence in literature that cultured *Syntrophomonas* sp. are capable of ethanol oxidation (indeed, the *Syntrophomonas wolfei* genome does not contain an annotated alcohol dehydrogenase gene), indicating that electrons may have been transferred between species. Thus, our results suggest that another bacterium may be required in a hitherto undescribed mutualistic relationship. For example, ethanol oxidation could proceed directly to acetate and hydrogen and hydrogen could be used to reduce acetate to an intermediate, such as crotonate, which *Syntrophomonadaceae* can convert to n-caproate. This hypothesis requires further research because it is only based on the taxonomy of genomic DNA sequences and thermodynamic calculations. If future work shows that some microbes oxidize ethanol in the process of providing substrate for *Syntrophomonas*, maintaining a low hydrogen partial pressure with hydrogenotrophic

methanogens may be more than an added benefit: it could be a requirement to sustain a functioning community that can elongate carboxylates if the chain elongation process does not itself consume hydrogen.

Simultaneous chain elongation and carbon dioxide reduction

We showed here that the product spectrum and product specificity of undefined mixed cultures for the carboxylate platform can be significantly altered by electron pushing and simultaneous *in-situ* product-specific extraction. Further, we demonstrated that electron pushing with ethanol resulted in two simultaneous product-upgrading reactions: chain elongation of acetate and n-butyrate to n-caproate and n-caprylate and reduction of carbon dioxide to methane. In doing so, we recovered carbon in the form of methane - a useful product - that would otherwise have been lost as carbon dioxide off gas. In fact, only small amounts of carbon dioxide were present in biogas, which consisted mainly of methane. Traditional thinking had included hydrogenotrophic methanogenesis as a major "barrier" to effective carboxylate bioproduction [Agler et al., 2011; Steinbusch et al., 2009]. The basis for this is that carboxylates are oxidized by syntrophic bacteria when hydrogen partial pressures are very low, which would be counter-productive. Here, we found that at bulk bioreactor conditions when most of the hydrogen was oxidized for methane production, carboxylate oxidation was still only barely thermodynamically feasible, not enough to support the growth of syntrophic microorganisms. It could be argued that more efficient product extraction (to remove all effluent carboxylates as n-caproate and n-caprylate) would result in more methane production, lower hydrogen partial pressures, and the onset of carboxylate oxidation. However, our metagenome functional ordinations showed that more efficient product

removal should also result in more efficient reduction of carbon dioxide with ethanol. This phenomenon could cause an *increase* in hydrogen partial pressures because there would be very little carbon dioxide remaining as an electron acceptor for hydrogen oxidation. In this case, bioreactor design could include a catalytic system to remove excess hydrogen or should allow for external carbon dioxide supplementation to encourage hydrogenotrophic methanogenesis.

Metagenomics yields valuable information to direct future work to improve stability

Based on the functional content of bioreactor metagenomes, we determined with statistical certainty that effective electron pushing with ethanol is only possible at low temperature (30^{o}C) and with efficient product-specific extraction. This system resulted in up to 54% n-caproate/n-caprylate specificity and fermentation product rates of n-caproate/n-caprylate that were 6 times those without product specific extraction. The approach we used combined relatively low-cost (~$250 per sample) metagenomic sequencing methods with ecological techniques to precisely determine the operating conditions/performance relationship in bioreactors converting dilute-acid pretreated corn fiber to n-caproate and n-caprylate. This application of metagenomics, which builds on work already performed by Dinsdale et al. [2008], is a diversification from previous bioreactor metagenomic studies that focus on covering as much of the metagenome as possible (at a higher cost per sample) to infer relationships and to discover new genes [Schluter et al., 2008]. This new application is important because it represents an opportunity to further improve performance of the carboxylate platform for which direct links between operating conditions and performance has until now yielded conflicting results.

5.5 Acknowledgements

This project was supported by the National Research Initiative of the USDA Cooperative State Research, Education and Extension Service, grant number 2007-35504-18256. A special thanks to Arjan Dekker and Jack Yi for support in development of the product extraction methods.

CHAPTER 6.

SUMMARY AND RECOMMENDATIONS FOR FUTURE WORK

This chapter is not published.

6.1 Summary

The carboxylate platform transforms biomass feedstocks into valuable biochemicals, using at least one bioprocess catalyzed by anaerobic undefined mixed cultures of microbes that transform the (pretreated) feedstock into carboxylates (Chapter 2). Bioprocesses with undefined mixed cultures of microbes have, thus far, largely focused on anaerobic digestion of biomass to produce methane as an end product (*via* carboxylates as intermediates). In all carboxylate platform processes, carboxylates are always an intermediate from primary fermentation (i.e., conversion of biomass into the products ethanol, acetate, propionate, lactate, and n-butyrate). Methane production is a secondary fermentation process (i.e., coupled oxidation of high energy primary fermentation products to reduction of low-energy primary fermentation products) that results in excellent product yields and specificity. While we have shown that methane production is a valuable application of the carboxylate platform for industries with high-energy waste streams (Chapter 3), we have also determined that application of principles that cause efficiency in anaerobic digesters can also guide new processing techniques that produce carboxylates as end products (Chapter 4 and Chapter 5). Development of carboxylate platform bioprocesses to produce carboxylates have, thus far, struggled to achieve high product yields and specificity because the systems are not well understood.

We showed that application of ecological methods to high-throughput analysis of bacterial community structure has the potential to bring more certainty to predictions relating function to environmental factors, such as end product inhibition (Chapter 4). We also found that the structure of bacterial communities were substrate dependent and that secondary fermentation processes should be manipulated to maximize yields and specificity (Chapter 4). Finally, we found that "electron pushing" (i.e., addition of a substrate, such as ethanol, to upgrade fermentation products) combined with *in-situ* product specific extraction can improve product specificity in carboxylate platform bioreactors (Chapter 5). Functional metagenomic analysis showed that the dynamic relationship between environment (i.e., operating conditions) and function (i.e., performance) can be revealed with ecological techniques and that these relationships generated information about further improving community performance (Chapter 5). In addition, we discovered that the pathway for chain elongation with ethanol (i.e., coupled ethanol oxidation and n-butyrate reduction to n-caproate and n-caprylate) in the bioreactors may proceed via a consortium of microorganisms and that this has implications for defining optimum operating parameters (Chapter 5). The findings here bring up new potential applications and further questions about functionality of the carboxylate platform. In light of the data from these studies, several recommendations for future work follow.

6.2 Recommendations for Future Work

Conversion of "beer" from the ethanol industry to medium-chain carboxylates

In Chapter 3, we found that by producing methane from thin stillage (i.e., essentially the waste left over after distillation to remove ethanol from fermented "beer"), corn-kernel to ethanol plants could offset a significant amount of the energy they consume. Most of the energy consumed in the plants is for distillation (Chapter 2), which upgrades ethanol from low concentrations in beer (with little value) to a 95% pure form that is valuable as a fuel and chemical feedstock. In Chapter 5, we found that ethanol pushing helped to increase the value of carboxylate products fermented from dilute-acid pretreated corn fiber to n-caproate and n-caprylate. Further, n-caproate and n-caprylate are easy to extract with membrane-based systems, which uses little energy (other than producing alkali chemicals to maintain the pH gradient). This represents a new method to indirectly recover ethanol while converting both the ethanol and lignocellulosics contained in "beer" to a specific end product. The economic and environmental sustainability of this process is unclear, and an assessment should include a full life-cycle analysis.

Lactate chain elongation in thermophilic bioreactors

In Chapter 4, we discovered that lactate was produced as an intermediate during the feeding cycle of the bioreactors producing primarily n-butyrate, because of fermentation of saccharides for pretreatment of corn fiber. Lactate was most likely consumed by a coupling of lactate oxidation to acetate and n-butyrate reduction to produce n-butyrate and n-caproate, respectively (i.e., lactate chain-elongation), perhaps by a member of the genus *Thermosinus*. In Chapter 5, we found that bioreactor communities were incapable of catalyzing ethanol chain-elongation at thermophilic (55^{o}C) temperatures, and functional metagenomics confirmed that the community was incapable of performing the

process at these conditions. Thus, lactate should be evaluated as an electron-pushing substrate to upgrade the product spectrum in thermophilic bioreactors. In that study we correlated n-caproate production with *Thermosinus*, but it is possible that *Thermosinus* is only involved in an aspect of the chain elongation. Therefore, the process should be evaluated in lab-scale carboxylate platform bioreactors, coupled with a functional metagenomic analysis to evaluate which factors contribute to lactate chain elongation so that the process can be optimized. Based on our results with ethanol chain elongation, the study should focus on whether product extraction is required for chain elongation and whether or not significant increases in extraction efficiency improve performance.

The role of community evenness in thermophilic bioreactors

Research has already revealed that community evenness is important in maintaining ecosystem function under stress in mixed microbial communities [Werner et al., 2011b; Wittebolle et al., 2009]. In Chapter 4 we discovered that our thermophilic bioreactor communities were relatively uneven, and it is unclear if this is a function of temperature, toxicity of end products, or both, or if an uneven structure is relative and is always a result of thermophilic temperatures. To study the stability of thermophilic systems, future research should implement high-throughput 16S rRNA gene surveys of microbial community structures in bioreactors to evaluate evenness under a range of conditions. One possible scenario would compare four bioreactors fed the same lignocellulosic substrate with key differences: 1. A mesophilic anaerobic digester supplemented with lactate and with optimum conversion of carboxylates to methane, 2. A thermophilic anaerobic digester supplemented with lactate and with optimum conversion of carboxylates to methane, 3. A thermophilic bioreactor supplemented with lactate to

accumulate a mix of carboxylates, and 4. A thermophilic bioreactor supplemented with lactate and with high-rate product specific extraction to remove nearly all carboxylates from the system. This scenario would determine whether thermophilic temperatures are cause for uneven communities in bioreactors, if product removal is responsible for improvements in evenness in thermophilic environments, or if anaerobic digestion results in an even community because of the series of metabolic conversions required to completely convert substrate to methane.

Chain elongation pathways in ethanol-supplemented bioreactors

Previous research demonstrated with selective 16S rRNA gene sequencing techniques (i.e., DGGE followed by manual band selection, isolation, and cloning) that chain elongation with ethanol as the electron pushing substrate at pH 7 was catalyzed by microbial communities dominated by *Clostridium kluyveri* (26/45 clones had 98% sequence similarity to *C. kluyveri*) in their bioreactors [Steinbusch et al., 2011]. In Chapter 5, our metagenomic survey indicated that more than one microorganism (including a member of the family *Syntrophomonadaceae*) might be responsible for chain elongation with ethanol at pH 5.5. If this is true, it is important to reveal the mechanisms of the chain elongation process to help reveal how different operating conditions would affect the process. For example, a distribution of the three metabolic functions ethanol oxidation, intermediate metabolite formation, such as crotonate, and conversion of intermediates to n-caproate would force a reevaluation of what is considered to be an optimum environment. Experiments should use high-throughput 16S rRNA sequencing, possibly combined with standard Sanger sequencing of isolated or enriched microbes or consortia and/or Sanger sequencing of isotope-labeled "heavy" 16S rRNA genes (i.e.,

DNA-SIP) to determine with more certainty which microorganisms are responsible for chain elongation. After this analysis, hypotheses can be made about whether or not direct oxidation of ethanol to acetate and hydrogen is necessary for chain elongation, or if other intermediates contribute to syntrophic relationships leading to chain elongation, and further experiments can determine the precise mechanisms in the bioreactors.

Further research on the implications of methanogenesis for chain elongation

In Chapter 5, we found that hydrogenotrophic methanogens could reduce carbon dioxide to methane side-by-side with chain elongation reactions that produce medium-chain carboxylates, even though the hydrogen partial pressure was very low. This finding alters the prevailing view that methanogens must be inhibited to prevent loss of product to competing processes [Agler et al., 2011; Steinbusch et al., 2009]. While we did show that n-butyrate oxidation would be unlikely at our bioreactor conditions, we did not perform experiments to prove that we did not experience some loss of product to oxidation reactions. We also were unable to determine if high-efficiency product extraction would allow the onset of carboxylate oxidation. If necessary, methanogens can be inhibited at both thermophilic (Appendix 2) and mesophilic [Steinbusch et al., 2009; Van Kessel and Russell, 1996] temperatures, but the two prevailing techniques, chemical additives and carboxylate inhibition, add cost and limit bioreactor productivity, respectively. Further, the added benefit of increased carbon recovery would be lost. Thus, experiments should determine with more certainty if a bioreactor pH of 5.5 at mesophilic temperatures prevents carboxylate oxidation so that methanogenesis and chain elongation with ethanol can exist together side-by-side (or if product extraction out-competes carboxylate oxidation). Experiments should also explore our hypothesis that

for chain elongation at pH 5.5, hydrogenotrophs are required to maintain a low hydrogen partial pressure for bioreactor functionality (Chapter 5).

Isolation and characterization of chain elongating microbes and/or consortium

In parallel to experiments studying optimization of chain elongation with lactate or ethanol at thermophilic and mesophilic temperatures, respectively, isolated microbes or microbial consortia should be cultured and characterized. In thermophilic systems, we expect this to include species within *Thermosinus* that catalyze chain elongation of acetate and n-butyrate with lactate. Because other related microbes have been described that convert lactate to n-caproate [Marounek et al., 1989], we hypothesize that one microbe may be responsible for this reaction. In mesophilic systems, we have hypothesized that a consortium of microorganisms is responsible for chain elongation with ethanol. Culturing the responsible consortia should be followed by metabolic analysis with stable isotopes to determine which intermediate chemicals are involved. If direct ethanol oxidation to acetate is involved, the ethanol-oxidizing microbe could be isolated on ethanol with artificial hydrogen removal or in culture with a hydrogenotrophic microorganism. Once intermediates are identified, the culture could be fed the intermediate substrate to enrich a specific community member and DNA-SIP could be used with a labeled carbon source to determine with certainty which microorganisms are responsible for chain elongation.

APPENDIX 1.

SUPPLEMENTAL INFORMATION FOR: THERMOPHILIC ANAEROBIC DIGESTION TO INCREASE THE NET ENERGY BALANCE OF CORN GRAIN ETHANOL

Summary

This supporting material provides additional information on bioreactor setup (A1.S1 and Figure A1.S1); the nitrogen mass balance (A1.S2); trace element limitations (A1.S3) and effluent COD and VS/TS characteristics (Table A1.S2); oxygen influx (A1.S4); the methane yield (Figure A1.S2); biomass characteristics (A1.S5 and Figures A1.S3 and A1.S4); energy supplement calculations (A1.S6 and Table A1.S2); pH over the operating period (Figure A1.S5); and SEM pictures and X-ray powder diffraction spectra for characterization of struvite (Figure A1.S6).

A1.S1 Experimental Setup

The experimental setup included two identical lab-scale bioreactors (Mid-Rivers Glassblowing, Inc., St. Charles, MO), R1 and R2, each with a 5-l working volume (Figure A1.S1). The bioreactors included a water jacket connected to a heating recirculator (Model 210, PolyScience, Niles, IL) to maintain a constant temperature of 55 ± 1^{o}C. Mixing was provided by recirculating headspace gas to the conical bottom of the bioreactor with a peristaltic pump (Cole-Parmer Instrument Co., Vernon Hills, IL). A glass tube extending to the 3-l level of the bioreactor was used to feed thin stillage once

every day without headspace gas loss. A similar tube was used to decant effluent with a peristaltic pump. The gas collection system included a foam collection bottle, a gas sampling port, pressurized balls to prevent air entrance during decanting of effluent, a bubble counter to visualize gas flow, and a gas meter (Actaris Meterfabriek B.V., Dordrecht, The Netherlands).

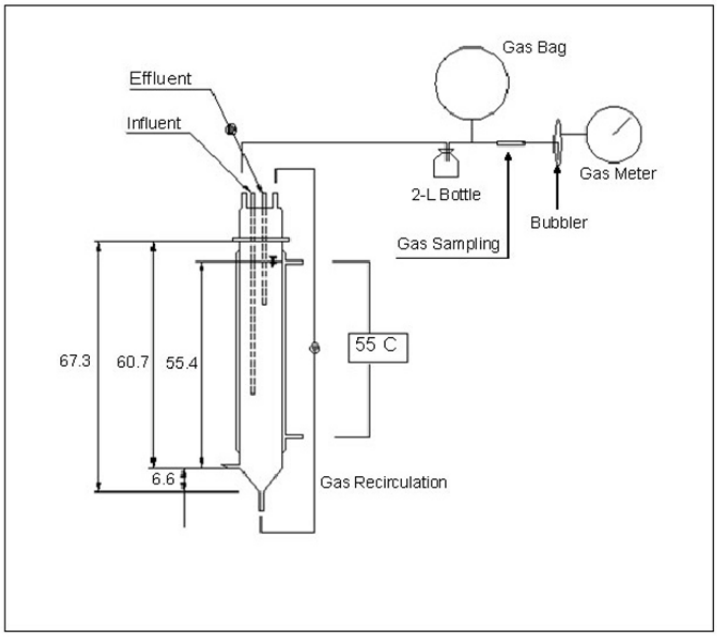

Figure A1.S1. Setup of a 5-l thermophilic anaerobic sequencing batch bioreactor (ASBR) for the bioconversion of thin stillage to methane (R1 and R2). Lengths in cm.

A1.S2 Nitrogen Balance

Assuming all nitrogen in the influent and effluent are contained in protein and ammonia species, the nitrogen balance was:

$$N_{total} = N_{protein} + N_{ammonium}$$

$$N_{protein} = \text{Protein} \cdot (\text{g N/g protein})$$

,where:

$N_{protein}$ = concentration of N bound in protein

$N_{ammonium}$= total concentration of NH_4^+-N (ammonia and ammonium)

Protein = concentration of total protein

(g N/g protein) = 0.16 g/g [Wang et al., 2003]

To measure the N composition of the struvite precipitate, a known amount of precipitate was dissolved in 1 mL concentrated hydrochloric acid and neutralized (to pH 7.0) by diluted sodium hydroxide. Next, the total ammonium concentration in the solution was measured by the colorimetric phenate method with an end point reading at 640 nm and ambient temperatures [APHA, 1998]. Total ammonium standards were made as described in *Standard Methods* [APHA, 1998], except we used a solution of sodium chloride instead of pure water with a concentration that was equal to that of the neutralized hydrochloric acid solution.

A1.S3 Trace Element Limitations

The initial start-up period of 49 days showed low total VFA concentrations of 170 mg CH_3COOH/l (SE =75.6, n =13) and 112 mg CH_3COOH/l (SE = 55.5, n = 13) in the effluent of R1 and R2, respectively, which showed that startup was progressing in a stable manner (Figure 3.1B of main text). However, on day 49 of the operating period the VFA levels began to rise in both bioreactors (Figure 3.1B). They continued to rise until day 78 (to ~ 2,900 mg CH_3COOH/l in R1), negatively impacting bioreactor performance with decreasing biogas production rates (Figure 3.1A). On day 78 of the operating period, 5 ml of a mixed solution of several trace elements was added to R1. A rapid decrease in the effluent VFA concentration to ~ 200 mg CH_3COOH/l by day 99 and an increase in biogas production was observed (Figures 3.1A and 3.1B), implicating trace element deficiencies as the reason for digester instability. After day 92, a cobalt solution was added to R2 rather than a mixed trace element solution. This was done after finding that adding solely iron on day 85 of the operating period had no effect on bioreactor performance. Similarly to the mixed trace element solution augmentation, the performance improved immediately after adding the cobalt solution with total VFA levels decreasing to ~ 200 mg CH_3COOH/l on day 99 and biogas production rates returning to stable levels (Figures 3.1A and 3.1B). A new batch of thin stillage feed was initiated on day 106 of the operating period with higher VS and TCOD concentrations (Table 3.1) without increasing the cobalt supplementation. A subsequent rise in the total VFA concentration in R2 from ~ 100 to ~ 900 mg CH_3COOH/l between days 113 and 119 was found (Figure 3.1B), which was immediately reversed after returning to the rate of cobalt augmentation of 1 ml/10 g influent TCOD once a week. The rate of augmentation of

cobalt solution was constant from day 120 until the end of the operating period for both bioreactors.

Table A1.S1. Characterization of effluent from thermophilic anaerobic digesters R1 and R2.

HRT (RX)	SCOD (g/l) % Removal	TCOD (g/l) % Removal	VS (g/l) % Removal	TS (g/l) % Removal
40 (R1)	3±0.5, n=3 96.97	16±3, n=2 83.68	6.65±2.77, n=4 82.17	9.85±3.76, n=4 76.6
40 (R2)	3.5±1.5, n=3 96.38	16±11.5, n=2 83.47	6.18±2.46, n=4 83.43	9.04±3.27, n=4 78.52
30 (R1)	5.5±2, n=3 94.52	14±5.5, n=4 85.33	4.72±0.15, n=3 87.34	8.26±0.37, n=3 80.38
30 (R2)	5.5±2.5, n=3 94.52	12±2.5, n=4 87.35	4.71±0.10, n=3 87.37	8.06±0.02, n=3 80.85
25 (R1)	2.5±1, n=3 97.33	7±1, n=3 93.01	4.97±0.07, n=3 89	8.63±0.13, n=3 82.72
25 (R2)	3.5±0.5, n=3 96.34	8.5±0.5, n=3 91.37	5.15±0.11, n=3 88.6	9.63±1.85, n=3 80.71
20 (R1)	3±0.5, n=4 96.85	6.5±2.5, n=4 92.8	4.19±0.51, n=6 89.82	7.66±0.76, n=6 83.31
20 (R2)	3±0.5, n=4 96.57	6.5±2.5, n=4 92.68	4.90±0.53, n=6 88.09	8.51±0.52, n=6 81.46
15 (R1)	2.5±0.5, n=7 97.11	8.5±2.5, n=6 89.73	3.71±0.97, n=11 89.23	7.13±1.14, n=11 81.79
15 (R2)	2.5±0.5, n=5 96.59	7.5±4, n=4 90.53	3.92±0.97, n=9 88.82	7.34±1.13, n=9 81.53
10 (R1)	3±0.5, n=3 96.27	7±0.5, n=3 90.48	3.41±0.78, n=4 89.29	6.94±0.83, n=4 81.05
10 (R2)	3±0.5, n=5 95.79	6±2.5, n=5 92.2	3.42±0.50, n=5 89.21	7.15±0.62, n=5 80.31

A1.S4 Oxygen Influx

Thirteen days after reaching the design HRT of 10 days, R1 was impacted by accidental oxygen exposure (day 284), while R2 continued to operate normally. Oxygen inhibition to methanogens severely retarded the stability of R1, and for the following 30

days, the effluent total VFA concentrations were above 2,000 mg CH_3COOH/l (Figure 3.1B). To stabilize R1, we reduced the HRT from 10 to 40 days on day 310 of the operating period (not indicated in Figure 3.1) and added diluted (1 M) sodium hydroxide on days 313 to 316 until the pH was increased from 6.64 to 6.86. The bioreactor pH subsequently began to increase without sodium hydroxide addition to 7.08 on day 319 (Figure A1.S5). The HRT was reduced to 30 days on day 319, and eventually to 10 days by a step-wise shortening of the HRT during a period of 43 days (day 319 to 362). Thus, R1 was able to recover from unstable conditions within a period of 2 months. This accident resulted in a shorter period of 30 days (3 HRT periods) during which R1 was operated at a 10-day HRT compared to R2 (121 days or 12 HRT periods).

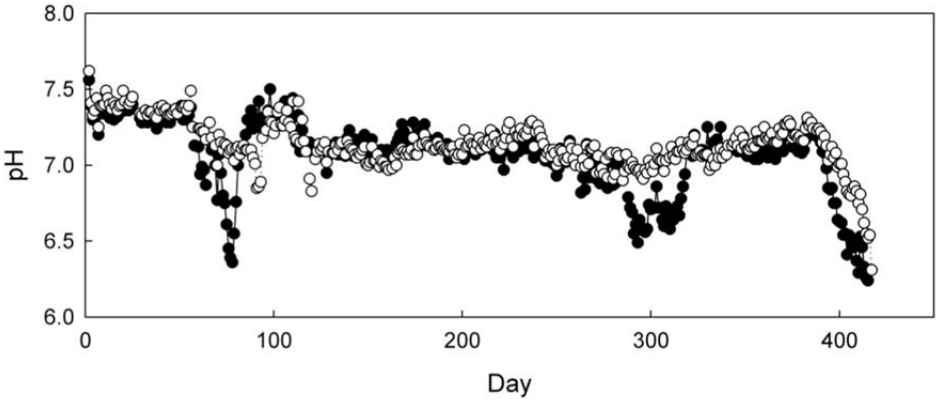

Figure A1.S5. pH level of bioreactor effluent over the operating period (● – R1; ○ – R2).

A1.S5 Biomass Characteristics

During the initial 200 days of the operating period, the VS concentrations in both bioreactors increased slowly and then reached a plateau (Figure 3.1C). There are two reasons for this increase in VS concentration: 1. no deliberate (by opening a valve) or natural wasting (by effluent flow) of biomass took place: during the initial 200 days of the operating period, the top of the biomass blanket had not reached the 3-l working volume height (the inlet of the effluent tube) after the settling period; and 2. the settleability of the biomass increased, which was shown by a decreased SVI (Figure A1.S3), resulting in a more dense biomass blanket. After day 200 of the operating period, VS levels in the effluent showed periodic spikes. For example, the temporary increases in effluent VS during the 15-day HRT around day 230 for R1 and days 255 and 330 for R2 were due to natural biomass wasting rather than bioreactor instability. This wasting of biomass was a natural process, which allowed for selection of better settling biomass. Despite not having a proper selection pressure on the bioreactors, some anaerobic granules (i.e., separate biomass entities after settling of most biomass with a

size of several mm) were found in the biomass of the bioreactor and floating on the top of the liquor (Figure A1.S4). Deliberate wasting of surplus biomass from the bioreactor by opening a valve can prevent periodic higher VS levels in the effluent during full-scale treatment (however we did not perform deliberate wasting in this study). A better settleability of the biomass after day 200 of the operating period, and thus a slightly higher SRT, resulted in the generally lower VS concentration in the effluent, with a combined average of 3.50 g/l (SE = 0.85 g/l, n = 69) during days 200-391 compared to 4.55 g/l (SE = 0.62 g/l, n = 73) during days 50-200 of the operating period (Figure 3.1C). At the design HRT of 10 days, the biomass VS averaged 12.0 g/l (Figure 3.1) and the methane production was 2.00 l CH_4/l/d (4.76 g CH_4-COD/l/d). Therefore, the calculated methanogenic activity based on mixed liquor VS was 0.40 g CH_4-COD/g VS/d.

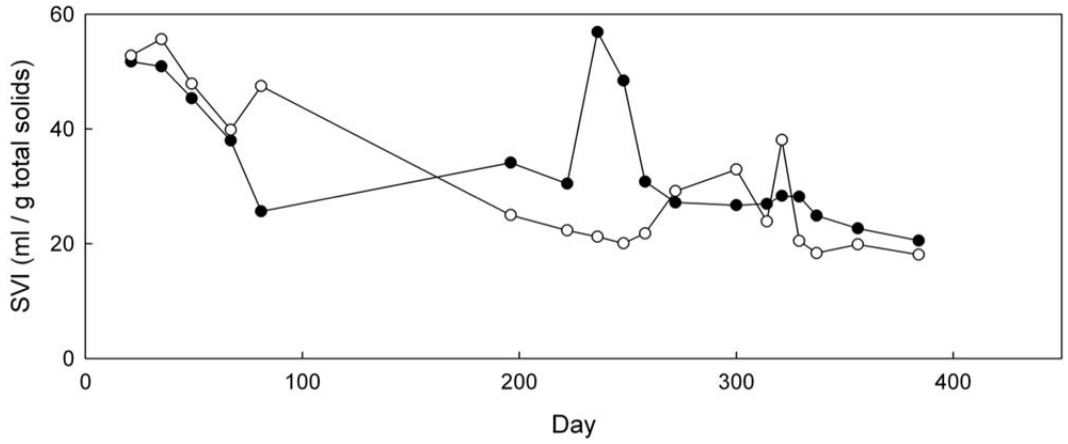

Figure A1.S3. Sludge volume index (SVI) of the ASBRs over the operating period (● – R1; ○ – R2).

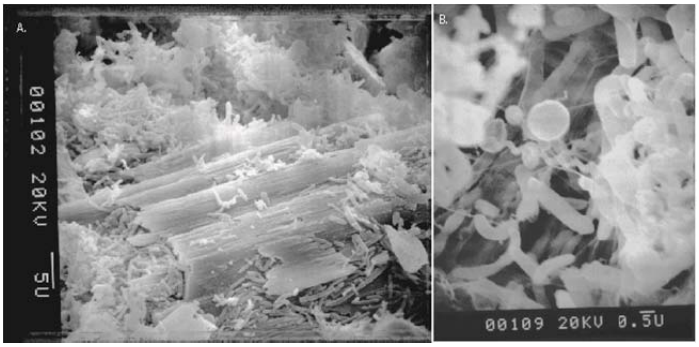

Figure A1.S4. SEM images of biomass granules. A. Biofilm growing in proximity of and on fiber particles (2,000 x magnification); and B. Surface of granule (10,000 x magnification).

A1.S6 Energy Supplement Calculations

To carry out energy supplement calculations, we used full-scale nonrenewable energy consumption and thin stillage production data for a $3.78 \cdot 10^8$ l ethanol per year (100 million U.S. gallon per year) dry-mill ethanol facility (Table A1.S1). Since wet distillers' grain and syrup dry weight data per volume of corn grain (kg/m^3) make up the dry weight of DDGS per volume of corn weight, we could use data from a full-scale dry mill to calculate the 45% feed mass reduction without syrup addition (Table A1.S1, a). The full scale facility used in this example has a typical natural gas requirement (for conventional dry mills, natural gas is used in boilers to produce steam, thermal oxidizers to remove volatile organic compounds from off gases, and flash dryers to dry DDGS) of $4.02 \cdot 10^8$ kJ/h. In our calculation this requirement is reduced by: **1.** the amount of natural gas that was originally dedicated to flash drying of syrup (7.62%) because syrup will no longer be added to wet distillers' grain for animal feed production. This percentage reduction was derived from the percentage of the total energy input dedicated to DDGS (16.86%) multiplied by the mass percentage of DDGS stemming from syrup (45.19%). The resulting natural gas requirement without syrup drying is $3.71 \cdot 10^8$ kJ/h (Table A1.S1, b);

and **2.** the amount of natural gas used at the conventional dry mill, which can be replaced by the methane generated in thermophilic anaerobic digestion (42.94%). The methane yield for the calculation (0.254 l CH_4/g TCOD) is the combined yield from R1 and R2 based on our study (Figure A1.S2). The calculation for energy production rate from methane is based on the lower heating value of methane in biogas (Table A1.S2, c). The percentage reduction from the energy required for a conventional plant is then 50.56% based on the energy production form methane (Table A1.S2, c) subtracted from the natural gas requirement without syrup drying (Table A1.S2, b). The processing energy input (per unit energy in ethanol) that was assessed by Hill et al. [2006] was reduced by this percentage of ~ 51% in Table A1.S2 (d-1 and d-2). We also reduced the energy output for feed credit (per unit energy in ethanol) (Table A1.S2, e) because of the ~ 45% reduction in animal feed quantity based on mass (Table A1.S2, a). The new values of 0.655 and 1.112, respectively (Table A1.S2, f), represent the new total input and output (per unit energy in ethanol) values for a dry mill with integrated thermophilic digestion of thin stillage, resulting in a new net energy balance (the ratio of output to input) of 1.70. We have not included the freed waste heat from circumventing evaporation in the calculation of the new net energy balance ratio. In conventional dry mills, triple or quadruple-effect evaporators (~ 80% efficiency) are used to evaporate the ~ 143,000 kg of water per h (data from a $3.78 \cdot 10^8$ l ethanol per year dry mill). All of the required $1.43 \cdot 10^8$ kJ/h of energy for thin stillage evaporation is provided from low-grade energy derived from the original $4.02 \cdot 10^8$ kJ/h input for steam generation and thermal oxidation.

Table A1.S2. Calculation of the percentage of required nonrenewable energy input that can be replaced by methane from thermophilic ASBRs and the change of the NEB ratio for a $3.78 \cdot 10^8$ l ethanol per year corn grain-to-ethanol plant with an integrated thermophilic ASBRs.

Energy Input Source (per unit energy in ethanol)	Ethanol	DDGS	Total		
Farm*	0.249	0.051	0.300		
Processing*	0.498	0.101	0.599		**d-1**
Construction and Labor*	0.008	0.001	0.009		
Transport*	0.042	0.008	0.050		
Total*	0.797	0.161	0.958		
Energy Output (per unit energy in ethanol)					
Ethanol*	1.000				
Feed Credit*	0.203				**e**
Total*	1.203				
Original Net Energy Balance Ratio*	1.26				
Processing					
Natural Gas Requirement in Conventional Plant** [kJ/h]	$4.02 \cdot 10^8$				
Percent of Total Energy input to DDGS (from processing data)*	16.86%	(due to flash drying)			
Processing with Anaerobic Digestion					
Wet Distillers' Grain in Conventional Plant** (dry weight in kg/m^3)	107.96				**a**
Syrup Production in Conventional Plant** (dry weight in kg/m^3)	89.00				**a**
Feed Mass Reduction without Syrup Drying**	45.19%				**a**
Natural Gas Requirement without Syrup Drying [kJ/h]	$3.71 \cdot 10^8$				**b**
Thin Stillage Flow** [l/h]	$1.90 \cdot 10^5$				**c**
Thin Stillage TCOD concentration*** [g TCOD/l]	$1.00 \cdot 10^2$				**c**
Methane Yield*** [l CH4/g TCOD]	$2.54 \cdot 10^{-1}$				**c**
Methane Production Rate [l CH4/h]	$4.83 \cdot 10^6$				**c**
Methane Heat Content**** [kJ/l CH_4] (Lower Heating Value)	$3.58 \cdot 10^1$		Energy Production [kJ/h]		$1.73 \cdot 10^8$
Percent Reduction From Conventional Plant (due to Methane Generation and without Syrup Drying)					50.56%
New Processing Energy Input (per unit energy in ethanol)	0.296				**d-2**
New Total Energy Input (per unit energy in ethanol)	0.655				**f**
New Total Energy Output (per unit energy in ethanol)	1.112				**f**
New Net Energy Balance Ratio	1.70				

*Hill et al. [2006]
**$3.78 \cdot 10^8$ l/yr full-scale dry mill data
***This Study
****Tchobanoglous et al. [2003]

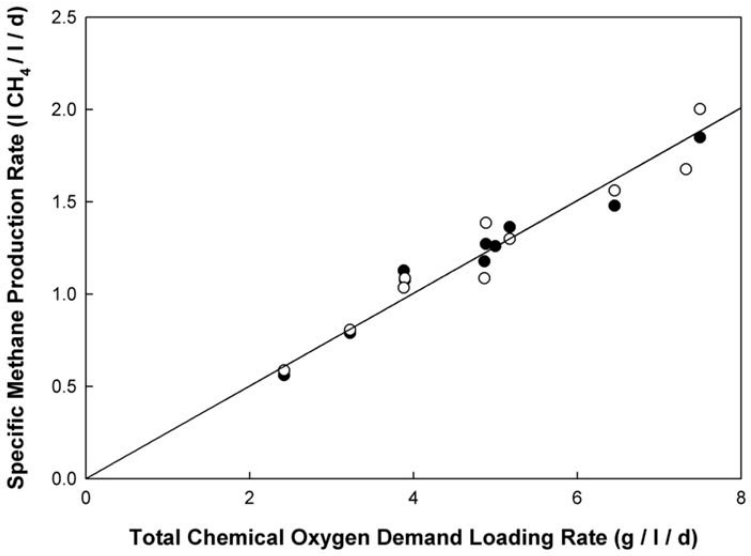

Figure A1.S2. Methane yield graph for R1 and R2. The combined yield was 0.254 l CH_4/g TCOD fed with a R^2 value of 0.99 (● – R1; ○ – R2).

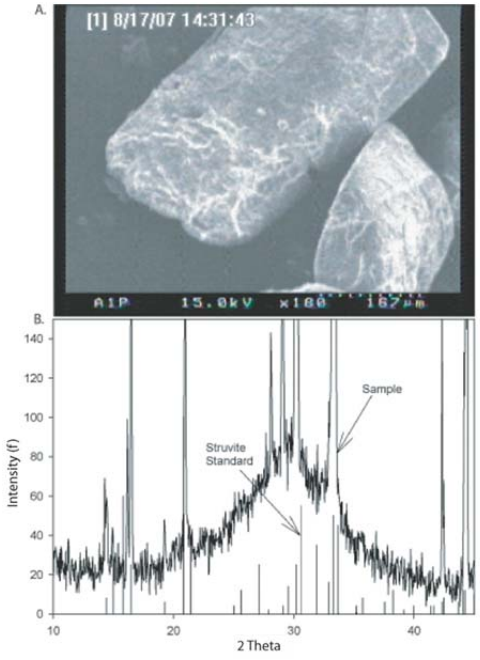

Figure A1.S6. Individual crystals of struvite: A. SEM view of the crystals (100 x magnification); and B. X-ray powder diffraction intensity scan of the crystals. The peak at 2Θ = 20 to 40 indicates an amorphous structure. This scale does not show the top of the peaks with the goal to provide a higher resolution. Standard is provided for reference.

APPENDIX 2.

HYDROGENOTROPHIC METHANOGEN INHIBITION DUE TO UNDISSOCIATED CARBOXYLIC ACID TOXICITY

A2.1 Introduction

Complete inhibition of methanogenesis has been implicated as being important in securing efficient production of carboxylates in the carboxylate platform [Shin et al., 2004]. Methods of inhibition for undefined mixed cultures of microbes include heat shock [Oh et al., 2003] and chemical additions (such as 2-bromoethanesulfonate) [Zinder and Koch, 1984], both of which add operational costs. Researchers have already shown that the undissociated form of carboxylic acids (specifically acetic acid) are toxic to methanogens at mesophilic (37^{o}C) conditions [Van Kessel and Russell, 1996]. They attributed the mechanism of toxicity to intracellular accumulation of carboxylate anions when bulk bioreactor pH was acidic. Therefore, to inhibit methanogens in a carboxylate platform process that is designed to produce (and thus would accumulate) carboxylate endproducts, low pH is an effective treatment. Here, we sought to determine if the same mechanism could inhibit hydrogenotrophic methanogenesis at thermophilic temperatures.

A2.2 Methods

Batch hydrogenotrophic methanogen inhibition

We inoulated 150-mL batch fermentation vessels with thermophilic sludge from a municipal wastewater treatment plant (Western Lake Superior Sanitary District, Duluth, MN). All batch reactions were carried out in triplicate. In short, in an anaerobic hood,

we added 7.5 mL basal medium (described elsewhere [Agler et al., 2010]), a predetermined amount of 1 M n-butyric acid (depending on the desired conditions), 100 mM MES to a total volume of 72.75 mL, 2.5 mL thermophilic sludge, corrected to the correct pH at 25^{o}C (corresponding to 5.5, 5.75, or 6.0 at 55^{o}C), added 0.25 mL Na_2S, capped the bottles with butyl rubber stoppers and crimp caps, and flushed each bottle with N_2 for 10 min. We incubated the bottles overnight with a 50/50 mixture of hydrogen/carbon dioxide and waited until methane headspace composition reached 10%. At this point we flushed bottles with nitrogen, added 75 kPa of 50/50 H_2/CO_2, and sampled periodically to record the rate of methane production. At the end of the run, we measured the volatile suspended solids (VSS) in the solution to normalize methane production rates for the amount of biomass in each batch bottle. Reported values are averages of the triplicates.

Batch hydrogenotrophic methane formation in bioreactor mixed liquor

We tested for hydrogenotrophic methane formation in mixed liquor taken from a bioreactor optimized for n-butyrate production during a 300-d operating period. We performed triplicate 150 mL batch fermentations, as described above, except that we used bioreactor mixed liquor as inoculum and the medium contained 48.5 mM acetate and 20.5 mM n-butyrate, approximately corresponding to the bioreactor composion. We added a 50/50 mixture of hydrogen/carbon dioxide, resulting in ~6-7 mmol of each per gram of volatile solids added as inoculum. This time we measured hydrogen, carbon dioxide, and methane biogas composition over the course of a 144-h operating period.

A2.3 Results

We tested inhibition of thermophilic hydrogenotrophic methanogens via carboxylate toxicity with batch incubations of thermophilic sludge from an anaerobic digester. We found that thermophilic hydrogenotrophic methanogenic activity (measured in terms of mL CH_4 g volatile suspended solids $(VSS)^{-1}$ d^{-1}) decreased substantially in the presence of high concentrations of total n-butyrate (Figure A2.1A, Table A2.1). The inhibition was much more pronounced at pH levels below 6, indicating that undissociated n-butyric acid may be responsible for inhibition. We extrapolated to 90% inhibition and found that it occurred in the range of 13.6 – 31.4 mM undissociated n-butyric acid at a pH of 5.5 – 6 (Table A2.1). This is a small range compared to the extrapolated 90% inhibition by total n-butyrate, which were 96.1 – 435.1 mM, which indicates that undissociated butyric acid is the inhibiting form of the acid.

Table A2.1. n-Butyrate and n-butyric acid levels (extrapolated from Figure A2.1A) to achieve 90% inhibition of hydrogenotrophic methanogenic activity.

pH	Total n-Butryate (mM)	Undissociated n-Butyric Acid (mM)
5.50	96.1	18.9
5.75	111.9	13.6
6.00	435.2	31.4

To determine if methanogen inhibition extended to actual thermophilic bioreactors in which the microbial community had been shaped by envirnmental conditions to be optimized for n-butyrate production (Chapter 4), we tested for hydrogenotrophic methanogenic activity in biomass from a thermophilic bioreactor that had been operated to convert dilute-acid pretreated corn fiber to n-butyrate at pH 5.5 for 300 days. The batch tests were run at conditions simulating the bioreactor environment, with a pH of 5.5 and initial concentrations of 48.5 mM total acetate and 20.5 mM total n-butyrate (8.1 mM and 4.0 mM of undissociated acetic acid and n-butyric acid, respectively). After 72 hours

we detected no accumulation of methane nor any significant decrease in hydrogen or carbon dioxide levels. Hydrogen levels did decrease slightly between measurements at 72 hours and 144 hours, but we did not detect any methane (Figure A2.1B) or acetate accumulation due to acetogenesis (not shown) and we expect that hydrogen diffused from the butyl bottle stoppers. Thus, hydrogenotrophic methanogen inhibition was complete in a thermophilic microbial community that was formed under conditions to optimize n-butyrate production.

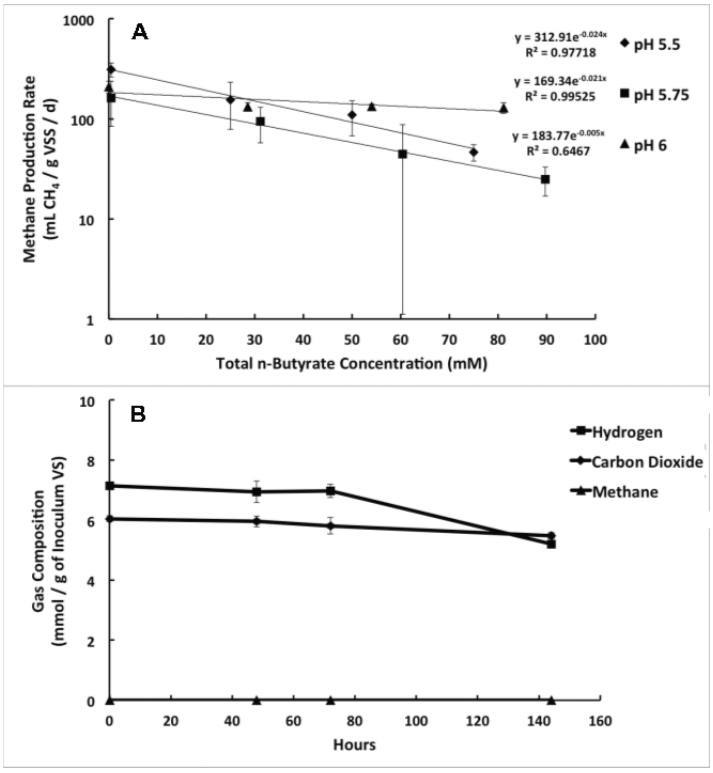

Figure A2.1. Inhibition of thermophilic hydrogenotrophic methanogens. A. Effect of the total n-butyrate concentration on hydrogenotrophic methanogenic activity at three pH levels; B. Inhibition of hydrogenotrophic methanogenesis in bioreactor sludge optimized for n-butyrate production.

A2.4 Discussion

Control of hydrogenotrophic methanogens is important because depending on the carboxylate platform application, partial pressures of hydrogen may need to regulated precisely for two reasons. First, the product distribution in primary fermentation (i.e., conversion of substrate carbon to ethanol, acetate, propionate, lactate, and n-butyrate) of carboxylates depends partly on hydrogen partial pressures because at partial pressures > ~60 Pa, oxidation of NADH with protons to balance electron pools is inhibited [Angenent et al., 2004]. Second, product specific extraction (i.e., removal of a specific bioproduct of interest from fermentation broths) is a method to increase fermentation product yields [Wu and Yang, 2003] and product specificity (Chapter 5). If methanogen inhibition is required for functionality or feasibility in a specific bioprocess, efficient product specific extraction may decrease system toxicity, resulting in the onset of methanogenesis.

We found that, similar to the results of others at mesophilic temperatures and with acetate [Van Kessel and Russell, 1996], inhibition of thermophilic hydrogenotrophic methanogens by n-butyrate appeared to be primarily due to the toxicity of the undissociated form of acid. Therefore, when methanogen inhibition is required and undissociated carboxylic acids cannot be maintained at high enough levels (e.g., at a pH of 7.0 or with product extraction), chemical inhibition of methanogens may be necessary. Further, our results with bioreactor inoculum demonstrated complete methanogen inhibition at ~ 12 mM of total undissociated carboxylic acids (total of acetic and n-butyric acids) even though n-butyric acid was only ~4 mM. This indicates that either the combination of acetate and n-butyrate are toxic, or that long-term community

conditioning in bioreactors may serve to eliminate methanogenic populations from biomass, but in reality both are likely contributors to inhibited methane production.

A2.5 Acknowledgements

Thanks to Jack Yi for help in development of the protocol for the batch methanogen inhibition study through many repeated trials.

APPENDIX 3.

SUPPLEMENTAL INFORMATION FOR: FUNCTIONALLY PREDICTIVE MICROBIAL COMMUNITY STRUCTURE LINKS OPERATING CONDITIONS TO n-BUTYRATE PRODUCTION

Summary

This appendix contains the following supplementary information: analysis of the effluent carbohydrates of R_{base} (A3.S1); operation of a bioreactor with nonpretreated corn fiber as substrate (A3.S2); startup of bioreactors R_{acid}, R_{base}, and R_{heat} (A3.S3); batch test results for lactate as an intermediate to n-butyrate (A3.S4); and community dynamics under perturbation in two identically operated bioreactors (A3.S5).

It contains the supplementary figures "Influent and effluent COD composition and effluent soluble carbohydrates for R_{acid}, R_{base}, and R_{heat}" (Figure A3.S1); "Biological solids hydrolysis" (Figure A3.S2); "Direct correlation between community composition and environmental gradients" (Figure A3.S3); "Rates of n-caproate formation are correlated with relative abundance of the genus *Thermosinus*" (Figure A3.S4); "Principal component analysis and evenness of microbial communities of R_{acid}-R_{heat} (Figure A3.S5); and "Community dynamics in identically perturbed bioreactors portray a nonrandom community structure" (Figure A3.S6).

Further, it contains supplementary methods descriptions and the following supplemental tables: pretreatment (Table A3.S1), operating conditions (Table A3.S2), bioreactor performance (Table A3.S3); and machine learning (Table A3.S4).

A3.S1: Analysis of the effluent carbohydrates of R_{base}

The dilute-alkali pretreatment solubilized more COD than the hot-water pretreatment (Table 4.1, main text), but we discovered that the soluble fraction of the hydrolysate was mostly composed of polysaccharides that were inefficiently degraded in R_{base}, resulting in soluble carbohydrates in the effluent (Figure A3.S1). We analyzed the effluent carbohydrates from R_{base} via HPLC, which revealed that the peak retention was close to that of other polysaccharides (slightly earlier than cellobiose) and that it had the same retention time and shape as a xylan standard. Although we did not perform techniques to identify the effluent carbohydrates with 100% certainty, xylan is the probable carbohydrate polymer because corn fiber is composed mostly of hemicellulose (Table A3.S1).

A3.S2 Operation of a bioreactor with nonpretreated corn fiber as substrate

We operated a fourth bioreactor for 100 days to convert nonpretreated corn fiber to n-butyrate. We discontinued operation because the nonpretreated pericarp (corn-kernel shell) fraction of the biomass was hydrophobic in nature, which caused poor degradation and mixing. Indeed, by day 90 of the operating period, total product formation rates in this bioreactor were only 50-60% of the levels of the other bioreactors. Besides hydrophobicity problems, the volatile solids (VS) loading rate in this bioreactor was 120-130% higher than for the other bioreactors due to the absence of pretreatment, and this combined with low productivity resulted in excessive buildup of solids in the bioreactor. We determined by day 100 that further operation was unsustainable, and stopped operating that bioreactor.

A3.S3: Startup of R_{acid}, R_{base}, and R_{heat}

We inoculated four bioreactors and immediately began an acidic pH regime (pH 5.5) to inhibit methanogens and promote n-butyrate metabolism. During the immediate startup period, significant methane partial pressures were observed (e.g., 30-45% of biogas on day 13), but these decreased below detection by day 125 of the operating period in bioreactors fed dilute-acid and dilute-alkaline pretreated substrates (R_{acid} and R_{base}, respectively) and by day 97 in the bioreactor fed hot-water pretreated substrate (R_{heat}). By day 120 of the operating period, production of short-chain carboxylates (acetate, n-butyrate, and n-caproate) became stable (Figure 4.1). The biogas hydrogen composition and effluent TCOD and SCOD had also stabilized in all three of the bioreactors (Figure A3.S1). Diversification of fermentation products from primarily acetate to a mixture of carboxylates and ethanol occurred as methane decreased and biogas hydrogen composition reached measurable levels (>1%) on day 13, 19, and 27 in R_{acid}, R_{base}, and R_{heat}, respectively. The distribution of bacterial phylotypes in all of the bioreactor communities became very uneven during startup (Figure A3.S5C). Simultaneously, the phylogenetic structure of the bioreactor bacterial communities, measured using weighted UniFrac [Lozupone and Knight, 2005], diverged from the inoculum, and each bioreactor community was identifiably unique after ~50 days (Figure A3.S5 A, B).

A3.S4: Batch test results for lactate as an intermediate to n-butyrate

We directly tested the potential for lactate production and the coupling of lactate oxidation with acetate reduction to n-butyrate in batch fermentations using mixed liquor from R_{acid} during Period 3 as inoculum. First, we performed batch fermentations of

cellobiose (a common biological degradation product of cellulose) at conditions similar to R_{acid}. In 44-h fermentations with 10mM cellobiose, most of the cellobiose carbon ended up in glucose (21%) or lactate (48%) and the pH decreased to 5.0, inhibiting further conversion (neither glucose nor lactate were detected in control batches with no cellobiose). In separate batch experiments we tested for lactate conversion to n-butyrate (via coupled oxidation of lactate with acetate reduction to n-butyrate) by adding 15mM or 30mM L-lactate to triplicate batch fermentations (with a control set without L-lactate). Indeed, while the control triplicate formed negligible amounts of n-butyrate, the triplicate with 15 mM L-lactate as substrate produced 2.88 ± 0.84 mM n-butyrate and consumed 1.30 ± 0.75 mM acetate in 3 days. The triplicate with 30mM L-lactate produced only 2.31 ± 1.42 mM n-butyrate and consumed 1.06 ± 1.16 mM acetate. In both cases the stoichiometry is ~2.2 n-butyrate per acetate, while estimates in literature are ~1.5-1.75 [Diez-Gonzalez et al., 1995; Duncan et al., 2004]. The low rates compared to the observed lactate utilization rates during the cycle analysis could be either due to absence of some nutrient that was available in the pretreated biomass, or due to oxygen intrusion during transfer of the effluent to batch bottles, or due to the fact that we only added L-lactate, while D-lactate may have been the available compound in the bioreactors.

A3.S5: Community dynamics in two identically operated and perturbed bioreactors

Because of long operating periods (419 days), we were only able to operate one replicate of each of R_{acid}, R_{base}, and R_{heat}. We wanted to test whether or not bioreactor bacterial communities were independent of the imposed bioreactor environment and if not, whether or not the community structure steady state was random. To test this "null" hypothesis, we inoculated two 5-l thermophilic bioreactors with effluent from R_{acid} during

Period 3 and subsequently semi-continuously fed them both acid pretreated corn fiber in a 48-h cycle at pH 5.5 and a 15-d HRT for ~200 days (identical conditions to R_{acid} during Period 3). Inoculation occurred at day -20 and on day 0 we combined both bioreactors into a bucket, exposed them to air, and evenly distributed the sludge back into the two bioreactors (Figure A3.S6). Next, on day 72 the temperature of the bioreactors was increased to 70 ^{o}C for one 48-h cycle. These two interruptions caused community disturbances that were nearly identical in both bioreactors (Figure A3.S6A and A3.S6B), indicating that the dynamic of the disturbance was controlled by environmental conditions. Interestingly, the taxonomic structure was not exactly the same state it was before the perturbation. Instead, a second population of bacteria existed alongside the previously dominant Clostridia. UniFrac principal coordinates 1 and 2 and evenness (Figure A3.S6C and A3.S6D, respectively) returned to pre-disturbance levels. The consistency between bioreactors indicates that the bioreactor community structure was not chaotic, even during a perturbation. Further, the steady-state of the bacterial community structure was not random and local, but was determined by the specific operating conditions.

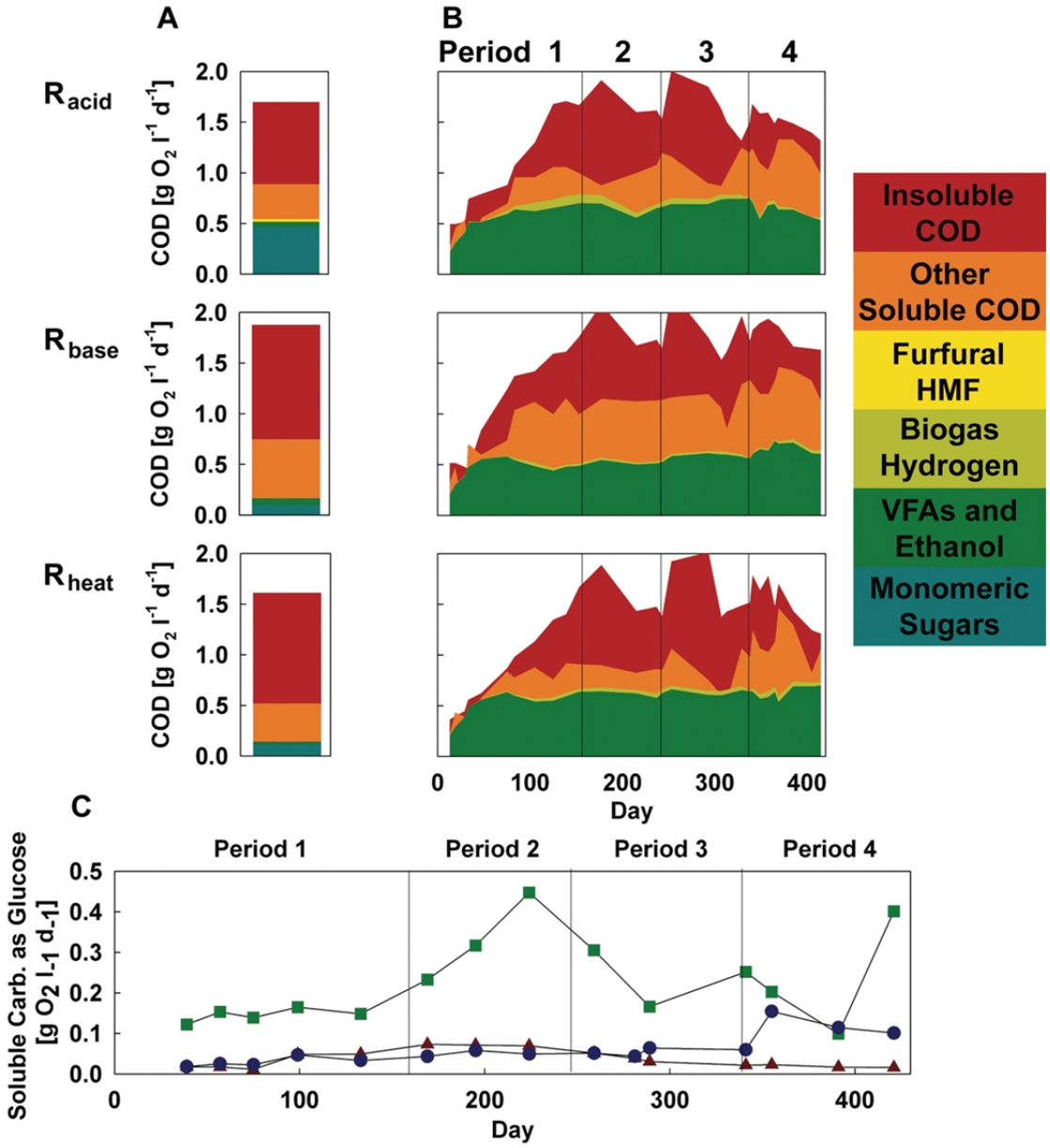

Figure A3.S1. COD composition in substrate and effluent for R_{acid}, R_{base}, and R_{heat}. A. Composition of COD in the dilute acid, dilute alkaline, and hot water, pretreated corn fiber hydrolysates; B. Composition of COD in the R_{acid}, R_{base}, and R_{heat} effluents; and C. Soluble carbohydrates in the effluent of R_{acid}, R_{base}, and R_{heat}, where red triangles are R_{acid}, green squares are R_{base}, and blue circles are R_{heat}.

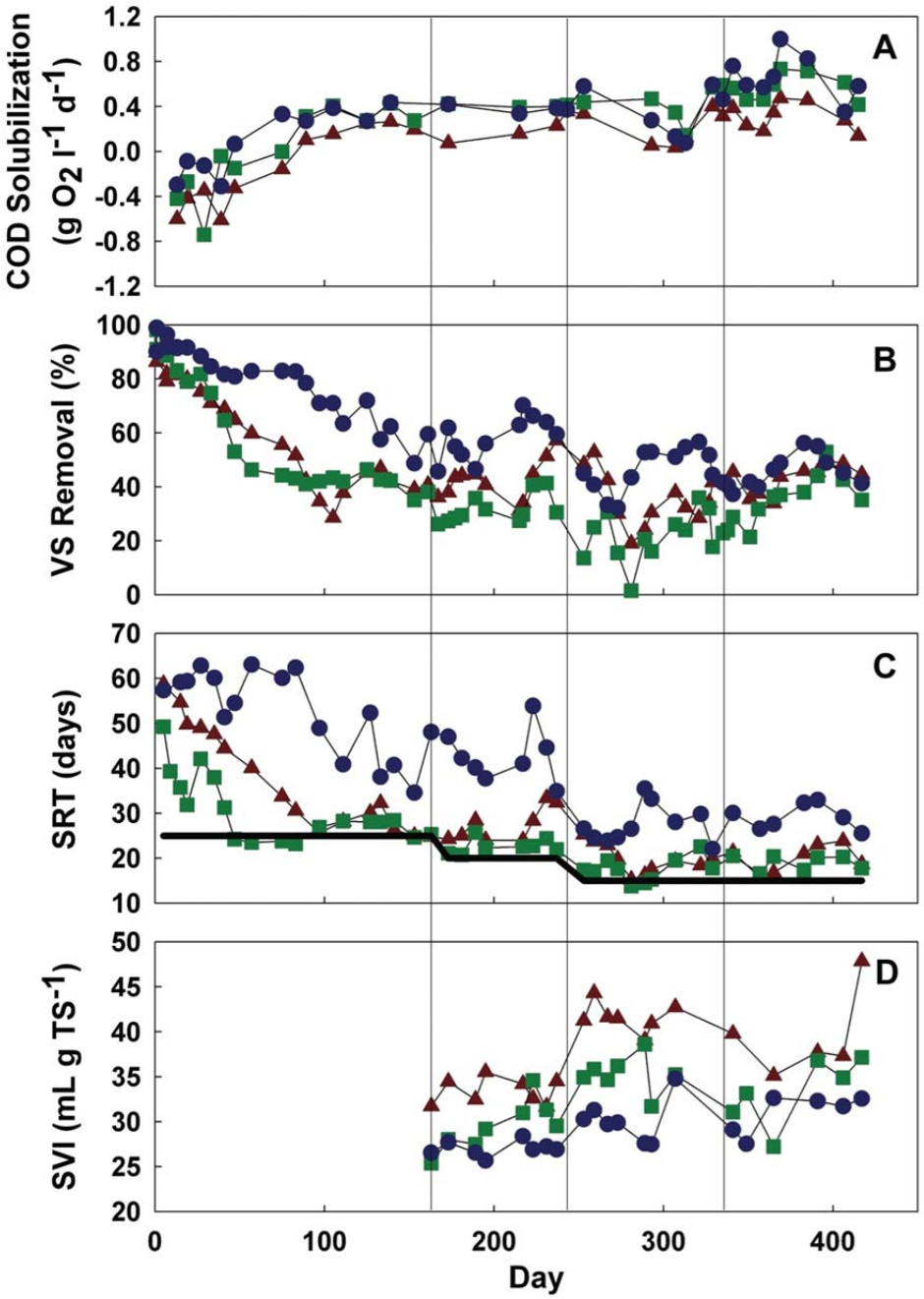

Figure A3.S2. R_{heat} was the most efficient at biological hydrolysis of solid substrate due to the best settling biomass. Red triangles are R_{acid}, green squares are R_{base}, and blue circles are R_{heat}: A. Rate of solubilization of particulate COD; B. Percent VS destruction during conversion to n-butyrate; C. SRT for R_{acid}, R_{base}, and R_{heat}. The black line indicates the hydraulic retention time for comparison; and D. SVI for the mixed liquor of the reactors, only measured in Period 2 - 4. A higher SVI indicates a relatively poorer settling sludge, and values are normalized for total solids content of the sludge.

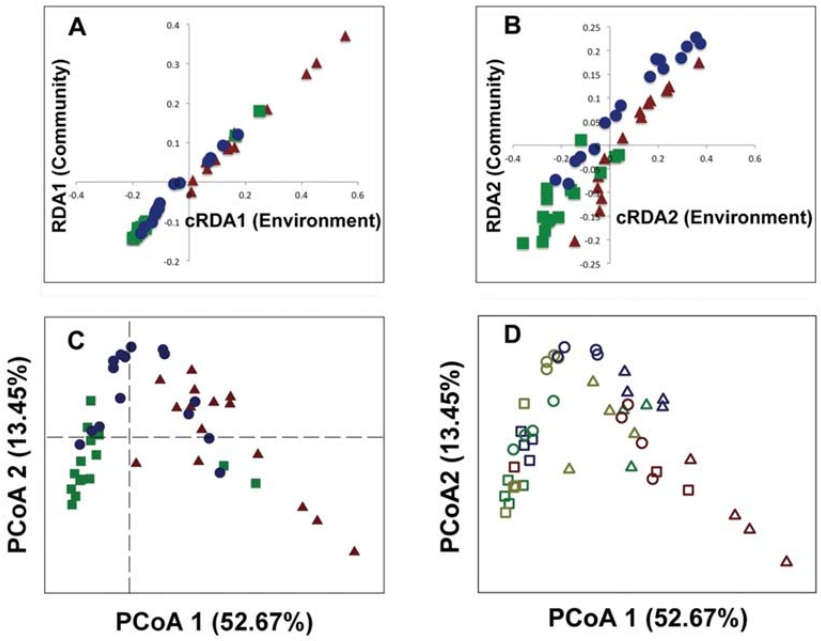

Figure A3.S3. Supplemental community structure analysis plots. In A-C, red triangles are R_{acid}, green squares are R_{base}, and blue circles are R_{heat}: A. and B. Plots of unconstrained (RDA) vs. constrained (cRDA) redundantly coordinated weighted UniFrac axes demonstrate that environmentally-constrained axes predict both within- and between-reactor community variation; C. First two principal coordinates of weighted UniFrac distances; and D. Same as C., colored by period (red: Period 1, green: Period 2, gold: Period 3, blue: Period 4).

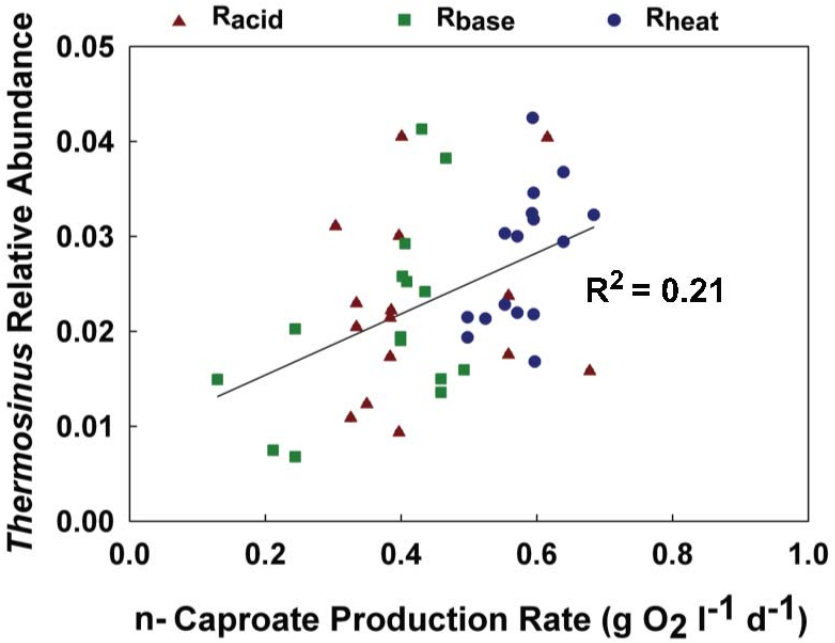

Figure A3.S4. Rates of n-caproate production are correlated with relative abundance of the genus *Thermosinus* across all bioreactors.

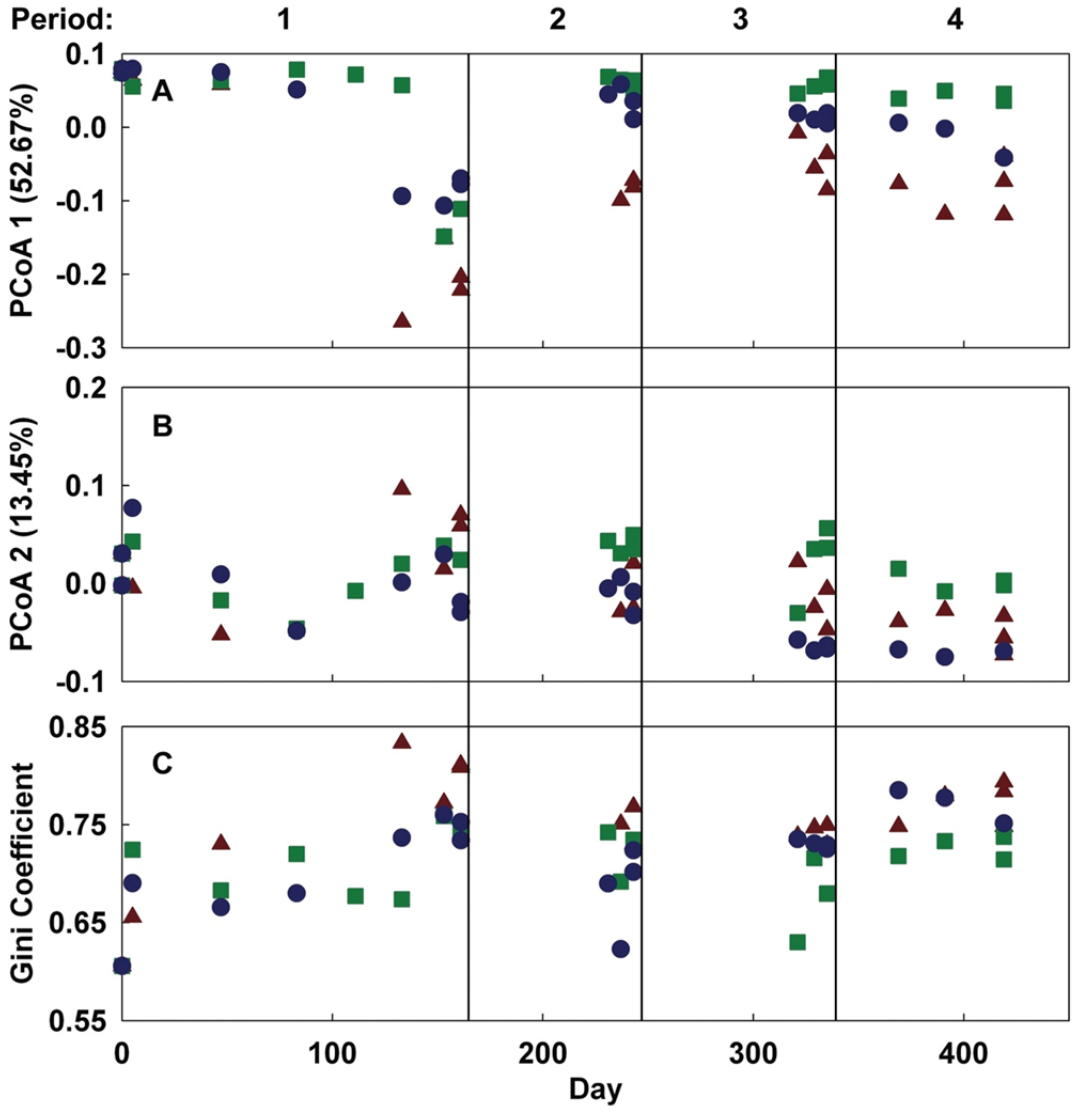

Figure A3.S5. Bacterial community information for R_{acid}, R_{base}, and R_{heat} during the operating period, where red triangles are R_{acid}, green squares are R_{base}, and blue circles are R_{heat}: A. Weighted UniFrac principal coordinate 1 describes 52.67% of community phylogenetic variation; B. Weighted UniFrac principal coordinate 2 describes 13.45% of community phylogenetic variation; and C. Evenness of the bacterial community, described by the Gini coefficient where 0 is a completely even community and 1 is a community dominated by only one phylotype.

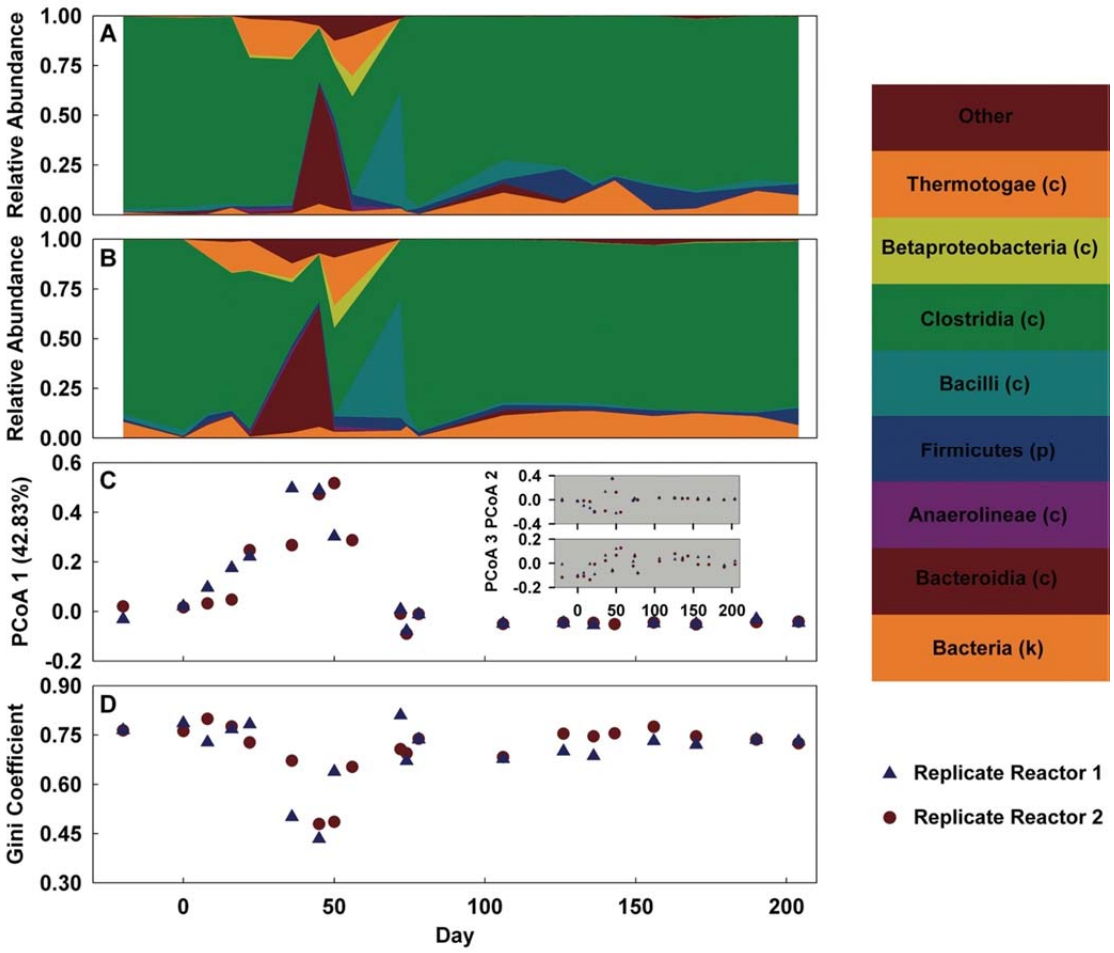

Figure A3.S6. Community dynamics in identically operated and perturbed bioreactors portray a nonrandom community structure; A. Taxonomic structure determined at the level of class in replicate bioreactor 1; B. Same as A for replicate bioreactor 2; C. Principal components plot of the community UniFrac distances reveal similar overall community structures; and D. Gini coefficient of the replicate bioreactors in which a coefficient of 0 is a completely even structure, and a coefficient of 1 is a structure dominated by a single phylotype.

Supporting Experimental Methods

Corn fiber pretreatment

Corn fiber pretreatment was performed at the USDA Agricultural Research Service in Peoria, IL, USA. 150g of corn fiber, which was received at ~45% solids content was mixed into a 316 stainless steel tube bioreactor with 320 ml of either dilute acid solution (0.5% w/w sulfuric acid), lime solution (1:10 $Ca(OH)_2$ to dry biomass), or distilled water. The bioreactors were incubated at 160^{o}C for 20 min in a fluidized-sand heating bath. At the end of a 20-min operating period, the reactors were immediately quenched in water. The bioreactor contents were subsequently transferred to shipping buckets and the bioreactors rinsed with 700 ml of distilled water, so that the concentration of total solids added to water was ~66 g l^{-1}. The buckets were shipped at 4^{o}C to Cornell University for anaerobic treatment and were frozen upon arrival, after mixing all buckets in a large container to assure homogeneity. The nonpretreated substrate was prepared at Cornell University by adding 150 g of corn fiber at ~45% solids content to 1 l of distilled water. All substrates were adjusted to pH 5.5 immediately before feeding to bioreactors by adding HCl or NaOH, as necessary. Table 4.1 and Table A3.S4 describe the characteristics of the three substrates as measured at Cornell University along with the nonpretreated substrate. The variation in substrate characteristics was low between prepared batches so the data in Table 4.1 and Table A3.S4 are averages over all batches.

Bioreactor Operation

Four identical 5-l bioreactors were designed to convert pretreated or nonpretreated corn fiber to n-butyrate. The bioreactors were anaerobic sequencing batch reactors (ASBRs), designed to settle for one hour before drawing effluent to increase the solids

retention times (SRT) compared to the hydraulic retention time (HRT). The bioreactors were timed to mix once per hour by biogas recirculation with a standard drive pump system (Masterflex, Cole-Parmer Instrument Company, Vernon Hills, IL). All bioreactors were controlled at pH = 5.5 with a pH controller/transmitter (Eutech Instruments pH 800, Thermo Scientific, Vernon Hills, IL), connected to fixed-speed drives (Masterflex) for automatic addition of 5M HCl or NaOH. The acid and base pumps shared a power source with the recirculation pumps so that addition of acid or base was only possible when the bioreactors were actively being mixed by gas recirculation. The bioreactors were temperature controlled at 55 ± 1^{o}C with water circulated through an external heating jacket with a heating recirculator (PolyScience, Inc., Niles, IL). The biogas collection system included a manometer-style pressure control system in which one bottle that was open to the bioreactor was connected via acidified water (to prevent microbial growth) to a second bottle that was open to the atmosphere. This insured that pressure inside the bioreactor would not drop below atmospheric pressure during drawing off and feeding or due to atmospheric pressure changes. The biogas then flowed through a gas sampling port, a bubbler to prevent air re-entry, and a gas meter (Model 1 l, Actaris Meterfabriek, Delft, The Netherlands)

The bioreactors were inoculated from a homogenous mix of three sources: 1. The rumen contents of a young sheep, which was strained to remove large fibrous foodstuffs; 2. Sludge from a full-scale thermophilic anaerobic digester treating primary and waste activated sludge (Western Lake Superior Sanitary District, Duluth, MN); and 3. Sludge from a lab-scale batch thermophilic anaerobic digester treating wheat straw. We inoculated with 1 l of inoculum (200 mL rumen fluid, 300 mL batch thermophilic

digester, and 500 mL full-scale thermophilic digester sludge), added 4 l of tap water, and allowed five days of acclimation at 55^{o}C before commencing feeding. We fed the bioreactors every other day, resulting in a 48-h cycle consisting of: instant feeding, a 47-h reaction period with intermittent mixing and pH adjustment every h, and a 58-min settling period followed by drawing off effluent (volume equal to the feeding volume) within two min. To compare conversion of corn fiber COD to n-butyrate COD, including any pretreatment losses, we always maintained a total COD loading rate to each bioreactor of 1.92 g O_2 l bioreactor^{-1} day^{-1} based on the COD of corn fiber slurry before pretreatment. The VS loading rate was constant, based on VS levels after pretreatment, with 1.01, 1.12, 1.11, and 1.35 g TS l bioreactor^{-1} day^{-1} for the acid, base, hot water, and nonpretreated corn fiber, respectively.

Chemical analysis

We used gas chromatography to measure the hydrogen content of the biogas on a Gow-Mac Series 350 TCD gas chromatograph. We determined the soluble constituents of the effluent by filtering with a 0.2-μm nitrocellulose membrane. Short-chain carboxylate and alcohol levels in the effluent were measured by gas chromatography (HP 5890 Series II) following acidification of filtered samples with 2% formic acid. Effluent soluble carbohydrates were determined colorimetrically by the phenol/sulfuric acid method using a 96-well plate reader (Bio-Tek, Winooski, VT).

Biomass sampling, DNA extraction, and amplification

We always sampled mixed liquor for subsequent sequencing at the end of a 48-hour cycle by first ensuring that the bioreactor was completely mixed, then rapidly collecting a sample from a side port on the bioreactor. The 2-ml biomass aliquots were centrifuged at

10,000 rpm for 10 min, the supernatant was disposed of, and samples were stored at 4^{o}C for up to 4 h before being transferred to -80^{o}C until subsequent processing.

Genomic DNA was extracted from 70 biomass samples using the MoBio PowerSoil 96-well gDNA isolation kit (MoBio Labs, Inc, Carlsbad, CA). DNA was extracted from ~200 mg of biomass according to the MoBio protocol, except that cell lysis was performed by beadbeating. PCR was carried out in triplicate for each sample to amplify 16S RNA genes. We also performed PCR on two water blanks carried through the extraction process. The PCR mastermix utilized 31.25 µl of water, 0.25 µl of 5U µl^{-1} Agilent Easy-A High Fidelity PCR Cloning Enzyme, 5 µl of 10X Easy-A reaction buffer, 1 µl each of 10 µM forward and reverse primers and 10 mM dNTP, 5 µl of 25mM $MgCl_2$, 3 µl of 10 mg ml^{-1} BSA, and 2 µl of sample. The forward primer combined the 454 primer 'B' and the universal bacterial primer 8F: 5'-GCCTTGCCAGCCCGCTCAGTC**AGAGTTTGATCCTGGCTCAG**-3'. The reverse primer was a concatenation of the 454 primer 'A', followed by a barcode, unique for each sample, followed by the universal bacterial primer 338R: 5'-GCCTCCCTCGCGCCATCAG*XXXXXXXXXXXX***CATGCTGCCTCCCGTAGGAGT**-3'. On each 96-well plate PCR we included three negatives composed of randomly selected reverse primers and no template. Triplicates were pooled with the Mag-Bind EZ Pure magnetic purification kit, and were eluted into 40 ul TE buffer according to the manufacturer's instructions. Pooled triplicates were run on a 1% agarose gel to verify the product. All negatives had no visible band and were not analyzed further. The concentration of dsDNA in each pooled triplicate was measured via fluourometric analysis with the PicoGreen dsDNA quantitation kit (Invitrogen Corp, Carlsbad, CA).

The samples were pooled in equimolar amounts into a single sample with a final concentration 19.2 ng μl^{-1} dsDNA. Sequencing was performed on the Roche 454 pyrosequencing platform using Titanium chemistry and beginning sequencing at 454 adaptor A (Engencore, Columbia, SC).

OTU prediction, taxonomy assignment, and OTU table preparation

We used the QIIME 1.2.1 pipeline [Caporaso et al., 2010] with default settings to denoise, quality filter, split sequences into the proper samples, and pick OTUs at 97% sequence identity with UCLUST [Edgar, 2010]. We aligned sequences to the GreenGenes (GG) core alignment template [DeSantis et al., 2006], trimmed to the V1-V2 region of 16S and filtered the alignment with the GG lanemask. We used the Bayesian classifier in mothur [Schloss et al., 2009] to assign taxonomy to OTUs using a 97%ID clustering of the GG database [Werner et al., 2011a]. We determined sample diversity with the Gini coefficient, a measure of the alpha diversity of each sample. The Gini coefficient is essentially unevenness on a scale from 0 to 1. Gini coefficients were calculated from 100 rarefactions of 400 sequences per sample. UniFrac is a beta-diversity index that calculates the phylogenetic distance between communities by determining the fraction of phylogeny the communities share [Lozupone and Knight, 2005]. We determined weighted and unweighted UniFrac distances based on 100 rarefactions of the OTU table at 500 sequences per sample. Both weighted and unweighted UniFrac metrics calculate distances between samples based on phylogenetic trees. Unweighted UniFrac considers only presence/absence of an OTU in a given sample (which makes it more affected by uneven communities or low-level contamination), whereas weighted UniFrac weights distances by abundance of each OTU. We only

report weighted UniFrac distances here because sample clustering was more informative than with unweighted UniFrac. We used principal coordinate decomposition to graphically display the phylogenetic distances between samples.

Batch tests for lactate as intermediate

To determine if lactate in R_{acid} could originate from glucose, we conducted a 44-h fermentation experiment in triplicate batches designed to resemble conditions in R_{acid}, with effluent from R_{acid} as the inoculum and as the medium. We added 0 or 10 mM of cellobiose as substrate. Cellobiose is a glucose dimer, and is a typical product of cellulose degradation by bacterial hydrolytic enzymes. After 44 h, we sampled the bottles, measured the pH, and measured glucose and lactate accumulation via HPLC and individual carboxylates and alcohol via GC. To study the feasibility of lactate and acetate conversion to n-butyrate, we again designed triplicate batch fermentations set up to resemble conditions in R_{acid} with effluent as inoculum and as medium and with 50mM of MES buffer (pH 5.5). The inoculum already contained 22.3 mM acetate and 32.7 mM n-butyrate and we added 0, 15, or 30 mM of L-lactate as substrate. We allowed the fermentation to proceed and sampled the bottles after three days. We measured the concentrations of acetate, n-butyrate, and n-caproate in the bottles at the end of the three days.

Table A3.S1: Additional substrate characteristics

Treatment	Hemicellulose ($g\ l^{-1}$) [%DM]	Cellulose ($g\ l^{-1}$) [%DM]	Lignin ($g\ l^{-1}$) [%DM]	HMF (mM)	Furfural (mM)	Succinate [mM]	Lactate [mM]	Acetate [mM]	Acetoin [mM]	Ethanol [mM]
Dilute Acid	0.49 ± 0.04 (n=2) [0.95%]	6.16 ± 0.00 (n=2) [11.90%]	1.19 ± 0.07 (n=2) [2.30%]	1.16 ± 0.25 (n=9)	5.25 ± 0.80 (n=9)	1.06±0.54 (n = 2)	4.22 ± 0 (n = 2)	20.15 ± 3.63 (n = 8)	3.12 ± 0.56 (n=2)	1.81 ± 0.33 (n=6)
Dilute Alkali	3.53 ± 0.07 (n=2) [5.54%]	8.27 ± 0.06 (n=2) [12.98%]	1.08 ± 0.09 (n=2) [1.70%]	0	0.044 ± .064 (n=9)	1.95±0.48 (n=2)	6.05 ± 0.55 (n = 2)	24.18 ± 1.04 (n = 8)	6.30 ± 2.01 (n=2)	1.70 ± .33 (n=6)
Hot Water	3.98 ± 0.07 (n=2) [7.06%]	8.36 ± 0.10 (n=2) [14.83%]	1.30 ± 0.04 (n=2) [2.31%]	0.043 ± .031 (n=9)	0.39 ± 0.21 (n=9)	1.95±0 (n=2)	3.83 ± 0.08 (n = 2)	2.41 ± 1.11 (n = 8)	2.26 ± 1.27 (n=2)	0.40 ± 0.62 (n=6)
None	21.41 ± 0.27 (n=2) [31.95%]	8.36 ± 1.94 (n=2) [12.48%]	2.14 ± 1.81 (n=2) [3.20%]	0	0	NA	NA	NA	NA	NA

n=represents the number of replicate measurements, and the value after ± is the standard deviation. Lignocellulose composition was only measured on one batch of substrate. We measured HMF, furfural, acetate, and ethanol for each batch of substrate we received (we also measured other short-chain carboxylates but found none). Succinate, lactate, and acetoin were measured only for the first two batches of substrate

Table A3.S2: Operating conditions for Period 1 through Period 4

		Period 1	Period 2	Period 3	Period 4
HRT (d)		25	20	15	15
pH		5.5	5.5	5.5	5.8
Substrate Dilution		2x	2.5x	3.33x	3.33x
VS Loading ($g\ l^{-1}\ d^{-1}$)	R_{acid}	1.01	1.01	1.01	1.01
	R_{alk}	1.12	1.12	1.12	1.12
	R_{HW}	1.11	1.11	1.11	1.11
COD Loading ($g\ O_2\ l^{-1}\ d^{-1}$)	R_{acid}	1.69	1.69	1.69	1.69
	R_{alk}	[1]1.88	[1]1.88	[1]1.88	[1]1.88
	R_{HW}	1.61	1.61	1.61	1.61

[1]Standard deviations for the total COD measurement of the substrate were very high, especially for R_{base}, and this value is not statistically higher than R_{acid} or R_{heat} ($p>0.05$), see Table 4.1 for standard deviations. The loading rate based on the nonpretreated biomass is 1.92 g O_2 l^{-1} d^{-1}.

Table A3.S3: Effects of changes in operating conditions for Period 1 to Period 4

		Period 1	Period 2	Period 3	Period 4
Undissociated Carboxylic Acid Concentration (mM)	R_{acid}	22.05 ± 1.72	18.07 ± 0.41	16.07 ± 0.09	6.76 ± 0.25
	R_{base}	19.05 ± 0.30	15.92 ± 0.48	13.91 ± 0.59	7.16 ± 0.41
	R_{heat}	21.12 ± 1.85	16.63 ± 0.33	14.16 ± 0.87	8.24 ± 0.51
Fermentation Product Rate ($g\ O_2\ l^{-1}\ d^{-1}$)	R_{acid}	0.644 ± 0.033	0.662 ± 0.010	0.744 ± 0.004	0.540 ± 0.020
	R_{base}	0.481 ± 0.005	0.511 ± 0.015	0.586 ± 0.023	0.590 ± 0.032
	R_{heat}	0.546 ± 0.043	0.591 ± 0.027	0.641 ± 0.027	0.671 ± 0.042
n-Butyrate Production Rate ($g\ O_2\ l^{-1}\ d^{-1}$)	R_{acid}	0.352 ± 0.009	0.395 ± 0.013	0.440 ± 0.005	0.273 ± 0.027
	R_{base}	0.197 ± 0.017	0.201 ± 0.011	0.253 ± 0.030	0.255 ± 0.006
	R_{heat}	0.205 ± 0.015	0.261 ± 0.015	0.300 ± 0.030	0.278 ± 0.010
n-Butyrate Specificity	R_{acid}	0.546 ± 0.022	0.596 ± 0.012	0.591 ± 0.010	0.504 ± 0.030
	R_{base}	0.385 ± 0.008	0.394 ± 0.011	0.430 ± 0.036	0.433 ± 0.026
	R_{heat}	0.376 ± 0.003	0.442 ± 0.005	0.468 ± 0.030	0.415 ± 0.012

Table A3.S4: OTUs determined by machine learning to be predictive of a bioreactor or combination of bioreactors

R_{acid}		R_{base}		R_{heat}		R_{acid}/R_{base}		R_{base}/R_{heat}		R_{acid}/R_{heat}	
OTU	**Taxonomy**	**OTU**	**Taxonomy**	**OTU**	**Taxonomy**	**OTU**	**Taxonomy**	**OTU**	**Taxonomy**	**OTU**	**Taxonomy**
1613	*Clostridium*	197	*Thermoanaerobacterium*	53	*Thermoanaerobacterium*	None		None		752	*Thermoanaerobacterium*
2879	Lachnospiraceae	1297	*Thermoanaerobacterium*	888	*Ethanoligenens*					3631	*Thermoanaerobacterium*
		2261	*Lactobacillus*	3479	*Thermoanaerobacterium*						

APPENDIX 4.

SUPPLEMENTAL INFORMATION FOR: DIRECTING MIXED MICROBIAL CULTURES TOWARD UPGRADING ACETATE, N-BUTYRATE, AND ETHANOL TO SPECIFIC MEDIUM-CHAIN CARBOXYLATES

Summary

This supporting material provides additional information on bioreactor setup and operating conditions (Figure A4.S1); volatile solids removal (Figure A4.S2); gene plots describing the significance of changes in gene abundance due to temperature or extraction (Figure A4.S3); correlations between taxonomy of the chain-elongation genes and the n-caproate/n-caprylate specificity (Figure A4.S4); energetics of n-butyrate and ethanol oxidation (Figure A4.S5); and taxonomic distribution of alcohol dehydrogenase genes in bioreactor communities (Figure A4.S6).

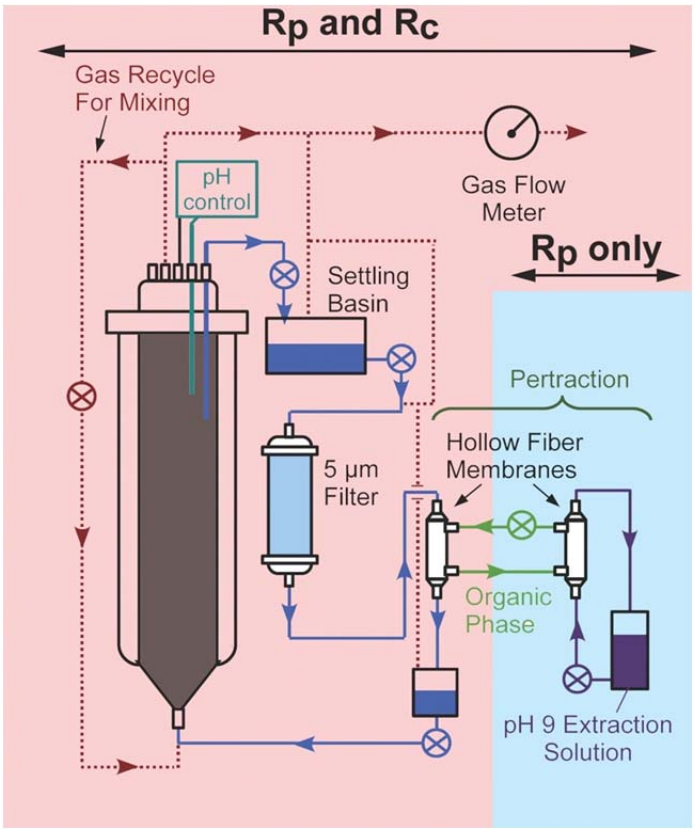

Figure A4.S1. Bioreactor setup for R_p (with *in*-situ product extraction) and R_c (without *in-situ* product extraction). Both bioreactors were operated identically, with automatic pH and temperature control. For R_p, we extracted n-caproate and n-caprylate in a membrane-based extraction system along a pH gradient. R_c was exposed to the same extraction solvent but the solvent was not regenerated along a pH gradient, and no extraction occurred.

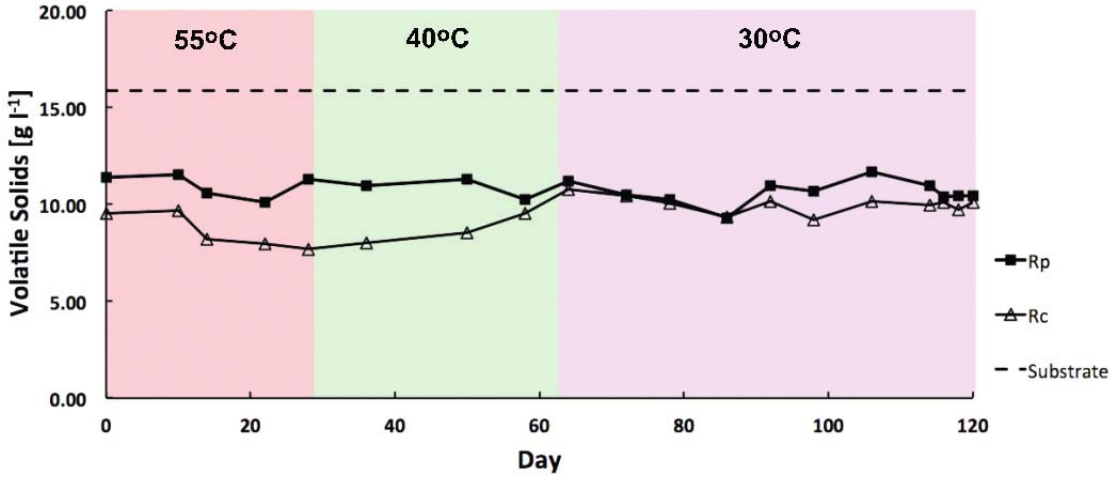

Figure A4.S2. Volatile solids (VS) removal in R_p and R_c for bioreactor operating periods across three temperatures. The dotted line indicates the concentration of VS in the dilute-acid pretreated substrate fed to both bioreactors.

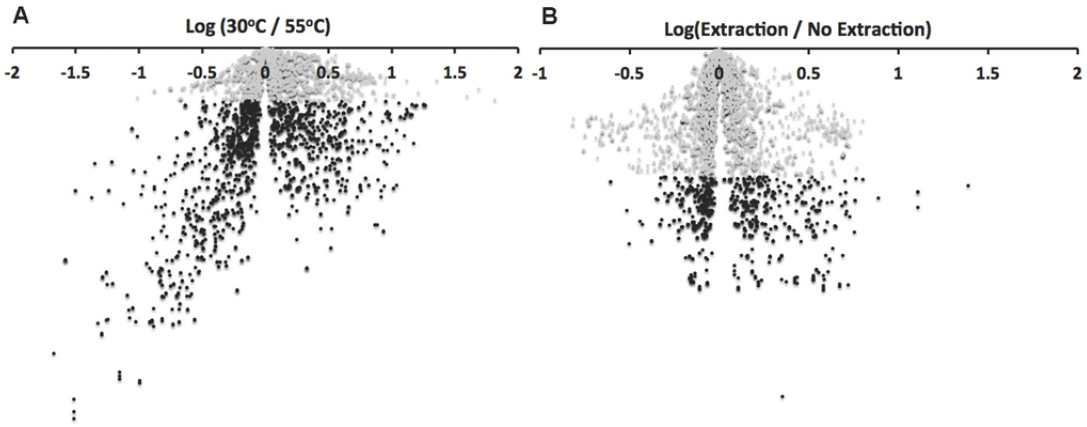

Figure A4.S3. Gene plots based on SEED subsystem-based functional abundances comparing gene abundance changes (as the log of the ratio of gene abundance at two conditions) due to temperature (A) and extraction (B). Black dots are genes with shifts that were statistically significant ($p < 0.05$). A 3-fold abundance change corresponds to a log-value of ± 0.477.

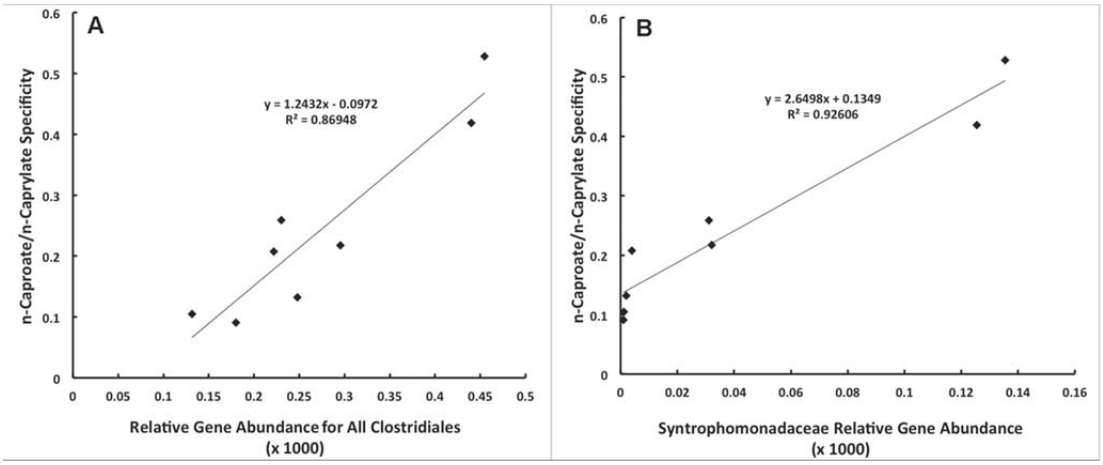

Figure A4.S4. Correlations between taxonomy of the chain-elongation genes and the n-caproate/n-caprylate specificity: A. n-Caproate/n-caprylate specificity vs. relative gene abundance (x 1000) for all Clostridiales ($R^2 = 0.87$); and B. n-Caproate/n-caprylate specificity vs. *Syntrophomonadaceae* relative gene abundance ($R^2 = 0.93$).

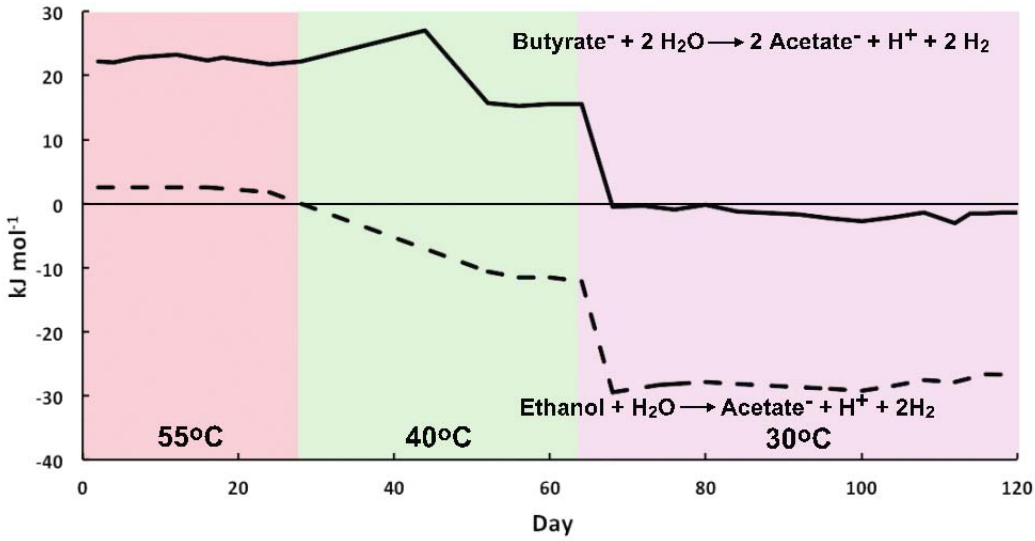

Figure A4.S5. Gibbs free energy of reaction (ΔG_r) for n-butyrate and ethanol oxidation at bulk bioreactor conditions during bioreactor operation.

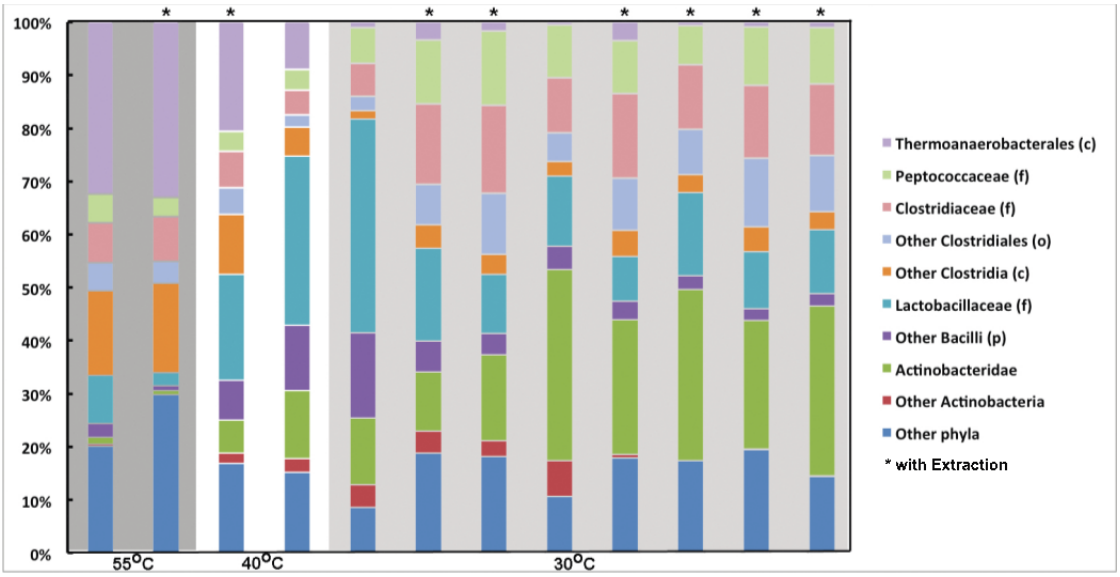

Figure A4.S6. Taxonomic distribution of alcohol dehydrogenase genes in bioreactor communities. organized first by temperature, then by increasing n-caproate/n-caprylate specificity. Bars with a * symbol are samples taken from the bioreactor with *in-situ* product extraction (R_p).

APPENDIX 5

PROTOCOLS

A5.1 Ammonia (ion-selective electrode method)

Materials:

Distilled-Deionized water
Stock ammonium chloride solution (1M)
Diluted standards of ammonium chloride (.001M, .01M, and .1M)

Procedure:

1. Place 25 mL of standard solution or sample into a 100-mL beaker
2. Immerse electrode while mixing with magnetic stirrer on a relatively low rate to minimize evaporation (if possible, cover with plastic wrap)
3. Add 1 mL of ammonia adjusting ISA solution to beaker
4. Allow time for electrode to equilibrate, and record mV reading

Calculations:

Prepare a stadard curve of concentration of ammonium chloride vs. mV readings on a semi-logarithmic graph. Fit a logarithmic curve to the points, with $R^2 > 0.98$. Last, fit sample points to the standard curve to find concentrations

A5.2 Chemical Oxygen Demand (COD) – Closed Reflux Titrimetric Method

Materials:

Standard potassium dichromate digestion solution, 0.0167M:
Add to about 500 mL distilled water: 4.913 g $K_2Cr_20_7$, 167 mL conc H_2SO_4, and 33.3 g $HgSO_4$. Dissolve, cool to room temperature and dilute to 1000mL.
Sulfuric acid reagent
Add 5.5g $AgSO_4$ per kg H_2SO_4, may need to dissolve 1-2 days
Ferroin indicator solution (available commercially)
Standard ferrous ammonium sulfate titrant (FAS), approximately 0.05M:
Dissolve 19.6 g Fe(NH4)2(SO4)2*6H2O in distilled water. Add 10mL conc H2SO4, cool, and dilute to 1000mL.

Procedure:

1. Dilute sample to less than 300 mg O_2/L
2. For soluble COD, filter through 0.22-um pore size nitrocellulose membrane
3. Acid wash culture tubes and caps thoroughly and dry before use.
4. Add 2.5 mL sample in culture tube, each sample at least in duplicate
5. Add 1.5 mL digestion solution.
6. Add 3.5 mL sulfuric acid reagent by carefully running down inside of vessel to maintain acid layer.
7. Tightly cap tubes or seal ampules and invert each several times to mix.
8. Place tubes in block digester set to 150^{o}C for120 minutes.
9. Cool to room temperature, remove caps, pour sample into small flask and add PTFE-covered magnetic stirring bar.
10. Add 1-2 drops of ferroin indicator and stir rapidly on magnetic stirrer while titrating with 0.05M FAS. The end point is a sharp color change from blue-green to red-brown.

Calculation:

$$\text{COD as mg } O_2\ l^{-1} = \frac{(A-B) \times M \times 8000}{mL\ sample}$$

Where:
A = mL FAS used for blank (typically should be ~3 for a clean blank)
B = mL FAS used for sample
M = molarity of FAS

A5.3 Volatile, Total, and Inert Solids (VS,TS, IS)

Materials:

1. Porcelain crucibles
2. 50 mL graduated cylinder
3. Solids samples

Procedure:

1. Place clean and dry crucible in desiccator for 15-30 minutes
2. Record the tare mass of the crucible
3. Add known volume of well-mixed sample, usually 25mL
4. Rinse graduated cylinder into crucible to get all solids out
5. Dry overnight at 105^{o}C, desiccate, and record mass
6. Burn at 550^{o}C in muffle furnace for 30-60 min, or until sample loses no more weight with subsequent burnings (60 min is usually sufficient).
7. Desiccate and record mass.

Calculation:

$$\text{VS} = \frac{(D-A)}{V}$$
$$\text{TS} = \frac{(D-T)}{V}$$
$$\text{IS} = \frac{(A-T)}{V}$$

Where:

T = Tare mass
D = Dry mass
A = Ash mass
V = Volume of sample

A5.4 Sludge Volume Index

Materials

1. 50 mL graduated cylinder or graduated centrifuge tube

Procedure

1. Determine the suspended solids concentration of a well-mixed sample of the suspension
2. For some sludges, suspended solids are difficult to determine, in that case just measure the total solids.
3. Determine the 30 min settled sludge volume by allowing the sample to settle for 30 minutes (dilution may be required first) in graduated container and record the settled and total volume.
4. Results are only comparable between samples measured in exactly the same manner.

Calculations

$$\text{SVI} = \frac{Settled\ sludge\ volume\ \left(\frac{mL}{L}\right) \times 1000}{Suspended\ solids\ \left(\frac{mg}{L}\right)}$$

A5.5 Batch Activity Assays

(Note: Always perform tests in triplicates for each sample)

Materials

1. Serum bottles, size is optional, depending on the application
2. Batch nutrient medium – depending on application. For methanogenic medium, a good reference is Rinzema et al., 1988 (I leave out the buffer and make a separate buffer solution).
3. Buffer solution – depending on application, BES is good for pH ~5.5, MES works closer to neutral pH. Carbonate buffers are standard for rumen fluid analysis, but are a little tricky to work with. Phosphate buffers should be avoided when working with methanogens because they are inhibiting at a neutral pH.

Procedure

Day 1

1. Weigh empty serum bottles
2. Weigh serum bottles filled with deionized water
3. Make anaerobic buffer solution by flushing buffered and pH-ready deionized water with nitrogen gas for 30 minutes.
4. Perform the following steps in an anaerobic hood.
5. Add nutrient medium at the desired concentration (for methanogens, 1:10 dilution of the above described medium is fine)
6. Add buffer solution to make up volume minus what you will add to correct pH.
7. If you are testing inhibition, add the compound of interest
8. Check that pH is at the expected level, correct if necessary
9. Add inoculum. The amount depends on the rates you need for getting accurate measurements
10. For methanogens, add 0.5 mL of 0.21M sodium sulfide solution
11. Seal bottle, remove from hood, and flush headspace with nitrogen gas for 5 minutes
12. If testing aceticlastic or hydrogenotrophic methanogens, add some substrate now to get growth going. For hydrogenotrophic methanogens, incubate until methane content of the headspace reaches ~5%. For aceticlastic methanogens, add acetate and incubate overnight.
13. Incubate at bioreactor conditions overnight on a shaker table set at 125 RPM

Day 2 (or when methane reaches ~5% for hydrogenotrophic methanogens)

1. Add substrate of interest
2. Check and correct pH to desired conditions

3. Seal bottles and flush with nitrogen gas for 5 minutes
4. Incubate on shaker table (125 RPM) for one hour, incubating at bioreactor conditions
5. Periodically, measure headspace gas composition and pressure, and liquid fraction for other assays.
    a. Pressure can easily be measured with a gas-tight syringe. Fill a known volume of water in the syringe and take a small volume of the headspace. Seal the syringe, remove, and allow water to displace gas (gas should be at the plunger end of the barrel, water at the needle end). Open the seal and record how much the volume increases. The pressure relative to atmospheric pressure is proportional to the volume increase.
6. Repeat step 5 periodically, depending on the rate of reaction. For methanogens, stay below ~3% methane if you are not correcting for pressure. If you rapidly reach this level, you are using too much inoculum.
7. Measure pH immediately after opening bottles
8. Weigh the bottles at the final volume
9. Measure volatile suspended solids (VSS) of solution in each bottle by vacuum filtration

Data Analysis for methanogenesis

1. Plot the increase in percent methane over time (days), correcting for pressure.
2. Calculate % methane per day from linear regression
3. Multiply by volume of headspace and divide by grams VSS to find mL methane / gVSS / day

A5.6 Gow-Mac GC Protocol (CH_4, CO_2, N_2, H_2, CO)

Notes:

1. BEFORE PROCEEDING MAKE SURE THAT THE CARRIER GAS IS PROPERLY TURNED ON AND FLOWING AT THE PROPER RATE
2. To measure hydrogen, nitrogen is the carrier gas at ~ 10 - 40 ml/min. To measure nitrogen, methane, and carbon dioxide, helium is the carrier gas at ~60 ml/min.
3. A faster flow rate or higher column temperature will cause the peak to elute faster.
4. To see the set and actual temperature for a component, press the desired button (e.g., detector) and use the other button to select "actual" or "set".

Procedure

Startup

1. **MAKE SURE THAT CARRIER IS FLOWING BY CHECKING WITH A BUBBLE COLUMN**
2. Turn on the GC (the switch is on the back)
3. Set the column temperature to 100^{o}C
4. Set the injector temperature to 110^{o}C
5. Set the detector temperature to 105^{o}C
6. Turn on the detector, set current to 70 – 110 mA. Higher current provides more resolution but may result in more noise.
7. Temperatures and current can be adjusted, but adjustments will affect the standard curve.

Calibration with PeakSimple

1. Calibrations are typically made on a percentage basis, where a full 500 ul syringe is 100%. You MUST start with the smallest calibration level if using PeakSimple.
2. Make an injection with, e.g., 10% (50 ul of 100% hydrogen in a 500 ul syringe). Then press the timebase button to start recording
3. Allow the peak to elute, then stop the recording by pushing the timebase button, or allow the recording to stop automatically.
4. If you did not already have a components file, right-click on the peak and press add component. Then, right click again and press edit component and add a peak name

1. Right-click on the peak and press calibrate.
2. If the program asks if you want to load a calibration file, press no.
3. Select the appropriate level, or "1" if it is the lowest level.
4. When the calibration opens, add the amount to the corresponding level and click "Accept".

5. Verify that your point has been added to the curve.
6. You can adjust the type of fitted curve if you desire (some GCs give non-linear response over a very large concentration range)
7. Continue until you injected all of your calibration samples
8. Save your calibration curve so that you don't have to make a complete new one every time.

Measurements

1. If you did not make a new calibration, make sure that you have a calibration file loaded.
1. Inject your sample, using the volume that corresponded to 100% for the sample.
2. The peak area ratios represent a molar fraction, so if you used 250ul of 100% hydrogen for a 50% standard, a sample with 50% hydrogen would contain 250ul in 500ul total.
3. After the peak elution, click on the page icon at the top bar. This should display results.
4. You can save your chromatogram for later analysis if so desired. Make a folder for yourself so as to not clutter the PeakSimple root folder.

A5.7 Individual Volatile Fatty Acid (VFA) Analysis

Sample Preservation and Storage:

- Samples should be filtered (0.22 um) to remove any suspended solids
- Dilute sample to ~500 mg/L total VFA (as acetate) with 2% formic acid
- For storage, filtered samples should be diluted at least 1:1 with 2% formic acid to lower the pH, and stored in 4^{o}C refrigerator for subsequent analysis
- If samples have precipitated (e.g., if your samples have phenolic monomers this may happen, re-filter)

Materials:

1. Stock solution of volatile fatty acids with 10mM each of: formic, acetic, propionic, isobutyric, butyric, isovaleric, valeric, isocaproic, caproic, and heptanoic acids (formic acid does not show up on the GC).

2. 2% formic acid solution for dilutions
   Note: people used to use HCl, but this is bad for capillary columns. Avoid it.

3. Standards of 1, 3, 5, and 7 mM, made by diluting with formic acid. Standards should be run weekly at least.

Procedure:

Start-up

1. **FIRST** Turn on the air, helium, and hydrogen cylinders, and turn the flow on at the GC (left hand side panel).
2. Add your name, date, and planned number of samples to the logbook so you don't forget. If the number changes, you can fix it later.
3. If the septum has not been replaced for over 50 injections, replace now.
4. If the glass injector sleeve has not been replaced for over 150 injections, replace now.
5. If you suspect the flow rate has changed, check it with the bubble meter. The flow of air, carrier (He), makeup (He), and hydrogen should be approximately: 350 ml/min, 10 ml/min, 20 ml/min, and 35 ml/min, respectively.
6. Turn the switch on the right side (when facing the front) of the machine on.
7. Turn on the communication module (separate unit to the left of the GC).
8. On the Windows 98 computer, open "Instrument 1 (online)" from the desktop.
9. If you have not already done so, skip to "**Loading Samples**", below.
10. Wait until GC reaches operating temperature (~15 minutes).
11. Push the Ignite button (on left panel of GC) to light the flame (if you don't hear it light, blow slightly in the exhaust port and it will light).
12. Allow 15 minutes to equilibrate.

13. Check that solvent A is fresh Methanol, solvent B is fresh DDI water, and empty the waste vials
14. Remove needle and check that the plunger moves smoothly through the barrel. Check that it takes up and dispels water properly. Replace needle properly.

Loading Samples (this can be performed while waiting for GC to warm up)

1. Load your samples into the autosampler. We recommend using a blank 2% formic acid sample every 5 samples (e.g., samples 1, 6, 11, etc.). Because the GC measurements can fluctuate after very long periods, we recommend a maximum of 50 samples at a time. For long runs, include a standard about every 25 samples and at the end of the run to ensure readings are the same all the way through or to adjust calibration if they are not.
2. Under the menu "Sequences" open "Sequence Table"
3. Click "Insert Vial Range" and put in the range of vials you will run on the autosampler (Method is: VFATRIAL, Injections: 1, Injection volume: 1). Click "OK".
4. Under the menu "Sequences" open "Sequence Parameters". Put in the name of the directory in which you want to store data files (e.g., mta81510). Click "OK".
5. Under the menu "Sequences" click on "Save Sequence" and give it a name (you can reuse the same file later by opening it and changing the sequence table and re-saving.)
6. Return to step 10 above, if you haven't already.

Starting Injections

1. When all of the above steps are complete, check that the computer reads "Ready"
2. If it is ready, press "Start"
3. Most problems occur in the first few injections, keep an eye out to make sure no problems arise.
4. If the autosampler gets stuck, it is usually a syringe problem. Remove the syringe, make sure the plunger moves freely, and replace. Restart the sequence.

Shutting Down

1. Shut off the program on the computer, and turn off the communication module.
2. Turn off the hydrogen valve at the machine to extinguish the flame.
3. Push [Oven Temp] and set to 25^{o}C, set [DetA Temp] to 50^{o}C, and [InjA Temp] to 50^{o}C.
4. After components have cooled at least to 100^{o}C, turn off the GC, then turn off the air and carrier valves.
5. **LAST** turn off the gas cylinders

Data Analysis

1. Open “Instrument 1 (offline)” on the computer
2. Go to “File” and “Load Signal”, and load your first standard vial
3. Go to “Calibration” and click “Add Peaks” and put in the calibration level (concentration) when prompted.
4. Remove (delete) unwanted peaks from the calibration table.
5. Use manual integration to ensure the baseline is proper for each peak.
6. Put in the names of the peaks
7. Load a new standard vial and under “Calibration” click on “Add Level”. The program should automatically recognize the proper peaks.
8. Once you have filled your calibration table, you can load your data signals, one at a time.
9. Click on the magnifying glass at the top right, which should bring up the report for your vial, with concentrations of the VFAs.
10. Until further notice, you have to write these down, we haven’t figured out yet how to export the data to excel.

A5.8 Peak Simple – Data analysis for GCs and HPLC

Materials

1. PeakSimple data collection system (model 302)
2. Wires, wiring supplies, and tools

Note: Peak Simple has a really handy function: Hold the mouse over any button or field to get a large information box about what that parameter will do.

Procedures

Data collection setup

1. Gow-Mac and HP GCs and Waters HPLCs have terminals for signal output in the range +/- 10mV. This can be wired directly to the channel terminals in the PeakSimple box.
2. HP GCs and HPLCs have terminal for a start signal or "remote" signal. This tells PeakSimple to begin recording when a run is started at the instrument. Wire this directly to the remote input in the PeakSimple box.

PeakSimple Operation

1. Open PeakSimple on the desktop computer
2. Open the control file that has the settings for your instrument
    a. A setting of 10Hz is typically appropriate for data collection.
    b. The timebase setting fixes which number (1-4) is pushed to start recording
    c. The record time should be set so that all peaks elute, or slightly shorter than the run time of the instrument if an autosampler is being used
3. Make sure the proper channel is showing in the recorder window
4. If available, load the component and calibration files for your peaks
5. If you have one, load your calibration curve (be sure to check that it is still valid, the GC parameters could have changed!)
6. To add a new peak or to use a peak for calibration, right click on the peak and select the appropriate option from the menu

If you use an autosampler, set the post-run settings so that chromatograms are automatically saved to file.

A5.9 gDNA Extraction and 16S rRNA Gene Amplification for High-throughput Barcoded 454 Pyrosequencing

Materials:

Extraction and Elution

1. Robot Disposables, wells and tips, Krackler Scientific, #38-960050088-EA, #38-960051017-EA
2. MoBio PowerSoil 96-well gDNA extraction kit. http://www.mobio.com/soil-dna-isolation/powersoil-htp-96-well-soil-dna-isolation-kit.html
3. PicoGreen dsDNA quantitation kit. http://products.invitrogen.com/ivgn/product/P11496

Gel

2. Agarose (Sigma-Aldrich)
3. 20X Borate Buffer
4. Ethidium Bromide (10mg/mL)
5. Gel Box and electrodes

PCR and Cleanup

1. Easy-A HIFI PCR cloning enzyme http://www.genomics.agilent.com/CollectionSubpage.aspx?PageType=Product&SubPageType=ProductDetail&PageID=1267
2. dNTPs http://www.promega.com/applications/products/PartsList.asp?subappid=51
3. Scaled up PCR mastermix recipe (see appendix below)
4. Primers: 8F + 454 linker / 338R + barcode+ 454 linker (V1/V2 region)
   8F: AGAGTTTGATCCTGGCTCAG + 454 "A" linker
   338R: CTGCTGCCTCCCGTAGGAGT + barcode (one per sample) + 454 "B" linker
   Primers: 515F + barcode + 454 linker / 806R + 454 linker (V4 region)
5. 96-well PCR plates, semi-skirted, Fisher scientific, # E951020401
6. 96-well PCR plate sealing tape, VWR, # 60941-074
7. Mag-bind EZ Pure magnetic purification beads, VWR #95059-680
8. Axygen "Max Recovery" filter pipet tips for DNA transfer, 20 ul, VWR #47749-870

Procedure:

Extraction and Elution

1. Load Powersoil 96-well extraction plate with samples (~0.25g / sample).
   a. For relatively dry samples, use sterile funnels to load plate wells

b. For more wet samples, use small spoon or cut pipet
c. Sterile funnels help prevent contamination of surrounding wells
d. Clean and flame the spoon or pipet between each sample

2. Cover plate and store at 4°C until beginning extraction.
3. Extraction is carried out with Eppendorf robot. Load the PowerSoil extraction protocol on the robot control computer and put samples and plates in robot container as the program demands.
    a. The beadbeating is 2 minutes for the Ley Lab beadbeater, Plate goes in with square mat facing out, and knobs finger-tight.
    b. Make sure the plates are balanced and completely seated in the centrifuge holder before spinning!
    c. After the first beadbeating step, the next robot step is to transfer the lysed samples to a new plate. Because of a high solids content at this step the robot can miss samples here that later have to be repeated. Unless you are running thousands of samples and can run a whole new plate to repeat failed extractions, **perform the sample transfer manually!!**
4. After extraction and before elution, samples can be stored at 4°C.
5. Elution involves several steps of washing, spinning, and then finally elution into a microplate. This should be done manually with a multichannel pipet. The detailed steps are given in the MoBio PowerSoil kit protocol.
6. For the first transfer to the spin plate, be sure to pipet the sample up and down to ensure it is well-mixed
7. Run samples on 0.8% agarose gel with ethidium bromide, view quality and photograph.
    a. Add agarose to 1X borate buffer, and microwave
        i. Higher concentration agarose can separate DNA strands close to one another in length. Longer DNA will run faster in a lower concentration gel. Typically, 0.8-1.2% is good for our shorter strands.
    b. Microwave until just when it starts boiling
    c. Remove and CAREFULLY swirl (if too hot, may overflow)
    d. Repeat until no solids remain
    e. Cool to ~60°C, just too hot to touch.
    f. Add ~2 drops ethidium bromide per 100mL of gel.
    g. Pour into box with comb and allow to solidify
    h. Usually 2 ul loading dye with 2-5ul DNA product is sufficient, you can run 96 wells at once. Use 12-channel pipet to do so.
    i. Run out at up to 150V, lower voltages run slower, and typically help keep bands from deforming.
    j. View under UV, with light on high. Capture on computer.

PCR and Cleanup – Use only filtered pipet tips!!!!!

1. For each sample, the PCR reaction must be run in triplicate to reduce

variation. If template DNA is extremely low and PCR products are not concentrated enough, quadruplicates may be necessary.

2. Along with samples run several water negatives, adding some random reverse primers with no template to randomly check that primers are not contaminated.
3. Keep all chemicals on ice here, when adding sample to PCR plate, also put it on ice
4. Make enough mastermix for all of the reactions you will need. Leave out the primer that is barcoded, this will be added individually to each sample.
5. Make up barcoded primers at 10 uM, one for each sample you are running. Add these to your spreadsheet so that you know which one corresponds to which sample.
6. Total volume in each well of the 96-well PCR plate will be 50 ul
7. To each well, add 48 uL of mastermix, 1 uL of sample-specific barcoded primer (10 uM), and 1 ul of sample. Before pipetting sample, centrifuge a few seconds to ensure no particulates are present
8. Run the following PCR cycle:
    a. 95^{o}C for 2 min
    b. 30 cycles of
        i. 95^{o}C, 30 sec
        ii. 54^{o}C, 30 sec
        iii. 72^{o}C, 1 min
    c. 72^{o}C, 7 min
    d. Hold at 4^{o}C
9. Pool triplicate PCR products and purify with magnetic kit and elute into 30-40ul. Eluting with less does not always result in higher concentration! Sometimes it is necessary to elute into larger volume to get all the DNA off of the beads. It may be worthwhile to experiment with ethanol precipitation in this case.
10. Quantify pooled PCR product with PicoGreen kit

Pooling

1. Use the "max recovery" tips for this part of the protocol.
2. The final pool should contain an equal amount of DNA from each sample.
3. Set up a spreadsheet to help calculate how much of each extracted sample to add to the pool to finish with 15-10 ng/ul.
4. Always pipet >10ul to avoid loss of product in the tip.
5. Quantify final product and run a gel with ladder and 2ul to include in shipment to the sequencing center.

A5.10 gDNA Extraction and Preparation for Illumina Sequencing for metagenomics

Materials:

1. MoBio PowerSoil DNA isolation kit
2. PicoGreen dsDNA quantification kit
3. Molecular biology grade ethanol (if gDNA concentration is necessary)

Procedure:

gDNA Isolation

1. Select samples for genomic sequencing, and determine if multiplexing (sequencing multiple samples in one 'lane') is necessary. If the sequencing center uses 'v3' reagents, you should get ~150 million quality reads per lane
2. Add ~0.2-0.3 g of sample to each extraction tube, or to each well if using the 96-well protocol.
3. If extracting with single sample tubes, follow MoBio instructions (except replace vortex step with bead beating on high for two minutes), pipetting by hand as necessary with filtered pipet tips
4. If extracting with 96-well plate protocol, follow MoBio instructions (bead beat on high for two minutes), using the MoBio protocol on the epMotion robot to perform necessary steps.
5. If using robot, perform the first sample transfer after bead beating by hand, because the robot often does a poor job with the high-solids samples.
6. Quantify endproduct DNA with the PicoGreen quantification kit. For Illumina, sequencing centers prefer 30-100 ng/ul of DNA (as much as possible) in 50 ul. We have sequenced with as little as 12 ng/ul with good results.
7. Run an agarose gel to visualize quality of gDNA bands (with mixed communities, these may not be one perfect band).
8. If you did not get enough DNA, precipitate with ethanol overnight in the freezer, centrifuge at 10,000 rpm for 30 min, gently pour off ethanol, completely dry, and elute into TE buffer.

REFERENCES

Agler, M., Wrenn, B., Zinder, S., and Angenent, L. (2011), Waste to bioproduct conversion with undefined mixed cultures: the carboxylate platform, *Trends in Biotechnology*, 29(2), 70-78.

Agler, M., Garcia, M., Lee, E., Schlicher, M., and Angenent, L. (2008), Thermophilic anaerobic digestion to increase the net energy balance of corn grain ethanol, *Environmental Science and Technology*, 42(17), 6723-6729.

Agler, M., Aydinkaya, Z., Cummings, T., Beers, A., and Angenent, L. (2010), Anaerobic digestion of brewery primary sludge to enhance bioenergy generation: A comparison between low- and high-rate solids treatment and different temperatures, *Bioresource Technology*, 101(15), 5842-5851.

Agler, M., Werner, J., Iten, L., Cotta, M., Dien, B., and Angenent, L. (2011), Functionally predictive microbial community structure links operating conditions to n-butyrate production, *Microbial Biotechnology*, *Submitted*.

Allison, S., and Martiny, J. (2008), Resistance, resilience, and redundancy in microbial communities, *Proceedings of the National Academy of Sciences*, *105*(Supplement 1), 11512-11519.

Amend, J. and Shock, E. (2001), Energetics of overall metabolic reactions of thermophilic and hyperthermophilic archaea and bacteria, *FEMS Microbiology Reviews*, 25(2), 175-243.

Angenent, L., and Wrenn, B. (2008), Optimizing mixed-culture bioprocessing to converting waste into bioenergy, in *Bioenergy*, edited by J. D. Wall, C. S. Harwood and A. Demain, ASM Press, Washington, DC.

Angenent, L., and Kleerebezem, R. (2011), Crystal ball – 2011 - Bioproducts from undefined mixed cultures: Electron pushing., *Microbial Biotechnology*, 4(2), 109-137.

Angenent, L., Zheng, D., Sung, S., and Raskin, L. (2002), Microbial community structure and activity in a compartmentalized, anaerobic bioreactor, *Water Environment Research*, 74(5), 450-461.

Angenent, L. Karim, K., Al-Dahhan, M., Wrenn, B., and Domiguez-Espinosa, R. (2004), Production of bioenergy and biochemicals from industrial and agricultural wastewater, *Trends in Biotechnology*, 22(9), 477-485.

APHA (1998), Standard methods for the examination of water and wastewater, 20th edition *Rep.*, American Public Health Association. Washington, D. C., USA.

Barker, H., Kamen, M., and Bornstein, B. (1945), The synthesis of butyric and caproic acids from ethanol and acetic acid by *Clostridium kluyveri*, *Proceedings of the National Academy of Sciences*, 31(12), 373-381.

Beaty, P., and McInerney, M. (1989), Effects of organic acid anions on the growth and metabolism of *Syntrophomonas wolfei* in pure culture and in defined consortia, *Applied and Environmental Microbiology*, 55(4), 977-983.

Belay, N., and Daniels, L. (1988), Ethane production by *Methanosarcina barkeri* during growth in ethanol supplemented medium, *Antonie Van Leeuwenhoek*, 54(2), 113-125.

Belenguer, A., Duncan, S., Holtrop, G., Anderson, S., Lobley, G., and Flint, H. (2007), Impact of pH on lactate formation and utilization by human fecal microbial communities, *Applied and Environmental Microbiology*, 73(20), 6526-6533.

Belyea, R., Clevenger, T., Singh, V., Tumbleson, M., and Rausch, K. (2006), Element concentrations of dry-grind corn-processing streams, *Applied Biochemistry and Biotechnology*, 134(2), 113-128.

Berezovsky, I., and Shakhnovich, E. (2005), Physics and evolution of thermophilic adaptation, *Proceedings of the National Academy of Sciences*, 102(36), 12742-12747.

Bories, A., Raynal, J., and Bazile, F. (1988), Anaerobic digestion of high-strength distillery wastewater (cane molasses stillage) in a fixed-film reactor, *Biological Wastes*, 23, 251-267.

Borja, R., Sánchez, E., Rincón, B., Raposo, F., Martín, M., and Martín, A. (2005), Study and optimisation of the anaerobic acidogenic fermentation of two-phase olive pomace, *Process Biochemistry*, 40(1), 281-291.

Bothast, R., and Schlicher, M. (2005), Biotechnological processes for conversion of corn into ethanol, *Applied Microbiology and Biotechnology*, 67(1), 19-25.

Bridger, G., Salutsky, M., and Starostka, R. (1962), Micronutrient sources, metal ammonium phosphates as fertilizers, *Journal of Agricultural and Food Chemistry*, 10(3), 181-188.

Butkus, M., Hughes, K., Bowman, D., Liotta, J., Jenkins, M., and Labare, M. (2011), Inactivation of *Ascaris suum* by short-chain fatty acids, *Applied and Environmental Microbiology*, 77(1), 363-366.

Cao, X., Huang, X., Liang, P., Boon, N., Fan, M., Zhang, L., and Zhang, X. (2009), A completely anoxic microbial fuel cell using a photo-biocathode for cathodic carbon dioxide reduction, *Energy and Environmental Science*, 2(5), 498-501.

Capar, S., Tanner, J., Friedman, M., and Boyer, K. (1978), Multielement analysis of animal feed, animal wastes, and sewage sludge, *Environmental Science and Technology*, 12(7), 785-790.

Caporaso, J.,Kuczynski, J., Stembaugh, J., Bittinger, K., Bushman, F., Costello, E., Fierer, N., Pena, A., Goodrich, J., Gordon, J., Huttley, G., Kelley, S., Knights, D., Koenig, J., Ley, R., Lozupone, C., McDonald, D., Muegge, B., Pirrung, M., Reeder, J., Sevinsky, J., Turnbaugh, P., Waters, W., Wildmann, J., Yatsunenko, J., Zaneveld, J., and Knight, R. (2010), QIIME allows analysis of high-throughput community sequencing data, *Nature Methods*, 7(5), 335-336.

Chan, W., and Holtzapple, M. (2003), Conversion of municipal solid wastes to carboxylic acids by thermophilic fermentation, *Applied Biochemistry and Biotechnology*, 111(2), 93-112.

Chen, M., and Wolin, M. (1977), Influence of CH_4 production by *Methanobacterium ruminantium* on the fermentation of glucose and lactate by *Selenomonas ruminantium*, *Applied and Environment Microbiology*, 34(6), 756-759.

Cheng, S., Xing, D., Call, D., and Logan, B. (2009), Direct biological conversion of electrical current into methane by electromethanogenesis, *Environmental Science and Technology*, 43(10), 3953-3958.

Clesceri, L., Greenberg, A., and Eaton, A. (1998), *Standard Methods for the Examination of Water and Wastewater*, APHA, AWWA, WEF, United Book Press, Inc., Baltimore, MD, USA.

Colomban, A., Roger, L., and Boyaval, P. (1993), Production of propionic acid from whey permeate by sequential fermentation, ultrafiltration, and cell recycling, *Biotechnology and Bioengineering*, 42(9), 1091-1098.

Cotta, M., and Forster, R. (2006), The Family Lachnospiraceae, Including the Genera *Butyrivibrio*, *Lachnospira*, and *Roseburia*, in *The Prokaryotes*, edited by M. Dworkin, S. Falkow, E. Rosenberg, K.-H. Schleifer and E. Stackebrandt, pp. 1002-1021, Springer New York.

Counotte, G., and Prins, R. (1981), Regulation of lactate metabolism in the rumen, *Veterinary Research Communications*, 5(1), 101-115.

De Schamphelaire, L., and Verstraete, W. (2009), Revival of the biological sunlight-to-biogas energy conversion system, *Biotechnology and Bioengineering*, 103, 296-304.

DeSantis, T., Hugenholtz, P., Larsen, N., Rojas, M., Brodie, E., Keller, K., Huber, T., Dalevi, D., Hu, P., and Andersen, G. (2006), Greengenes, a chimera-checked 16S rRNA gene database and workbench compatible with ARB, *Applied and Environmental Microbiology*, 72(7), 5069-5072.

Dien, B., Iten, L., and Bothast, R. (1999), Conversion of corn fiber to ethanol by recombinant *E. coli* strain FBR3, *Journal of Industrial Microbiology and Biotechnology*, 22(6), 575-581.

Diez-Gonzalez, F., Russell, J., and Hunter, J. (1995), The role of an NAD-independent lactate dehydrogenase and acetate in the utilization of lactate by *Clostridium acetobutylicum* strain P262, *Archives of Microbiology*, 164(1), 36-42.

Ding, H.-B., Tan, G.-Y., and Wang, J.-Y. (2010), Caproate formation in mixed-culture fermentative hydrogen production, *Bioresource Technology*, 101(24), 9550-9559

Dinsdale, E., Edwards, R., Hall, D., Angly, F., Breitbart, M., Brulc, J., Furlan, M., Desnues, C., Haynes, M., and Li, L. (2008), Functional Metagenomic Profiling of Nine Biomes, *Nature,* 452(3), 629-633.

Duncan, S., Louis, P., and Flint, H. (2004), Lactate-utilizing bacteria, isolated from human feces, that produce butyrate as a major fermentation product, *Applied and Environmental Microbiology*, 70(10), 5810-5817.

Edgar, R. (2010), Search and clustering orders of magnitude faster than BLAST, *Bioinformatics*, 26(19), 2460-2461.

Egg, R., Sweeten, J., and Coble, C. (1985), Grain sorghum stillage recycling: effect on ethanol yield and stillage quality, *Biotechnology and Bioengineering*, 28, 1735-1738.

Enari, T., and Suihko, M. (1983), Ethanol Production by Fermentation of Pentoses and Hexoses from Cellulosic Materials, *Critical Reviews in Biotechnology*, 1(3), 229-240.

Farrell, A., Plevin, R., Turner, B., Jones, A., O'Hare, M., and Kammen, D. (2006), Ethanol can contribute to energy and environmental goals, *Science*, 311(5760), 506-508.

Fathepure, B. (1987), Factors affecting the methanogenic activity of *Methanothrix soehngenii* VNBF, *Applied and Environmental Microbiology*, 53(12), 2978-2982.

Foley, J., Rozendal, R., Hertle, C., Lant, P., and Rabaey, K. (2010), Life cycle assessment of high-rate anaerobic treatment, microbial fuel cells, and microbial electrolysis cells, *Environmental Science and Technology*, 44(9), 3629–3637.

Fornero, J., Rosenbaum, M., and Angenent, L. (2010), Electric power generation from municipal, food, and animal wastewaters using microbial fuel cells, *Electroanalysis*, 22(7-8), 832-843.

Frimmer, U., and Widdel, F. (1989), Oxidation of ethanol by methanogenic bacteria, *Archives of Microbiology*, 152(5), 479-483.

Gaertner, C., Serrano-Ruiz, J., Braden, D., and Dumesic, J. (2009), Catalytic coupling of carboxylic acids by ketonization as a processing step in biomass conversion, *Journal of Catalysis*, 266(1), 71-78.

Ganapathi, G. (1984), A comprehensive treatability study on alcohol stillage using aerobic and anaerobic suspended growth systems, Doctor of Philosophy thesis, Oklahoma State University.

Gianoulis, T., Raes, J., Patel, P., Bjornson, R., Korbel, J., Letunic, I., Yamada, T., Paccanaro, A., Jensen, L., Snyder, M., Bork, P., and Gerstein, M. (2009), Quantifying environmental adaptation of metabolic pathways in metagenomics, *Proceedings of the National Academy of Sciences*, 106(5), 1374-1379.

Glinski, M., Koziol, A., Lomot, D., and Kaszkur, Z. (2007), Catalytic ketonization over oxide catalysts: Part XII. Selective reduction of carboxylic acids by formic acid, *Applied Catalysis A: General*, 323, 77-85.

Grethlein, A., Worden, R., Jain, M., and Datta, R. (1991), Evidence for production of n-butanol from carbon monoxide by *Butyribacterium methylotrophicum*, *Journal of Fermentation and Bioengineering*, 72(1), 58-60.

Hanselmann, K. (1991), Microbial energetics applied to waste repositories, *Cellular and Molecular Life Sciences*, 47(7), 645-687.

Hashsham, S., Fernandez, A., Dollhopf, S., Dazzo, F., Hickey, R., Tiedje, J., and Criddle, C. (2000), Parallel processing of substrate correlates with greater functional stability in methanogenic bioreactor communities perturbed by glucose, *Applied and Environmental Microbiology*, 66(9), 4050-4057.

Hendriks, A., and Zeeman, G. (2009), Pretreatments to enhance the digestibility of lignocellulosic biomass, *Bioresource Technology*, 100(1), 10-18.

Hill, J., Nelson, E., Tilman, D., Polasky, S., and Tiffany, D. (2006), Environmental, economic, and energetic costs and benefits of biodiesel and ethanol biofuels, *Proceedings of the National Academy of Sciences*, 103(30), 11206-11210.

Hollister, E., Forrest, A., Wilkinson, H., Ebbole, D., Malfatti, S., Tringe, S., Holtzapple, M., and Gentry, T. (2010), Structure and dynamics of the microbial communities underlying the carboxylate platform for biofuel production, *Applied Microbiology and Biotechnology*, 88(1), 389-399.

Holtzapple, M., and Granda, C. (2009), Carboxylate platform: the MixAlco process part 1: comparison of three biomass conversion platforms, *Applied Biochemistry and Biotechnology*, 156(1), 95-106.

Holtzapple, M., Davison, R., Ross, M. Albrett-Lee, S., Naguani, M., Lee, C.M., Lee, C., Adelson, S., Kaar, W. Gaskin, D., Shirage, H., Chang, N.S., Chang, V.S., and Loescher, M. (1999), Biomass conversion to mixed alcohol fuels using the MixAlco process, *Applied Biochemistry and Biotechnology*, 79(1), 609-631.

Hutnan, M., Hornak, M., Bodik, I., and Hlavacka, V. (2003), Anaerobic treatment of wheat stillage, *Chemical and Biochemical Engineering Quarterly*, 17(3), 233-241.

Ingledew, W. (2003), Water reuse in fuel alcohol plants: Effect on fermentation. Is a "Zero discharge" concept attainable?, in *The Alcohol Textbook*, edited by T. P. Lyons, pp. 343-354, Nottingham University Press, Nottingham, UK.

Jeganathan, J., Nakhla, G., and Bassi, A. (2006), Long-term performance of high-rate anaerobic reactors for the treatment of oily wastewater, *Environmental Science and Technology*, 40(20), 6466-6472.

Jin, Q. (2007), Control of hydrogen partial pressures on the rates of syntrophic microbial metabolisms: A kinetic model for butyrate fermentation, *Geobiology*, 5, 35-48.

John, R., Nampoothiri, K., and Pandey, A. (2007), Fermentative production of lactic acid from biomass: an overview on process developments and future perspectives, *Applied Microbiology and Biotechnology*, 74(3), 524-534.

Kim, M., Gomec, C., Ahn, Y., and Speece, R. (2003), Hydrolysis and acidogenesis of particulate organic material in mesophilic and thermophilic anaerobic digestion, *Environmental Technology*, 24(9), 1183 - 1190.

Kim, S., and Holtzapple, M. (2005), Lime pretreatment and enzymatic hydrolysis of corn stover, *Bioresource Technology*, 96(18), 1994-2006.

Kim, S., Han, S.-K., and Shin, H.-S. (2006), Effect of substrate concentration on hydrogen production and 16S rDNA-based analysis of the microbial community in a continuous fermenter, *Process Biochemistry*, 41(1), 199-207.

Kleerebezem, R., and Stams, A. (2000), Kinetics of syntrophic cultures: A theoretical treatise on butyrate fermentation, *Biotechnology and Bioengineering*, 67, 529-543.

Kleerebezem, R., and van Loosdrecht, M. (2007), Mixed culture biotechnology for bioenergy production, *Current Opinion in Biotechnology*, 18(3), 207-212.

Kleerebezem, R., Rodriguez, J., Temudo, M., and van Loosdrecht, M. (2008), Modeling mixed culture fermentations; the role of different electron carriers, *Water Science and Technology*, 57(4), 493-497.

Leadbetter, J., Schmidt, T., Graber, J., and Breznak, J. (1999), Acetogenesis from H_2 Plus CO_2 by Spirochetes from Termite Guts, *Science*, 283(5402), 686-689.

Lee, S., Krajmalinik-Brown, R., Zhang, H., and Rittman, B. (2009), An electron-flow model can predict complex redox reactions in mixed-culture fermentative bioH_2: Microbial ecology evidence, *Biotechnology and Bioengineering*, 104(4), 687-697.

Lee, Y.-E., Lowe, S., and Zeikus, J. (1993), Regulation and characterization of xylanolytic enzymes of *Thermoanaerobacterium saccharolyticum* B6A-RI, *Applied and Environmental Microbiology*, 59(3), 763-771.

Lettinga, G. (1995), Anaerobic digestion and wastewater treatment systems, *Antonie Van Leeuwenhoek*, 67, 3-28.

Levy, P., Sanderson, J., Kispert, R., and Wise, D. (1981), Biorefining of biomass to liquid fuels and organic chemicals, *Enzyme and Microbial Technology*, 3(3), 207-215.

Li, Z., Qin, W., and Dai, Y. (2002), Liquid-liquid equilibria of acetic, propionic, butyric, and valeric acids with trioctylamine as extractant, *Journal of Chemical and Engineering Data*, 47(4), 843-848.

Liu, H., Grot, S., and Logan, B. (2005), Electrochemically assisted microbial production of hydrogen from acetate, *Environmental Science and Technology,* 39(11), 4317-4320.

Liu, S.-Y., Rainey, F., Morgan, H., Mayer, F., and Wiegel, J. (1996), *Thermoanaerobacterium aotearoense* sp. now., a slightly acidophilic, anaerobic thermophile isolated from various hot springs in New Zealand, and Emendation of the genus *Thermoanaerobacterium*, *International Jouranl of Systematic and Evolutionary Microbiology*, 46(2), 388-396.

Logan, B., Hamelers, B., Rozendal, R., Schröder, U., Keller, J., Freguia, S., Aelterman, P., Verstraete, W., and Rabaey, K. (2006), Microbial fuel cells: Methodology and technology, *Environmental Science and Technology*, 40(17), 5181-5191.

Lozupone, C., and Knight, R. (2005), UniFrac: a new phylogenetic method for comparing microbial communities, *Applied and Environmental Microbiology*, 71(12), 8228-8235.

Machado, M., and Sant'Anna, G. (1987), Study of the acidogenic phase of the anaerobic fermentation of stillage from ethanol distilleries, *Biotechnology Letters*, 9(7), 517-522.

Mackie, R., and Bryant, M. (1995), Anaerobic-digestion of cattle waste at mesophilic and thermophilic temperatures, *Applied Microbiology and Biotechnology*, 43(2), 346-350.

Marounek, M., Fliegrova, K., and Bartos, S. (1989), Metabolism and some characteristics of ruminal strains of *Megasphaera elsdenii*, *Applied and Environmental Microbiology*, *55*(6), 1570-1573.

Marták, J., and Schlosser, Š. (2008), Liquid-liquid equilibria of butyric acid for solvents containing a phosphonium ionic liquid, *Chemical Papers*, 62(1), 42-50.

Martin, H. Ivanova, N., Kunin, V., Warnecke, F., Barry, K., McHardy, A., Yeates, C., He, S., Salamov, A., Szeto, E., Dalin, E., Putnam, N., Shapiro, H., Pangilinan, J., Rigoutsos, I., Kyrpides, N., Blackall, L., McMahon, K., and Hugenholtz, P. (2006), Metagenomic analysis of two enhanced biological phosphorus removal (EBPR) sludge communities, *Nature Biotechology*, 24(10), 1263-1269.

McFarlane, J., Ridenour, W., Luo, H., Hunt, R., DePaoli, D., and Ren, R. (2005), Room temperature ionic liquids for separating organics from produced water, *Separation Science and Technology*, 40(6), 1245 - 1265.

McInerney, M., Bryant, M., Hespell, R., and Costerton, J. (1981), *Syntrophomonas wolfei* gen. nov. sp. nov., an anaerobic, syntrophic, fatty acid-oxidizing bacterium, *Applied and Environment Microbiology*, 41(4), 1029-1039.

Meyer, F., Paarman, D., D'Souza, M., Olson, R., Glass, E., Kubal, M., Paczian, T., Rodriguez, A., Stevens, R., Wilke, A., Wilkening, J., and Edwards, R. (2008), The metagenomics RAST server - a public resource for the automatic phylogenetic and functional analysis of metagenomes, *BMC Bioinformatics*, 9(1), 386.

Mosier, N., Wyman, C., Dale, B., Elander, R., Lee, Y., Holtzapple, M., and Ladisch, M. (2005a), Features of promising technologies for pretreatment of lignocellulosic biomass, *Bioresource Technology*, 96(6), 673-686.

Mosier, N., Hendrickson, R., Brewer, M., Ho, N., Sedlak, M., Dreshel, R., Welch, G., Dien, B., Aden, A., and Ladisch, M. (2005b), Industrial scale-up of pH-controlled liquid hot water pretreatment of corn fiber for fuel ethanol production, *Applied Biochemistry and Biotechnology*, 125(2), 77-97.

Murray, W., and van den Berg, L. (1981), Effects of nickel, cobalt, and molybdenum on performance of methanogenic fixed-film reactors, *Applied and Environmental Microbiology*, 42(3), 502-505.

Nagase, M., and Matsuo, T. (1982), Interactions between amino-acid degrading bacteria and methanogenic bacteria in anaerobic digestion, *Biotechnology and Bioengineering*, 24, 2227-2239.

Nevin, K., Woodard, T., Franks, A., Summers, Z., and Lovley, D. (2010), Microbial electrosynthesis: Feeding microbes electricity to convert carbon dioxide and water to multicarbon extracellular organic compounds, *mBio*, 1(2), e00103-00110

Noureddini, H., and Byun, J. (2010), Dilute-acid pretreatment of distillers' grains and corn fiber, *Bioresource Technology*, 101(3), 1060-1067.

Odelson, D., and Breznak, J. (1983), Volatile fatty acid production by the hindgut microbiota of xylophagous termites, *Applied and Environment Microbiology*, 45(5), 1602-1613.

Oh, S.-E., Van Ginkel, S., and Logan, B. (2003), The relative effectiveness of pH control and heat treatment for enhancing biohydrogen gas production, *Environmental Science and Technology*, 37(22), 5186-5190.

Oksanen, J., Blanchet, F., Kindt, R., Legendre, P., O'Hara, R., Simpson, G., Solymos, P., Stevens, M., and Wagner, H. (2011), vegan: Community ecology package. R package version 1.17-10, edited.

Owens, F., Secrist, D., Hill, W., and Gill, D. (1998), Acidosis in cattle: a review, *Journal of Animal Science*, 76(1), 275-286.

Ozadali, F., Glatz, B., and Glatz, C. (1996), Fed-batch fermentation with and without on-line extraction for propionic and acetic acid production by *Propionibacterium acidipropionici*, *Applied Microbiology and Biotechnology*, 44(6), 710-716.

Park, Y., Shaffer, C., and Bennett, G. (2009), Microbial formation of esters, *Applied Microbiology and Biotechnology*, 85(1), 13-25.

Rabaey, K., Bützer, S., Brown, S., Keller, J., and Rozendal, R. (2010), High current generation coupled to caustic production using a lamellar bioelectrochemical system, *Environmental Science and Technology*, 44(11), 4315-4321.

Ragauskas, A., Williams, C., Davison, B., Britovsek, G., Cairney, J., Eckert, C., Frederick, W. Jr., Hallett, J., Leak, D., Liotta, C., Mielenz, J., Murphy, R., Templer, R., and Tschaplinski, T. (2006), The Path Forward for Biofuels and Biomaterials, *Science*, 311(5760), 484-489.

Rausch, K., and Belyea, R. (2006), The future of coproducts from corn processing, *Applied Biochemistry and Biotechnology*, 128(1), 47-86.

Read, S., Dutta, P., Bond, P., Keller, J., and Rabaey, K. (2010), Initial development and structure of biofilms on microbial fuel cell anodes, *BMC Microbiology*, 10, 98.

Reimann, I., Klatt, A., and Markl, H. (2002), Treatment of fat-containing wastewater from the food processing industry with a thermophilic microorganism, *Chemie Ingenieur Technik*, 74(4), 508-512.

Ren, N., Wang, B., and Huang, J. (1997), Ethanol-type fermentation from carbohydrate in high rate acidogenic reactor, *Biotechnology and Bioengineering*, 54(5), 428-433.

Ren, N., Xing, D., Rittmann, B., Zhao, L., Xie, T., and Zhao, X. (2007), Microbial community structure of ethanol type fermentation in bio-hydrogen production, *Environmental Microbiology*, 9(5), 1112-1125.

Ren, N., Cao, G., Wang, A., Lee, D.-J., Guo, W., and Zhu, Y. (2008), Dark fermentation of xylose and glucose mix using isolated *Thermoanaerobacterium thermosaccharolyticum* W16, *International Journal of Hydrogen Energy*, 33(21), 6124-6132.

Richter, H., Qureshi, N., Heger, S., Dien, B., Cotta, M., and Angenent, L. (2011), Prolonged conversion of n-butyrate to n-butanol with *Clostridium saccharoperbutylacetonicum* in a two-stage continuous culture with *in-situ* product removal, *Biotechnology and Bioengineering*, *Submitted*.

Rodriguez, J., Kleerebezem, R., Lema, J., and van Loosdrecht, M. (2006), Modeling product formation in anaerobic mixed culture fermentations, *Biotechnology and Bioengineering*, 93(3), 592-606.

Rosenbaum, M., Bar, H., Beg, Q., Segrè, D., Booth, J., Cotta, M., and Angenent, L. (2011), *Shewanella oneidensis* in a lactate-fed pure-culture and a glucose-fed co-culture with *Lactococcus lactis* with an electrode as electron acceptor, *Bioresource Technology*, 102(3), 2623-2628.

Rozendal, R., Leone, E., Keller, J., and Rabaey, K. (2009), Efficient hydrogen peroxide generation from organic matter in a bioelectrochemical system, *Electrochemical Communications*, 11(9), 1752-1755.

Russell, J., and Hino, T. (1985), Regulation of lactate production in *Streptococcus bovis*: A spiraling effect that contributes to rumen acidosis, *Journal of Dairy Science*, 68(7), 1712-1721.

Russell, J., and Wilson, D. (1996a), Why Are Ruminal Cellulolytic Bacteria Unable to Digest Cellulose at Low pH?, *Journal of Dairy Science*, 79(8), 1503-1509.

Saha, B., and Bothast, R. (1999), Pretreatment and enzymatic saccharification of corn fiber, *Applied Biochemistry and Biotechnology*, 76(2), 65-77.

Schaefer, S., and Sung, S. (2008), Retooling the ethanol industry: Thermophilic anaerobic digestion of thin stillage for methane production and pollution prevention, *Water Environment Research*, 80(2), 101-108.

Schink, B. (1997), Energetics of syntrophic cooperation in methanogenic degradation, *Microbiology and Molecular Biology Reviews*, 61(2), 262-280.

Schirmer, A., Rude, M., Li, X., Popova, E., and del Cardayre, S. (2010), Microbial biosynthesis of alkanes, *Science*, 329(5991), 559-562.

Schloss, P., Westcott, S., Ryabin, T., Hall, J., Hartmann, M., Hollister, E., Lesnewski, R., Oakley, B., Parks, D., Robinson, C., Sahl, J., Stres, B., Thallinger, G., van Horn, D., and Weber, C. (2009), Introducing mothur: Open-source, platform-independent, community-supported software for describing and comparing microbial communities, *Applied and Environmental Microbiology*, 75(23), 7537-7541.

Schlüter, A., Bekel, T., Diaz, N., Dondrup, M., Eichenlaub, R., Gartemann, K., Krahn, I., Krause, L., Krömehe, H., Kruse, O., Mussgnug, J., Neuweger, H., Niehaus, K., Pühler, A., Runte, K., Seczepanowski, R., Tauch, A., Tilker, A., Viehöver, P., and Goesmann, A. (2008), The metagenome of a biogas-producing microbial community

of a production-scale biogas plant fermenter analysed by the 454-pyrosequencing technology, *Journal of Biotechnology*, 136(1-2), 77-90.

Schnoor, J. (2006), The debate is over, *Environmental Science and Technology*, 40(9), 2861-2861.

Seedorf, H., Fricke, W., Veith, B., Brüggemann, H., Liesegang, H., Strittmatter, A., Miethke, M., Buckel, W., Hinderberger, J., Li, F., Hagemeier, C., Thauer, R., and Gottschalk, G. (2008), The genome of *Clostridium kluyveri*, a strict anaerobe with unique metabolic features, *Proceedings of the National Academy of Sciences*, 105(6), 2128-2133.

Segers, L., Verstrynge, L., and Verstraete, W. (1981), Product patterns of non-axenic sucrose fermentation as a function of pH, *Biotechnology Letters*, 3(11), 635-640.

Shin, H.-S., Youn, J.-H., and Kim, S.-H. (2004), Hydrogen production from food waste in anaerobic mesophilic and thermophilic acidogenesis, *International Journal of Hydrogen Energy*, 29(13), 1355-1363.

Shock, E. (1995), Organic acids in hydrothermal solutions; standard molal thermodynamic properties of carboxylic acids and estimates of dissociation constants at high temperatures and pressures, *American Journal of Science*, 295(5), 496-580.

Shock, E., and Helgeson, H. (1990), Calculation of the thermodynamic and transport properties of aqueous species at high pressures and temperatures: Standard partial molal properties of organic species, *Geochimica et Cosmochimica Acta*, 54(4), 915-945.

Shojaosadati, S., Sanaei, H., and Fatemi, S. (1996), The use of biomass and stillage recycle in conventional ethanol fermentation, *Journal of Chemical Technology and Biotechnology*, 67(4), 362-366.

Shu, C., Cai, J., Huang, L., Zhu, X., and Xu, Z. (2011), Biocatalytic production of ethyl butyrate from butyric acid with immobilized *Candida rugosa* lipase on cotton cloth, *Journal of Molecular Catalysis B: Enzymatic*, *In Press, Corrected Proof*.

Smith, D., and McCarty, P. (1989), Reduced product formation following perturbation of ethanol- and propionate-fed methanogenic CSTRs, *Biotechnology and Bioengineering*, 34(7), 885-895.

Smith, D., and McCarty, P. (1989), Energetic and rate effects on methanogenesis of ethanol and propionate in perturbed CSTRs, *Biotechnology and Bioengineering*, 34(1), 39-54.

Solomon, B., Barnes, J., and Halvorsen, K. (2007), Grain and cellulosic ethanol: History, economics, and energy policy, *Biomass and Bioenergy*, 31, 416-425.

Speece, R. (1996), *Anaerobic biotechnology for industrial wastewaters*, Archae Press, Nashville.

Speece, R., Boonyakitsombut, S., Kim, M., Azbar, N., and Ursillo, P. (2006), Overview of anaerobic treatment: thermophilic and propionate implications, *Water Environment Research*, 78(5), 460-473.

Steinbusch, K. (2010), Liquid Biofuel Production from Volatile Fatty Acids, Thesis, 139 pp, Wageningen Uiniversity, Wageningen, the Netherlands.

Steinbusch, K., Hamelers, H., and Buisman, C. (2008), Alcohol production through volatile fatty acids reduction with hydrogen as electron donor by mixed cultures, *Water Research*, 42(15), 4059-4066.

Steinbusch, K., Arvaniti, E., Hamelers, H., and Buisman, C. (2009), Selective inhibition of methanogenesis to enhance ethanol and n-butyrate production through acetate reduction in mixed culture fermentation, *Bioresource Technology*, 100(13), 3261-3267.

Steinbusch, K., Hamelers, H., Plugge, C., and Buisman, C. (2011), Biological formation of caproate and caprylate from acetate: fuel and chemical production from low grade biomass, *Energy and Environmental Science*, 4(1), 216-224.

Steinbusch, K., Hamelers, H., Schaap, J., Kampman, C., and Buisman, C. (2010), Bioelectrochemical ethanol production through mediated acetate reduction by mixed cultures, *Environmental Science and Technology*, 44(1), 513-517.

Stiles, M. (1996), Biopreservation by lactic acid bacteria, *Antonie Van Leeuwenhoek*, 70(2), 331-345.

Stover, E. (1984), Use of methane gas from anaerobic treatment of stillage for fuel alcohol production, paper presented at 39th Industrial Waste Conference, Butterworth Publishers, Purdue University.

Tashiro, Y., Takeda, K., Kobayashi, G., Sonomoto, K., and Yoshino, S. (2004), High butanol production by *Clostridium saccharoperbutylacetonicum* N1-4 in fed-batch culture with pH-Stat continuous butyric acid and glucose feeding method, *Journal of Bioscience and Bioengineering*, 98(4), 263-268.

Tchobanoglous, G., Burton, F., and Stensel, H. (2003), *Wastewater Engineering, Treatment and Reuse: Metcalf and Eddy*, 4 ed., McGraw Hill, New York, NY.

Temudo, M., Kleerebezem, R., and van Loosdrecht, M. (2007), Influence of the pH on (open) mixed culture fermentation of glucose: A chemostat study, *Biotechnology and Bioengineering*, 98(1), 69-79.

Thanakoses, P., Mostafa, N., and Holtzapple, M. (2003), Conversion of sugarcane bagasse to carboxylic acids using a mixed culture of mesophilic microorganisms, *Applied Biochemistry and Biotechnology*, 107(1), 523-546.

Thauer, R. (1998), Biochemistry of methanogenesis: a tribute to Marjory Stephenson. 1998 Marjory Stephenson Prize Lecture, *Microbiology*, 144(9), 2377-2406.

Thauer, R., Jungermann, K., and Decker, K. (1977), Energy conservation in chemotrophic anaerobic bacteria, *Bacteriological Reviews*, 41(1), 100-180.

Tibshirani, R., Hastie, T., Narasimhan, B., and Chu, G. (2002), Diagnosis of multiple cancer types by shrunken centroids of gene expression, *Proceedings of the National Academy of Sciences*, 99(10), 6567-6572.

Tong, X., Smith, L., and McCarty, P. (1990), Methane fermentation of selected lignocellulosic materials, *Biomass*, 21(4), 239-255.

Tong, Y., Hirata, M., Takanashi, H., Hano, T., Kubota, F., Goto, M., Nakashio, F., and Matsumoto, M. (1998), Extraction of lactic acid from fermented broth with microporous hollow fiber membranes, *Journal of Membrane Science*, 143(1-2), 81-91.

USDA (2008), Illinois ethanol corn and co-products processing value, USDA - IL Department of Ag Market News, Springfield, IL.

Van Kessel, J., and Russell, J. (1996), The effect of pH on ruminal methanogenesis, *FEMS Microbiology Ecology*, 30, 205-210.

Vavilin, V., Fernandez, B., Palatsi, J., and Flotats, X. (2008), Hydrolysis kinetics in anaerobic degradation of particulate organic material: An overview, *Waste Management*, 28(6), 939-951.

Villano, M., Aulenta, F., Ciucci, C., Ferri, T., Giuliano, A., and Majone, M. (2010), Bioelectrochemical reduction of CO_2 to CH_4 via direct and indirect extracellular electron transfer by a hydrogenophilic methanogenic culture, *Bioresource Technology*, 101(9), 3085-3090.

Wang, J., Burken, J., Zhang, X., and Surampali, R. (2005), Engineered struvite precipitation: Impacts of component-ion molar ratios and pH, *Journal of Environmental Engineering*, 131(10), 1433.

Wang, Z., Shen, W., Kotler, D., Heshka, S., Wielopolski, L., Aloia, J., Nelson, M., Pierson, R., Jr., and Heymsfield, S. (2003), Total body protein: a new cellular level mass and distribution prediction model, *American Journal of Clinical Nutrition*, 78(5), 979-984.

Werner, J., Koren, O., Hugenholtz, P., DeSantis, T., Walters, W., Caporaso, J., Angenent, L., Knight, R., and Ley, R. (2011a), Impact of training sets on classification of high-throughput bacterial 16S rRNA gene surveys, *The ISME Journal*, *In Press*.

Werner, J., Knights, D., Garcia, M., Scalfone, N., Smith, S., Yarasheski, K., Cummings, T., Beers, A., Knight, R., and Angenent, L. (2011b), Bacterial community structures are unique and resilient in full-scale bioenergy systems, *Proceedings of the National Academy of Sciences*, 108(10), 4158-4163.

Wilkie, A., Riedesel, K., and Owens, J. (2000), Stillage Characterization and Anaerobic Treatment of Ethanol Stillage from Conventional and Cellulosic Feedstocks, *Biomass and Bioenergy*, 19, 63-102.

Wittebolle, L., Marzorati, M., Clement, L., Balloi, A., Daffonchio, D., Heylen, K., De Vos, P., Verstraete, W., and Boon, N. (2009), Initial community evenness favours functionality under selective stress, *Nature*, 458(7238), 623-626.

Committee on water implications of biofuels production in the United States (2007), Water Implications of Biofuels Production in the United States, National Academy of Sciences, Washington, DC.

Wu, Z., and Yang, S.-T. (2003), Extractive fermentation for butyric acid production from glucose by *Clostridium tyrobutyricum*, *Biotechnology and Bioengineering*, 82(1), 93-102.

Zehnder, A., Huser, B., Brock, T., and Wuhrmann, K. (1980), Characterization of an acetate-decarboxylating, non-hydrogen-oxidizing methane bacterium, *Archives of Microbiology*, 124(1), 1-11.

Zhang, T., Liu, H., and Fang, H. (2003), Biohydrogen production from starch in wastewater under thermophilic conditions, *Journal of Environmental Management*, 69, 149-156.

Zigová, J., and Šturdík, E. (2000), Advances in biotechnological production of butyric acid, *Journal of Industrial Microbiology and Biotechnology*, 24(3), 153-160.

Zinder, S., and Koch, M. (1984), Non-aceticlastic methanogenesis from acetate: acetate oxidation by a thermophilic syntrophic coculture, *Archives of Microbiology*, 138, 263-272.

Zoetemeyer, R., Arnoldy, P., Cohen, A., and Boelhouwer, C. (1982), Influence of temperature on the anaerobic acidification of glucose in a mixed culture forming part of a two-stage digestion process, *Water Research*, 16(3), 313-321.